General Disclaimer

One or more of the Following Statements may affect this Document

- This document has been reproduced from the best copy furnished by the organizational source. It is being released in the interest of making available as much information as possible.

- This document may contain data, which exceeds the sheet parameters. It was furnished in this condition by the organizational source and is the best copy available.

- This document may contain tone-on-tone or color graphs, charts and/or pictures, which have been reproduced in black and white.

- This document is paginated as submitted by the original source.

- Portions of this document are not fully legible due to the historical nature of some of the material. However, it is the best reproduction available from the original submission.

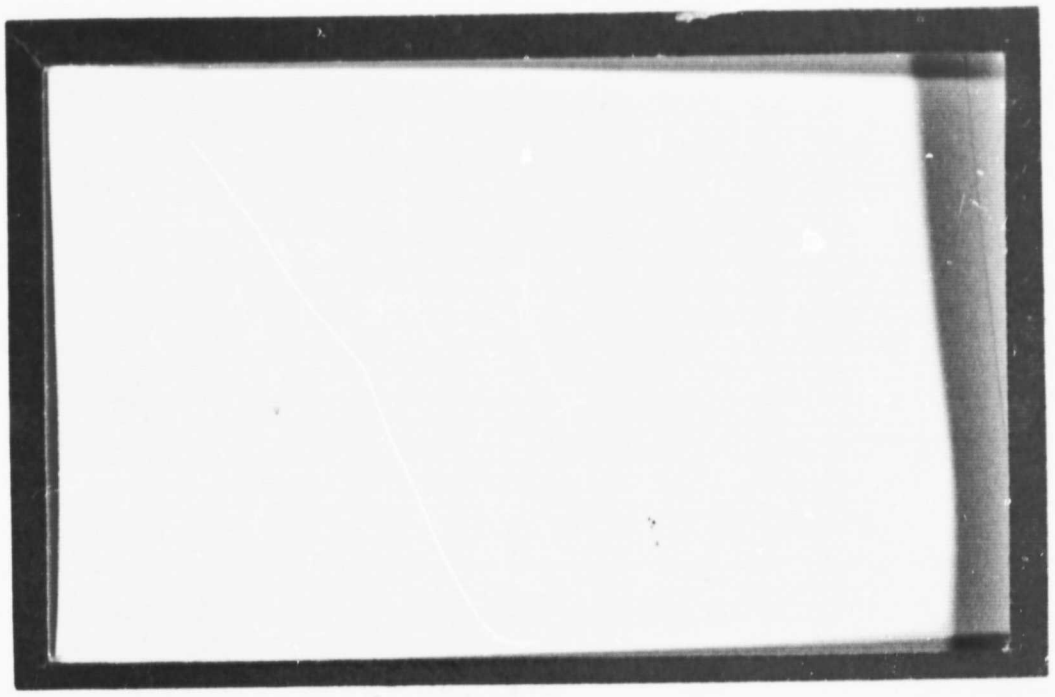

SYRACUSE UNIVERSITY

SYRACUSE UNIVERSITY : FOUNDED A·D·1870 : SUOS CULTORES SCIENTIA CORONAT

Contract No. 950831

STUDY OF NOVEL REFRIGERATION METHODS

William E. Gifford

Syracuse University Research Institute
Mechanical and Aerospace Engineering Department

FINAL REPORT

October 1966

This work was performed for the Jet Propulsion Laboratory, California Institute of Technology, sponsored by the National Aeronautics and Space Administration under Contract NAS7-100.

Jet Propulsion Laboratory

California Institute of Technology
4800 Oak Grove Drive
Pasadena, California 91103

TABLE OF CONTENTS

		Page No.
I.	Introduction	1
II.	The General Problem of Cryogenic Refrigeration	3
	1. The Heat Exchange Means	
	2. Multi-Staging Cryogenic Refrigeration Systems	
III.	Cryomatic Gas Balancing (The Gifford-McMahon Cycle)	12
	1. General Theory	
	2. Cryomatic Gas Balancing Model Results and Potential	
	3. Gas Balancing Thermal Loss Analysis	
	4. Experimental Apparatus	
	5. Results	
	6. Discussion	
IV.	Pulse Tube Refrigeration	32
	1. Surface Heat Pumping Effect	
	2. Pulse Tube Refrigeration Characteristics	
	3. Test Results	
	4. Empirical Formulation	
	5. Multi Stage Pulse Tubes	
V.	Reversible Pulse Tube Refrigeration	48
	1. Theory	
	2. Pulse Tube Refrigerator Ideal Volume Ratio	
	3. Objectives of Test Program	
	4. Description of Experimental Apparatus	
	5. Results of Reversible Pulse Tube Test Program	
	6. Reversible Pulse Tube Efficiency	

TABLE OF CONTENTS

Page No.

VI. Compact Cryogenic Refrigerators 67

1. Introduction

2. Test Results

Figures

References

Bibliography

LIST OF ILLUSTRATIONS

Figure Number	
1	Basic Cryogenic Refrigerator Schematic
2	Basic Refrigerator Temperature Patterns
3	Pressure-Volume Diagram for a Gas Balancing Refrigerator
4	Temperature Position Diagram for a Thermal Regenerator
5	Motional Heat Transfer Temperature Patterns
6	Single Stage Cryomatic Gas Balancing Refrigerator, Schematic Diagram
7	Two Stage Cryomatic Gas Balancing Refrigerator, Schematic Diagram
8	Temperature-Entropy Diagram for First Batch of Gas to Enter Refrigerator
9	Temperature-Entropy Diagram for Batch of Gas Entering the Refrigerator when the Pressure Has Been Built Up Half Way
10	Refrigeration Cycle Performance Curves
11	Two Stage Gas Balancing Refrigerator Model
12	Single Stage Gas Balancing Test Refrigerator
13	Test Apparatus Setup
14	Pressure Volume Diagram
15	Variation of Available Refrigeration as a Function of Displacer Speed
16	Pressure and Volume Changes with Time
17	Gas and Wall Temperature vs. Position for Surface Heat Pumping Cycle
18	Gas and Wall Temperature vs. Position for Elements at Different Radii with Viscous Effects
19	Pulse Tube Refrigerator Configuration
20	Test Setup

LIST OF ILLUSTRATIONS (continued)

Figure no.	
21	Schematic Diagram of Thermocouple Circuit
22	Heat Pumping Rate vs. Cold End Temperature
23	Heat Pumping Rate vs. Low Pressure at Constant High Pressure and Pressure Ratio
24	Heat Pumping Rate vs. Speed for Constant Pressures
25	Heat Pumping Rate vs. Cold End Temperature for Tubes of Different Length Ratios
26	Watts Out/Length vs. Cold End Temperature for Three Different Length Pulse Tubes
27	Heat Pumping Rate vs. Cold End Temperature for Different Diameter Tubes at Same Value of ND^2
28	Photograph of Pulse Tubes 25, 27, 28, 29, 30 and 32
29	Photograph of $\frac{1}{4}$" Diameter Pulse Tube Mounted on Conduction Type Calorimeter
30	Correlation of Test Data with Helium
31	Correlation of Test Data with Air
32	Pulse Tube Cycle Diagrams
33	Integrated P-V Diagram for Gas Packets in Pulse Tube
34	T-S Diagram for Brayton Cycle
35	Pulse Tube Refrigeration as a Function of Cold End Temperature
36	Volume Ratio vs. Temperature Ratio
37	Reversible Pulse Tube Experimental Setup Photograph, Showing Variable Volume Extension
38	Photograph of Multitube Pulse Tube Refrigerator Without Regenerator and Flow Straighteners
39	Typical Valved Pulse Tube Refrigerator
40	Reversible Pulse Tube Refrigerator to be Tested
41	Photograph of Experimental Model of Reversible Pulse Tube Refrigerator

LIST OF ILLUSTRATIONS (continued)

Figure no.	
42	Photograph - Experimental Set Up Used to Test Reversible Pulse Tube
43	Performance of Reversible and Standard Pulse Tube Refrigerators
44	Performance of Reversible Pulse Tube Refrigerator
45	Effects of Compressor Speed on Reversible Pulse Tube Performance
46	Typical Pressure Time Relations at Equal P_h/P for Valved and Reversible Pulse Tubes
47	System Power Losses in Reversible Pulse Tube Testing Apparatus
48	Heat Loss vs. SCFM Helium
49	Inefficiency Vs. SCFM Helium
50	Variation in Regenerator Inefficiency with Regenerator Length for a Phenolic Tube and Bronze Screens
51	Variation in Regenerator Inefficiency with Regenerator Length for a Phenolic Tube and Bronze Screens
52	Variation in the Regenerator Inefficiency with Regenerator Length for a .010 in. thick Stainless Steel Walled Regenerator and Bronze Screens
53	Variation in Regenerator Inefficiency with Regenerator Length for a .020 in. thick Stainless Steel Walled Regenerator and Stainless Steel Screens
54	Variation in Regenerator Inefficiency for Lead Spheres .015 to .018 in. diameters
55	Variation in Regenerator Inefficiency for Lead Spheres .006 to .009 in. diameters
56	Regenerator Inefficiency Variations with Helium Flow Rate
57	Regenerator Inefficiency Variation with Helium Flow Rate
58	Regenerator Inefficiency Variation with Helium Flow Rate for a Stainless Steel Walled Regenerator
59	Regenerator Inefficiency Variation with Helium Flow Rate
60	Variation in Regenerator Inefficiency with Packing Density for 150 Mesh Stainless Steel Screens

LIST OF ILLUSTRATIONS (continued)

Figure no.

61 Variation in Regenerator Inefficiency with Packing Density for 150 Mesh Bronze Screens

62 Variation in Regenerator Inefficiency with Screen Packing Density

63 Variation in Regenerator Inefficiency with Screen Packing Density

64 Variation in Regenerator Inefficiency for a 2" Long Regenerator with Variable End Conditions

65 Regenerator Test Flow Diagram

I. INTRODUCTION

The object of this contract has been to advance the general cryogenic refrigeration capability. The effort has been principally with "Pulse Tube Refrigeration" and "Cryomatic Gas Balancing," both promising cryogenic refrigeration methods originated at Syracuse University.

The goal for the work has been the low temperature of 4.2°K. Much of the work has been experimentation at much higher temperatures as the methods are new and a considerable amount of study and understanding is required before designing for a temperature as low as 4.2°K.

This is especially true for "Pulse Tube Refrigeration." Even after a program full of worthwhile progress, the understanding is still not adequate for designing for 4.2°K. In fact, even at the finish of the program the degree of understanding is only adequate for single stage units for the temperature range 125-175°K. It is even presently doubted that it would ever be a good method for temperatures lower than about 30°K. Temperatures to 43°K have been achieved.

Better results were obtained with "Cryomatic Gas Balancing." Units were built both at Syracuse University and at the Jet Propulsion Laboratory with which temperatures of 4.2°K were attained and maintained reliably.

In general, great progress was made with the understanding of both methods and with experimental verification of many conclusions.

In addition to the work with these two refrigeration methods, a considerable investigation of "Thermal Regenerators" was started. Thermal regenerators are a very important component of these two refrigeration methods as well as of several of the other successful cryogenic refrigeration methods. Though thermal regenerators are simple devices to build, they present very difficult analytical problems and are also difficult to investigate experimentally.

During the period of this program work other than that described was carried out which led to no fruitful results as yet and therefore is not reported here. Such work included such things as analysis to lead to optimal design, especially in the multi-stage aspects of both the Pulse Tube and Gas Balancing Refrigeration methods.

II. THE GENERAL PROBLEM OF CRYOGENIC REFRIGERATION

Refrigeration consists of removing heat at some temperature which is substantially lower than the surroundings. In order to do this it is necessary to find a means of doing something to a material which will drop its temperature. There are various things which can be done, however, by far the most significant temperature changes can be achieved over a wide range of temperatures by allowing a gas to expand.

The first law of thermodynamics tells us that for an isolated gas mass the heat transfer to the gas δQ will be equal to the sum of the change in internal energy $d U$ plus the work done by the gas δW.

$$\delta Q = d u + \delta W$$

Since gases are very compressible, a large amount of work may be performed on them or by them. If this is done with no heat transfer δQ the result will be large changes in the internal energy $d U$.

$$\delta W = -d U$$

or large changes in temperatures

$$\delta W = C_v d T$$

Where C_v = constant volume specific heat.

It may be shown that for a reversible adiabatic expansion (such an expansion is also called isentropic), without heat transfer the final temperature T_2 will be

$$T_2 = T_1\left(\frac{P_2}{P_1}\right)^{\frac{\gamma - 1}{\gamma}}$$

Where

T_1 = Initial temperature

P_1 = Initial pressure

P_2 = Final pressure

γ = Ratio of specific heats $\frac{C_p}{C_v}$

1.666 for helium gas

A drop in pressure to one fifth the initial pressure will drop the temperature to .525 the initial value T_1 or give a temperature drop of 242°F from room temperature. This obviously is a means by which refrigeration may be obtained in substantial quantities and overlarge temperature differences.

Temperature drops may also be achieved in rubber by compression and expansion. However, the effect is small. Also, work may be carried out and temperature changes reduced by magnetization of paramagnetic salts. Here also the effect is small except at very low temperatures where heat capacities are tiny, so that though work is small the temperature changes are a large part of the total temperature.

$$\Delta W = -C_v \quad \Delta T$$

A gas can expand without doing work through a valve and this will give no change in temperature for an ideal gas. However, if the gas is sufficiently dense during

this expansion it will do work on intermolecular forces and cool. This is a positive Joule-Thomson effect and it can and has been used to achieve low temperature refrigeration. The temperature drops achieved depend of course on the pressures and the temperature at which the expansion occurs. The effect is very large for temperatures just above the critical point for the gas used and diminishes as the temperature is increased, finally it reverses at a sufficiently large temperature. This reversal occurs at about 30°K for helium, about 100°K for hydrogen, and well above room temperature for air or nitrogen. Thus the Joule-Thomson effect may be used for refrigeration from room temperature. Both helium and hydrogen require precooling.

1. THE HEAT EXCHANGE MEANS

We have seen that getting low temperature refrigeration will involve the manipulation of gases as that is the one means by which we may induce large temperature changes. However, the temperature changes are not enough for the low temperatures we are interested in (4 to 100°K). The temperature changes possible for three methods of gas expansion are summarized in the fcllowing table.

	Drop	Final Temp. from Room Temp. 300°K
Joule-Thomson	.05 to .20 T_1	285 to 240°K
Isentropic	.2 to .6 T_1	240 to 120°K
Semi-isentropic (Gifford-McMahon, etc.)	.2 to .33 T_1	240 to 200°K

A cryogenic refrigerator must have another important part - an efficient heat exchange means for precooling the gas to be expanded with the gas which has just expanded. Basically, the heat exchange means, which can be a counter flow heat exchanger or a thermal regenerator, does not produce any cooling effect. It simply

provides for gas expansion to occur at a low temperature and keeps the loss of the refrigeration, produced by the gas expansion, to a tolerably low level.

The function of the heat exchange means is shown by considering the simplest basic cryogenic refrigeration system shown schematically in Figure 1. It is composed of an expansion engine, a counter flow heat exchanger, a compressor, an after cooler, and a means of absorbing a heat load Q. A temperature plot for the heat exchanger and expansion engine system is shown in Figure 2.

The load is assumed to be at $50^{\circ}K$. The gas must expand from $60^{\circ}K$ to $30^{\circ}K$ because of $10^{\circ}K$ ΔT of the heat exchanger. The heat load is absorbed by the gas in warming up from $30^{\circ}K$ to the $50^{\circ}K$. Thus only 2/3 of the refrigeration produced is used absorbing the load. The other 1/3 is lost due to the heat exchanger ΔT of $10^{\circ}K$.

It is interesting to note that as is always the case with cryogenic refrigeration, the heat exchanged in the heat exchanger is much larger than the refrigeration produced. The heat exchanged in the heat exchanger Q_1

$$Q_1 = \dot{m} C_p (T_1 - T_2)$$

where $\dot{m}$ = mass flow

C_p = specific heat at constant pressure

$$Q_1 = \dot{m} C_p \, 240$$

The refrigeration produced Q_e

$$Q_e = \dot{m} C_p (T_2 - T_3)$$

$$= \dot{m} C_p \, 30$$

Thus eight times as much heat is exchanged as is refrigeration achieved by the expansion.

It is intersting to note that if the heat exchanger ΔT were $30^{\circ}K$ no refrigeration would be available. A heat exchange means inefficiency I_e is defined the ratio of ΔT to temperatures at either end of the heat exchange means.

$$I_e = \frac{\Delta T}{T_1 - T_4}$$

The inefficiency as shown would be only $\frac{10}{250} = 4\%$. An inefficiency of 12% would result in no available refrigeration. It can be seen readily from this that for good performance in cryogenic refrigerators, highly efficient heat exchange means are required. Efficiencies of 97% or better are really needed because, without this, other losses will result in very poor overall refrigerator efficiencies.

Achieving such an efficiency in small devices is not a simple matter. Two gas streams must run physically separated by walls while in very intimate thermal contact throughout the length of the heat exchanger. If the efficiency is to be 97% or greater, and the length only 10-12 inches, the gas passages must be of the order of .020 to .080". This is necessary in order to get sufficiently high heat transfer coefficients h and areas A to achieve the needed degree of efficiency. At the same time the counterflowing stream passages must be intermingled. Such devices are not easy to devise and build. Conduction through the metal of the heat exchanger must be high between the two gas streams and low from end to end.

A thermal regenerator serves the same function as the counterflow heat exchanger in a different way. In its case the gas flows in for a period and then out for a similar period. In a regenerator the heat is not transferred continuously from in-flowing gas to out-flowing gas. Rather, the heat flows from

the gas on its way in to find a solid matrix material in the regenerator and is stored there. Then, later on its way out it picks up the heat again.

It serves the same purpose though in that it allows a gas to flow in from room temperature, be cooled to almost any low temperature by storing heat in the regenerator at a continuum of temperatures, expand at the low temperature giving refrigeration, exhaust through the regenerator picking up the heat previously stored so that its temperature is only a small ΔT cooler than it entered. In this way only a small part of the refrigeration produced by the expansion of the gas at the low temperature might be lost.

It has many practical advantages over heat exchangers.

1. For same size the efficiency can be made much better than heat exchangers.
2. They are very simple and therefore not costly to build.
3. They are very insensitive to impurities. Small amounts of oil and water vapors do not cause plugging.

Any cryogenic refrigeration system consists of a means of compressing a gas at room temperature and dissipating the heat generated

$$Q_c = \dot{m} C_p T_1 \left[\left(\frac{P_h}{P}\right)^{\frac{\gamma - 1}{\gamma}} - 1 \right]$$

where

$\dot{m}$ = mass flow rate

C_p = constant pressure specified heat

T_1 = temperature of compression

$\gamma = \frac{C_p}{C_v}$

Then gas after cooling in a heat exchange means is allowed to expand with a resultant refrigeration temperature drop T_r. This makes refrigeration available at a low temperature equal to

$$Q_r = \dot{m} C_p T_r$$

A part Q_T of this ideally available refrigeration is lost due to the inefficiency I_e of the heat exchange means.

$$Q_T = \dot{m} C_p I_e (T_1 - T_r)$$

where

T_r = temperature of refrigeration

In a broad sense all the gas refrigeration processes achieve their refrigeration in this way. It is true for the Stirling Cycle, Brayton Cycle, turbine systems, expansion engines, and even the Gifford-McMahon Cycle, Cryomatic Gas Bal cing and Pulse Tube Refrigeration.

The means by which they achieve expansion and compression may be complex and novel. However, effectively it is true. A Joule-Thomson system is a special case which will be treated elsewhere.

2. MULTI-STAGING CRYOGENIC REFRIGERATION SYSTEMS

In all gas expansion cryogenic refrigeration methods the temperature drop giving refrigeration is directly proportional to the temperature from which the gas is expanded. Therefore, the amount of refrigeration available per unit mass of gas is roughly proportional to the temperature at which the gas expands. Since it is all compressed at room temperature the amount of work required in the

compressor per unit of heat removed $\frac{W}{Q}$ is roughly inversely proportional to the temperature. Some examples of exact functions are

$$\frac{W}{Q} = \frac{T_h - T_c}{T_c}$$

for the Carnot Cycle and

$$\frac{W}{Q} = \left[\frac{T_h}{T_c}\left(\frac{P_h}{P_\ell}\right)^{\frac{\gamma-1}{\gamma}} - 1\right]$$

for the Brayton Cycle

where

T_h = High temperature of compression

T_c = Temperature of expansion

P_h = High pressure

P_ℓ = Low pressure

From this it may be seen readily that it is advantageous to do the expansion at as high a temperature as possible and thus reduce the work required.

Most low temperature applications for refrigeration have two or more needs for heat removal. At least one of these may be taken at a temperature higher than the lowest one with a resultant decrease in work requirement. For example, in any problem there are heat leaks into the cold region by thermal radiation. This may put a larger heat removal load on the refrigerator than the main item to be cooled. This thermal radiation heat leak will be almost the same from 300°K to 20°K. Removal of this heat load at 80°K with a stage of refrigeration will reduce the compressor's

work requirement to about one quarter. Similar examples may be cited for conduction heat leak.

Another reason for multi-staging is to reduce the efficiency required of heat exchangers or regenerators. If a heat exchanger is to operate between 300°K and 10°K, and have a ΔT of 3°K in order that even the most efficient expansion device would give available refrigeration, it would have to have an efficiency of 99%..... an almost impossible construction job. If it operated from 70°K, only an efficiency of 95% would be needed, an easy construction job.

III. CRYOMATIC GAS BALANCING (THE GIFFORD-McMAHON CYCLE)

1. GENERAL THEORY

Cryomatic gas balancing is a preferred method of achieving the Gifford-McMahon Cycle. A considerable part of its merit lies in the simplicity of components which are required. In addition to simplicity, the components promise very high reliability which is an essential feature required of many cryogenic refrigerators.

Some individuals have questioned whether the Gifford-McMahon cycle is a new cycle or not.

This can best be answered by considering the definition for a cycle. A cycle is defined as follows[1]: "When a system in a given state, and the system can be a mass of gas, goes through a number of different processes and finally returns to its initial state, the system has undergone a cycle." In the Gifford-McMahon Cycle all the gas does not proceed through the same series of processes. Here each little batch of gas goes through a different series of processes but does return to the initial state. The net result is the sum of the actions of all the different batches of gas which act similarly but differently and return to the same initial state. Since the definition of a cycle does not preclude this possibility, the Gifford-McMahon Cycle may legitimately be called a cycle.

It is different from most cycles in the way in which it was devised. Most cycles were devised by planning a series of processes for a gas mass by which refrigeration or power might be generated efficiently. These can be worked out before any consideration is given to the equipment with which the gas will be caused to pass through these processes. For the Gifford-McMahon Cycle, the procedure was just the opposite. The operation of some simple equipment was devised which gave a very significant refrigeration effect and had many practical advantages. At a much later date the series of processes (the cycle) which the gas passes through in such equipment was worked out and described. It is very unlikely that

one would go from the cycle diagrams for the Gifford-McMahon Cycle to the equipment. The series of processes when seen on a TS diagram are so complex that one would question the reason for them unless one thinks of the equipment with which it would be carried out.

The fact that many little segments of the operating gas act differently causes a problem when an attempt is made to describe it thermodynamically, such as by plotting it on a Temperature-Entropy diagram. The processes followed by systems operating on other cycles, such as turbines operating on the Brayton cycle, can be described by a single line on a T-S diagram. A single area is enclosed and the areas under lines have special significance. The Gifford-McMahon Cycle, however, involves a continuum of lines, thus giving areas which overlap. To get a clear idea of the cycle through reference to a T-S diagram it is necessary to plot several different T-S diagrams for a selection of different batches of gas which show the different processes which are occurring.

The reasons for the Gifford-McMahon Cycle being useful are of a practical nature, such as simplicity, reliability and ease of construction. There is, however, a small sacrifice in efficiency compared to more ideal systems. It is interesting that in making the constructional details simple, as compared to the Stirling cycle devices, one makes the thermodynamic analysis aspects more complex.

In order to make an analysis of the Gifford-McMahon Cycle it is necessary to have a model to refer to as we show the processes followed by different batches of gas. This is shown by the schematic diagram, Figure 6., for the new method, Cryomatic Gas Balancing[2], which applies the Gifford-McMahon Cycle with a minimum of device complexity. The method achieves refrigeration in a system composed of a volume divided into several chambers by a free-floating displacer. Motion of the displacer is caused by the unbalance of pressures in these chambers resulting from the delivery and exhaustion of gas through the simple rotary cored valve.

As is shown, the closed volume created by the two coaxial cylinders of different size is divided into three variable chambers by the free-floating displacer. The size of each chamber depends on the position of the displacer. Chamber (2) at the intersection of the two cylinders and Chamber (3) at the end of the large cylinder are interconnected by a small, highly efficient thermal regenerator of small pressure drop so that both of these chambers are always maintained at approximately equal pressure. A suitable seal separates Chamber (1) from Chamber (2) so that the pressure in Chamber (1) can be different from that in Chambers (2) and (3). A rotary cored valve is used to raise the pressure by delivering high pressure gas from a compressor, or to lower the pressure by exhausting to the low pressure line from either Chamber (1) or Chambers (2) and (3). The timing between pressurizing and depressurizing the chambers may be set by the location of the parts connecting the chambers with the valve.

At the beginning of the series of operations, the displacer is in its topmost position so that the volumes of Chambers (1) and (2) are zero and Chamber (3) is at a maximum volume, with the rotating valve reference X at 11:00 o'clock. Low pressure is in all three chambers since the low pressure slot is opposite both connecting tubes.

When the valve rotates counterclockwise so that reference X passes 9:00 o'clock, it allows high pressure gas to be delivered to Chamber (1) only, forcing the displacer to move to the bottom position. Gas is transported from Chamber (3) to Chamber (2). If Chamber (3) is colder, some gas will be exhausted through the valve as a result of expansion back to the inlet temperature.

When the rotating valve (reference X) passes 6:00 o'clock, high pressure gas is let into Chambers (2) and (3). This builds the pressure there to the high pressure while the high pressure is still maintained in Chamber (1). The displacer does not move.

When the rotating valve (reference X) passes 3:00 o'clock the pressure drops in Chamber (1) because of the movement of the low pressure cored slot to a position in register with the Chamber (1) connecting tube. This causes an unbalance of pressure on the displacer so that it moves to its topmost position transferring the gas in Chamber (2) at a constant high pressure to Chamber (3). If Chamber (3) is colder, as it will be in operation, additional high pressure gas will be supplied through the valve during this transfer.

When the rotating valve (reference X) passes 12:00 o'clock, it allows the pressure in Chambers (2) and (3) to drop to a low value because the low pressure cored slot in the valve is now opposite the Chamber (2) and (3) connecting tubes. Chamber (1) retains its low pressure as the low pressure slot is still opposite its connecting tube, so this process takes place without the displacer moving. This completes the series of operations which is repeated with each revolution of the valve.

The general nature of the cycle may be shown on a T-S diagram by following what happens to a small part of the gas involved. In Figure 8 is shown a T-S diagram for the first gas to enter the refrigerator which contributes to the refrigeration achieved. It enters the valve at room temperature, T_R, point 1, and expands through the valve isenthalpically to very nearly the low pressure, P_ℓ, point 2. It is then transferred into Chamber (2) with only a slight pressure increase. There it is compressed back to the high pressure, P_h, point 3, by the addition of more gas.

In the act of being transferred out of Chamber (2) when the displacer moves up it will be mixed with additional gas from the supply and comes to a lower temperature, T_c, point 4. It is then cooled in the regenerator to the cryogenic temperature, T_R, point 5.

After Chamber (3) has reached its maximum volume the valve next allows this

cold high pressure gas to be exhausted. The expansion before it leaves Chamber (3) allows it to drop slightly in temperature to 6, giving the refrigeration effect, before being heated again in the regenerator to 7 and passing through the valve expanding isenthalpically to the low pressure, point 8, at a temperature close to that of the mixing temperature. Compression and cooling to pass from 8 to 1 is not shown on the diagram as it would obscure the clarity of the other lines. The complete cycle, of course, involves this also.

It is to be remembered that this only represents the action for the first small fraction of gas to enter the refrigerator. Every other small fraction of gas will have different diagrams. For example, gas that enters the refrigerator after the pressure is about half way up will follow the diagram of Figure 9 where numbers have the same significance as in Figure 8 . All of the gas that is added at the high pressure during the period when the displacer is moving up does not proceed through the processes 1 to 4 but mixes directly with the initial pressurizing gas, proceeding from point 1 directly to point 4. A complete set of lines for all segments of the gas involved would give many overlapping areas. It thus is a very difficult cycle to put on a T-S diagram.

The diagrams of Figure 8 and 9 , do, however, represent the nature of the cycle for the gas masses which achieve the refrigeration. They are not very similar to the Stirling cycle but do enclose an area as any power or refrigeration cycle must. It can be noticed that they have added features not at all included in the Stirling cycle.

The reason one prepares any diagram showing any functional relationship, series of operations, or a cycle, is for the purpose of making it more understandable by a simple direct picture. A T-S diagram is selected for many cycles because it makes it possible to see clearly the overall operation quickly and simply including pictorially the heat and work quantities involved. A T-S diagram

does not accomplish this for the Gifford-McMahon cycle. It makes the cycle more obscure by presenting a rather difficult intellectual problem. Therefore, there is really no good reason for attempting to put it on a T-S diagram. It is rather like solving a heat transfer problem, involving a rectangular block, in spherical coordinates.

The best method for computing the performance of the Gifford-McMahon cycle has been shown in previous papers[3], [4], [5] by consideration of what is going on in the chambers in an overall way, rather than integrating the effects of all the different batches of gas with varying actions.

It has been shown that the total refrigeration, Q, is

$$Q = \oint VdP = \oint PdV$$

for the expansion space or

$$Q = V(P_h - P_\ell) \tag{1}$$

where V is the volume of Chamber (3), P_h the high pressure, and P_ℓ the low pressure.

In the analysis of a refrigeration cycle, the desired result is an ability to compute the ideal performance of a proposed system and then also show how each factor which detracts from this ideal performance affects the total performance. For a refrigerator the thing you want to know is how much work, W, at room temperature, T_R, is required to remove an amount of heat, Q, at a low temperature T_r.

The work required to compress a given mass of gas, m, in an adiabatic process is

$$W = mC_pT_R\left[(P_h/P_\ell)^{(\gamma-1)/\gamma} - 1\right] \tag{2}$$

where C_p is the specific heat of the gas at constant pressure; γ is the ratio of specific heats, and T_R is the temperature of the gas entering the compressor.

The mass of gas used in the Gifford-McMahon cycle would be the difference between the mass of gas in Chamber (3), m_3, at the low temperature T_r and high pressure P_h, and the mass of gas in Chamber (2) at temperature T_c, and at the low pressure P_ℓ. In an actual system the volume of Chamber (1) is small relative to Chamber (2) and little accuracy is lost if it is assumed to be so small that Chamber (2) is equal in volume to Chamber (3).

$$m = m_3 - m_2 \tag{3}$$

Assuming the perfect gas relation is valid,

$$m = \frac{P_h V_3}{RT_r} - \frac{P_\ell V_2}{RT_c} \tag{4}$$

where R is the gas constant.

The work per cycle is thus

$$W = C_p T_r \left(\frac{P_h V_3}{RT_r} - \frac{P_\ell V_2}{RT_c}\right) \left[\left(\frac{P_h}{P_\ell}\right)^{(\gamma-1)/\gamma} - 1\right] \tag{5}$$

Dividing Equation (5) by (1)

$$\frac{W}{Q} = \frac{C_p T_R \left[(P_h V_3/RT_r - P_\ell V_2/RT_c)\right]\left[(P_h/P_\ell)^{(\gamma-1)/\gamma} - 1\right]}{V_3(P_h - P_\ell)} \tag{6}$$

The assumption that Chamber (2) is equal to Chamber (3) and that $T_R/T_c \simeq 1$ allows the relation to simplify to

$$\frac{W}{Q} = \frac{C_p\left[(P_h/P_\ell)(T_R/T_r) - 1\right]\left[(P_h/P_\ell)^{(\gamma-1)/\gamma} - 1\right]}{R(P_h/P_\ell - 1)} \tag{7}$$

It is interesting to note that the work per unit heat removed at a low temperature, W/Q, increases as the temperature ratio increases, just as it does for Brayton cycle refrigerators. For T_R of 300°K and T_r of 80°K, Figure 10 shows a plot of W/Q as a function of pressure ratio from Equation (7) assuming helium is the refrigerant. Also shown on the same plot is the relationship for the Carnot cycle and the Brayton cycle, with and without work recovery. The relation for the Carnot cycle is well known as

$$\frac{W}{Q} = \frac{(T_R - T_r)}{T_r} \tag{8}$$

and the relation for the Brayton cycle is

$$\frac{W}{Q} = [(T_R/T_r)(P_h/P_\ell)^{(\gamma-1)/\gamma} - 1] \tag{9}$$

The Brayton cycle is really the ideal cycle for the refrigerators that are said to be Stirling cycle refrigerators. The Stirling cycle calls for isothermal compression and expansion, and the Brayton cycle isentropic compression and expansion. The .01 second allowed for compression and expansion in the Stirling cycle devices does not give time for the transfer of an appreciable amount of heat during these processes. It is not sufficient to cool after compression. To achieve Stirling cycle efficiency the cooling must occur during the compression.

The Brayton cycle is also the ideal cycle of small expansion engine or turbine refrigerators, if the work of the expansion device is not recovered. If not, the ratio of W/Q is given by Equation (9) with the one deleted.

The Gifford-McMahon cycle as seen from the curves requires more work for a given amount of refrigeration than the Brayton cycle. However, the difference is not great for small compression ratios which is the way any refrigerator designed to use these cycles should be operated. A Gifford-McMahon cycle at a pressure ratio of 2 is about equivalent to a Brayton cycle at a pressure ratio of 3.5.

Gifford-McMahon cycle devices work very well with pressure ratios of 1.5 to 2.5. There is no need to go to higher pressure ratios and thus poorer efficiencies. The Gifford-McMahon cycle does sacrifice some potential efficiency for its many practical advantages; this sacrifice, however, is not very great.

2. CRYOMATIC GAS BALANCING MODEL RESULTS AND POTENTIAL

The Cryomatic Gas Balancing refrigerator is quite an easy device to build, as it involves only two slow-moving parts. Operating speed is only about 50 to 150 cycles per minute. It can make an excellent refrigerator. Temperatures as low as 23°K have been reached in Chamber (3) with a $1\frac{1}{4}$" diameter displacer operating at 120 RPM.

It is relatively simple to make a multi-stage unit (Figure 7) where refrigeration is developed at two different low temperatures. Only one additional moving part, the displacer, and an additional thermal regenerator is required. Several such machines have been built which achieve temperatures as low as 12°K. An actual two-stage experimental refrigerator of this type is shown in Figure 11. It has 4 watts refrigeration capacity at 16°K and 18 watts at 50°K and has served as the base for a 4.2°K refrigerator which achieved .7 watts at 4.2°K.

The practical advantages, as have been described in previous papers, [3],[4],[5] are numerous. They all should lead to high reliability because the basic equipment components are simple, slow-moving, and not highly stressed components. This is especially true for the new method, Cryomatic Gas Balancing [2] which applies the Gifford-McMahon cycle with only two slow-moving parts. The gas seal on the displacer moves at a rate of 2 to 5 inches per second rather than 30 to 50 inches per second as in some small cryogenic refrigerators. This should make continuous operating times of 5,000 to 10,000 hours a high probability.

An added advantage of the new method is the relative simplicity with which a different model of new capacity may be developed. There are only a few basic parts which are all relatively easy to construct so that prototype model development costs may be greatly reduced.

3. GAS BALANCING THERMAL LOSS ANALYSIS

In a previous section a ratio of compressor work W to heat removed Q at a low temperature was derived assuming ideal no loss perfect operation. As with any actual refrigerator, there will be many causes for losses. The most significant ones are the following:

1. Expansion efficiency.
2. Loss due to ΔT of regenerator.
3. Loss due to pressure drop through the regenerator.
4. Loss due to end to heat leak along the displacer.
5. Loss due to gas requirement to fill regenerator which gives no refrigeration.

It would be an advantage to compute a performance efficiency for each of these effects so that an actual $\left(\frac{W}{Q}\right)_a$ could be computed from the ideal one $\left(\frac{W}{Q}\right)_a$ of equation (7) divided by all the various efficiencies.

$$\left(\frac{W}{Q}\right)_a \left(\frac{W}{Q}\right)_i \quad \frac{1}{E_e \, E_{\Delta T} \, E_p \, E_M \, E_V}$$

Where

E_e = Expansion space efficiency

$E_{\Delta T}$ = Heat exchange system efficiency

$E_{\Delta p}$ = An efficiency taking into account Δp losses

E_M = An efficiency taking account of motional heat leak

E_V = An efficiency taking into account excess volume in the system.

Each of the E's may be a function of the system parameters and other E's for that matter. A derivation of the functional relations for these E's follows:

1. The expansion space efficiency E_e will probably be quite as we are including the losses usually included in expansion engine efficiencies elsewhere. It probably should be about .95.

2. The efficiency due to ΔT of the regenerator may be computed from calculating what fraction of refrigeration available is not lost due to the ΔT of the regenerator.

The refrigeration available from the expansion space would be

$$Q_e = E_e V (P_h - P_l)$$

The loss due to regenerator inefficiency I_e will

$$Q_{\Delta T} = I_e (T_R - T_r)$$

Therefore

$$E_{\Delta T} = \frac{E_e V (P_h - P_l) - I_e (T_R - T_r)}{E_e V (P_h - P_l)}$$

$$E_{\Delta T} = 1 - \frac{I_e (T_R - T_r)}{E_e V (P_h - P_l)}$$

$$P_h V = R T_r$$

$$E_{\Delta T} = 1 - \frac{C_p I_e (T_R - T_r)}{\frac{E_e R T_r}{P_h} (P_h - P_l)}$$

$$E_{\Delta T} = 1 - \frac{I_e \left[\frac{T_R}{T_r} - 1\right]}{\frac{E_e R}{C_p} \left[1 - \frac{P_l}{P_h}\right]}$$

It is interesting to note that this heat exchange efficiency of the system is a function of temperatures, pressures, expansion space efficiency, E_e and inefficiency of the regenerator. It is not to be confused with the regenerator efficiency $(1 - I_e)$. A regenerator inefficiency of 1% can cause $E_{\Delta T}$ to be 60% or even lower.

3. The efficiency caused by pressure drop losses $E_{\Delta p}$ will be the ratio of the refrigeration with Δp losses to that under ideal conditions with no losses.

4. E_m is the motional heat leak efficiency. It is the biggest, heat leak into small refrigerators of this type. It is due to reciprocating motion of two surfaces with steep temperature gradients in them. The effect may be understood by reference to Figure 5. The temperature of the displacer and cylinder will only be the same for the displacer half way down. When it is at the top it will be everywhere colder than the cylinder and heat will be transferred from the cylinder to the displacer.

At the bottom the displacer will be hotter and heat will be transferred from the displacer to the cylinder.

In the center, heat will be transferred back and forth between the displacer and the cylinder. Each transfer, however, will pass the heat one stroke S further down the cylinder. The net heat reaching bottom can be computed from conduction across gas layer when displacer is at the bottom.

$$Q_m = \frac{E\ k\ A\ \Delta T}{L}$$

Where

k = Thermal conductivity of the gas

A = Surface area = $S\pi D$

ΔT_o = Temperature difference built up at bottom

$$= \frac{(T_R - T_r)\ S}{2L_g}$$

L = Thickness of gas layer t

E = Amount of time of displacer with maximum ΔT_o

= to approximately 1/3

$$Q_m = \frac{k\ S\pi D\ (T_R - T_r)\ S}{3\ t_g\ 2L_g}$$

$$Q_m = \frac{k\pi S^2 D\ (T_R - T_S)}{6\ t_g\ L_g}$$

The E_m will be the ratio of ideal refrigeration available minus Q_m to ideal refrigeration

$$E_m = \frac{N\ \forall\ (P_h - P_l) - \frac{k\pi S^2 D\ (T_R - T_r)}{6\ t_g\ L_g}}{N\ \forall\ (P_h - P_l)}$$

$$E_m = 1 - \frac{k\ \pi S^2 \not{D}\ (T_R - T_r)\ 4}{6 t_g\ L_g\ \ \pi\ \not{D}^2\ S}$$

$$E_m = 1 - \frac{2\ k\ S\ (T_R - T_r)}{3 t_g\ L_g\ D\ N\ (P_h - P_l)}$$

5. The E_v can be computed by taking ratio of gas required to operate expansion space to this gas plus the gas required to raise and lower the pressure in the regenerator.

$$E_v = \frac{\frac{V_e P_h}{T_r}}{\frac{V_e P_h}{T_r} + \frac{V_R (P_h - P_l)}{T_\alpha}}$$

Where

T_α = Average temperature in regenerator.

$$E_V = \frac{1}{1 + \frac{V_r T_r (P_h - P_l)}{V_e T_\alpha P_h}}$$

4. EXPERIMENTAL APPARATUS

The gas balancing test refrigerator is a single stage cryogenic refrigerator designed to provide the data needed to evaluate its performance. The test refrigerator used and the test setup are shown in Figures 12 and 13.

The refrigerator's instrumentation consisted of two pressure transducers, one connected to the expansion chamber and the second to the top of the regenerator, a displacement transducer connected to the displacer, and six thermocouples. A regenerator insert was also provided to facilitate easy removal of regenerators for regenerator performance tests.

To ascertain the refrigerator's performance a PV diagram for the expansion chamber was established by connecting the first transducer to the vertical input of an oscilloscope and the displacement transducer to the horizontal input of the oxcilloscope. The area inscribed by the PV diagram thus gave the available refrigeration produced by the unit. The actual refrigeration produced was measured by the electrical heater mounted to the heat exchanger. The temperature at which the refrigeration was available was recorded by a thermocouple.

The effect of regenerator length; using 150 mesh bronze screens, on the performance of the unit was found by varying the regenerator's length and recording the heat load at a given refrigeration temperature.

Calculations

a. Maximum available refrigeration

$$W = NV\Delta P$$

V = volume = $8.275 \times 10^{-4} ft^3$

$\Delta P = (P_h - P_L = 385 - 150 = 235 \text{ psi} = 3.381 \times 10^4 \frac{LB_f}{Ft^2}$

N = Piston speed = 140 rpm

$W = 88.6$ watts

b. Actual available refrigeration

$W = (82\%)(88.6)$ watts $= 72.5$ watts

c. Heat added

$$Q_a = \frac{V^2}{R} = \frac{(95)^2}{204} = 44.2$$

d. Heat losses

$$Q_L = (72.5 - 44.2) \text{ watts} = 28.3 \text{ watts}$$

e. Efficiency

$$n = \frac{44.2}{72.5} = 61\%$$

f. Regenerator losses

$$Q_R = (2\dot{m})C_p\Delta T = I_e(2\dot{m})C_p(T_h - T_c)$$

$$C_p = 1.25 \frac{Btu}{LB_m\,^\circ R}$$

$$(T_h - T_c) = (300°K - 82°K) = 218°K = 392°R$$

$$\dot{m} = N \frac{PV}{RT}$$

$$N = \text{piston speed} = 140 \text{ rpm}$$

$$P = (240 + 14.7)\text{psia} = 3.67 \times 10^4 \frac{LB_f}{Ft^2}$$

$$V = 8.275 \times 10^{-4} \text{ ft}^3$$

$$R = 386.0 \frac{Ft\text{-}LB_f}{LB_m °R}$$

$$T = 82°K - 148°R$$

The mass flow is

$$\dot{m} = 0.0744 \frac{LB_m}{min}$$

and

$$Q_R = I_e(1281)\text{watts}$$

From regenerator inefficiency tests, I_c was found to be 1% for 150 mesh bronze screens and a 10 SCFM flow rate. This gives

$$Q_R = 12.81 \text{ watts}$$

g. Motional heat leak

$$Q_m = \frac{k_g \pi D S^2 C_t \ (T_{h_w} - T_c)}{2L \ t_g}$$

$S = .0775$ ft

$D = .125$ ft

$(T_{h_w} - T_c) = 461°R$ (Temp. difference recorded by thermocouples 3 and 6 Fig. 38.)

$L = .544$ ft

$t_g = .005$ ft

$k_g = .06 \frac{Btu}{hr\ ft°F}$ @82°K

$C_T = 1/3$

and

$Q_m = 14.8$ watts

h. Calculated losses

$Q_L = 14.8$ watts + 12.81 watts = 27.61 watts

5. RESULTS

At the present level of development, the gas balancing refrigerator can achieve an efficiency of 61%. This efficiency was obtained for the operating conditions:

P_h = 385 psig

P_L = 150 psig

N = 140 RPM

T_c = 82°K

Reg. length = 3.5 in., 150 mesh bronze screens

A displacer speed of 140 was selected for these performance tests because, as shown in Figure 15, the available refrigeration reached its maximum value in this region. Under these operating conditions the PV diagram shown in Figure 14 was recorded, and from the diagram the available refrigeration was calculated at 72.5 watts. The applied heat load was 44.2 watts resulting in losses amounting to 28.3 watts. These losses, however, can be accounted for by the regenerator thermal loss and the motional heat leak loss.

Previous regenerator tests showed that for a flow rate of 10 SCFM, the regenerator inefficiency is 1%. A 1% regenerator inefficiency for this unit results in a thermal loss of 12.8 watts. From motional heat leak theory, the calculated motional heat leak is 14.8 watts. This gives a total calculated heat loss of 27.6 watts as compared to the measured loss of 28.3 watts.

Heat Load--Regenerator Length Characteristics

Speed (RPM)	Mesh	Reg. Length (in.)	Temp. °K	Heat Load (watts)
140	150	3.5	82	44
140	150	5.0	82	39

This table gives the heat loads recorded for a 150 mesh regenerator 3.5 in. long and a 150 mesh regenerator 5 in. long. The increase in refrigeration for the

3.5 in. regenerator can be attributed to the increase in the inscribed area of the PV diagram. The 5 in. regenerator caused an increase in the pressure drop across the regenerator. Thus as the piston moves down, expelling the gas, it experiences a larger upward force due to the pressure increase in the expansion chamber. The decrease in the PV area is shown by the short dashed line in Figure 14.

Figure 15 shows that both the available refrigeration and the refrigeration temperature, recorded by thermocouple number and located at the base of the heat exchanger, Figure 13, attain optimum values in the neighborhood of 140 RPM. The available refrigeration curve was found by applying to the unit, at each piston speed setting, a heat load that would maintain thermocouple number 2 at 82°K. At each speed setting the available refrigeration was calculated from the inscribed area of the recorded PV diagram. The temperature variation curve was found by applying a constant heat load, 44.2 watts, to the system and then recording the temperature of thermocouple number 2 at each piston speed setting.

Theoretically, the temperature should continue to decrease and the available refrigeration should continue to increase as the piston speed is raised above 140 RPM. For the available refrigeration this is readily apparent from Equation (10) which shows that W is directly proportional to the N. This increase in W, with the heat load, Q_c, held constant, also makes available more cooling in the gas passing from the heat exchanger to the regenerator. Thus the cold end of the regenerator will become colder, and in turn lower the temperature sensed by thermocouple number 2. However, to achieve this ideal operation would require a gas having no viscosity, and a friction free piston seal assembly. Since neither is possible, time lags present in the piston motion and the expansion chamber pressurization and depressurization processes reduce the available refrigeration above 140 RPM. In Figure 16a, the ideal piston motion and pressure changes are represented by the square waves. Under this ideal operation there is no overlapping of the curves.

of the curves. That is, the step changes in each of the curves occur while the other curve remains at a constant value. The corresponding PV diagram for this square wave operation is given by the curve 1, 2, 4, 5, 1 in Figure 16b. The time lag, however, produces periods when both curves are changing magnitude at the same time, and the overlapping of the curves causes a rounding off of the corners of the PV diagram as shown by curve 1, 3, 4, 6, 1 in Figure 16b. As the piston speed is further increased, the overlapping becomes greater and the PV diagram takes the elliptical shape shown by curve 1,4,1 in Figure 16b.

These curves reveal that there is an optimum operating range for the gas balancing refrigerator, and they enabled an optimum speed to be selected for the thermal loss analysis presented in this section.

6. DISCUSSION

From this experimental investigation a more precise understanding of thermal losses in a gas balancing refrigerator was gained. These losses, as was shown, manifest themselves primarily in regenerator losses and motional heat leak. These two thermal losses contribute to a unit inefficiency of 39%.

The unit's inefficiency calculations were based on an inscribed PV area of 82% of the theoretical maximum area, and from the diagram the mass flow was calculated at .0744 Lb_m/min. Since only 82% of the theoretical diagram was achieved it would seem reasonable to expect that the best way to improve the unit's performance would be to increase the area of the PV diagram. By increasing the diagram to 100% of the theoretical diagram the available refrigeration would go up from 72.5 to 88.6 watts. However, a square diagram would mean that the expansion chamber has to be filled with gas at the high pressure instead of gas at some lower pressure. Thus the mass flow would increase to .1165 Lb_m min., resulting in thermal regenerator losses of 20.1 watts instead of 12.8 watts.

Because of the increase in the thermal regenerator losses the unit's efficiency

would not be improved. This shows that in order to improve the refrigerator's performance, investigations will have to be concentrated towards reducing the thermal losses.

IV. PULSE TUBE REFRIGERATION

The heat pumping mechanism of pulse tube refrigeration is not just found in the cylindrical pulse tubes that are currently being investigated, but also occurs in any other closed volume that is subject to a systematic pressurization and depressurization. In its more general form the heat pumping mechanism is called surface heat pumping

1. SURFACE HEAT PUMPING EFFECT

Surface heat pumping is caused by an unusual interaction between fluid displacement along a surface, energy change in the fluid, and heat exchange with the surface, as a result of a periodic change of pressure of the gas. The mechanism can best be visualized from consideration of the closed tubular model shown in Figure 17 A small element of gas at x' with temperature T_1' is displaced to X" as a result of pressurizing the tube by supplying gas from the left end. Also, as a result of pressurizing the element of gas there is an energy increase in the gas which produces a change in the temperature of the gas. It is possible that the element will be in thermal equilibrium with the wall but more likely the gas will be compressed along a polytropic path, or if the pressure change is fast enough so that essentially no heat is transferred from the element, then an isentropi path is followed, as shown by the dashed line in Figure 1, reaching a temperature of $T_1"$. If the pressure in the tu' e is now held constant, heat will flow from the gas to the wall, eventually cooling to T_2'. When gas is now allowed to flow out of the tube and the pressure reduced to its initial value the element will return to the vicinity of its initial position but will have a temperature $T_2"$ which is lower than T_1'. The cycle is completed by maintaining the pressure constant while heat flows from the gas to the wall, returning the temperature to T_1'.

The net effect of this cycle has been the removal of heat from the wall at X' and the depositing of that heat in the wall at X". This effect occurs throughout the tube and produces a heat pumping effect from the open end to the closed end.

While this effect occurs in any volume, there are several factors which enhance the effect. First, the flow should be smooth and uniform so that a regular and not a random pattern of heat pumping is established. Second, the heat exchange with the walls when the gas is at its extreme positions should be large relative to the heat that is exchanged while it is moving.

For the present it will be considered that there is no viscous drag from the surfaces so that the gas flowing back and forth in the volume shown in Figure 8 has a constant velocity across the cross section of the tube. If the pressure change occurs fast enough then heat transfer during the pressure change is negligible and the gas follows an isentropic path. The temperature is thus related to the pressure, P, according to the well known thermodynamic relation,

$$T'' = T'(P''/P')^{(\gamma-1)/\gamma} \tag{1}$$

in which a single prime denotes the initial condition and the double prime denotes the final condition.

The assumption of an isentropic process throughout the tube with uniform velocity across the cross section also permits the use of the relation between temperature and displacement.

$$T'' = T'(X'/X'')^{\gamma-1} \tag{2}$$

At any given point along the wall the temperature will assume some value between the temperature of the gas adjacent to it when the pressure is low and the temperature of the gas when the pressure is high. Heat will be exchanged

with the wall and pumped along the wall until the condition is reached that the gas temperature coincides with the wall temperature everywhere along the tube. If now the temperature at $X = X_o$ is held at T_o (Figure 17) and the temperatures in the rest of the tube are allowed to come to equilibrium with the gas, under the condition in which no heat is being pumped, then the temperature in the tube at X, T(x) will be

$$\frac{T(x)}{T_o} = \left(\frac{X_o}{X}\right)^{\gamma-1} \tag{3}$$

This action will occur for virtually any pressure change which causes a displacement of the gas in the tube. Small pressure ratios of 1.5 to 2.0 will cause the mechanism which will give the heat pumping action. As can be seen, the temperature changes built up in the walls depend on volume ratios in the tube. Therefore, the temperature differences it would be possible to build up in a tube would be very great relative to that defined by the pressure changes in Equation (1).

As the temperature pattern gets near to that defined by Equation (3) the temperature differences become smaller and smaller and the heat pumping action is greatly reduced. One might expect to approach this temperature pattern but in an actual tube there would be some conduction and heat exchange losses which would prevent one from actually reaching it.

Let us now see how the viscous drag of the tube surfaces will affect the heat pumping action. To visualize this best, let us consider our oscillating flow again in the same tube. Due to the fact that the walls cause a viscous drag on the gas, the flow will be slower at the walls and faster in the center when the pressure oscillations are instigated. As a result, the gas near the walls will not be displaced as far by the pressure oscillations as the gas in the center of the tube.

To see how this variation in gas displacement will affect the heat pumping phenomenon, let us assume the tube has the ideal temperature pattern in it defined by Equation (3) and shown in Figure 18. In such a case the gas that is displaced the average distance will not have a temperature difference which will cause a heat transfer with the walls. As this gas is displaced its temperature will coincide with that of the wall. Thus, this gas would have no tendency to create a heat pumping action.

The gas near the surfaces, however, will vary as much in temperature as the average gas but will not move so far. It will only be displaced from X_1' to X_1'', instead of the average displacement from X_2' to X_2'' as shown in Figure 2. As a result it will be hotter than the tube at X_1'' and colder at X_1'. It will, therefore, heat the tube at X_1'' with cooling of the gas and cool the tube at X_1' with heating of the gas. The net result is the transfer of heat from X_1' to X_1'' against a temperature gradient. This action is, of course, true for every section of the tube. There thus is a very positive heat pumping action at the surface even when the effect described, assuming no viscosity, is no longer possible.

At the center of the tube gas will be displaced farther than the average, between X_3' and X_3'' and will build up temperature differences with respect to the walls which would tend to pump heat in the opposite direction if there were heat transfer between this gas and the walls. However, the walls are not available to the central gas and thus its temperature will just rise and fall with the displacements in an essentially reversible manner.

2. PULSE TUBE REFRIGERATION CHARACTERISTICS

The basic mechanism which produces the heat pumping is initially a pressure change which builds a temperature pattern in the gas followed by heat transfer to the walls. This is followed by a decrease in pressure, building another tem-

perature pattern in the gas followed by heat transfer from the walls to the gas. The temperature patterns are such that heat received from the walls is transferred back to the wall at a point closer to the closed end giving the heat pumping effect.

The pressure changes may be made at any speed. Time, however, must be allowed for heat transfer from the gas to the wall. The time can be either too short so that very little of the heat is transferred to the walls, or so long that time is wasted when little or nothing is happening. There thus is an optimum or more or less ideal speed.

Determining the exact temperature changes in the gas with pressure, displacement, and heat transfer is very complex. However, due to a great similarity in problems of non-steady heat transfer from volumes, it is possible to deduce some fundamental characteristics about the optimum pulse rate for a round closed tube even though the exact time temperature pattern in the tube is now known.

If most of the heat is exchanged with the walls at a constant pressure, then the significant terms in the heat transfer equation are

$$\frac{\partial T^*}{\partial \tau^*} = \frac{\alpha}{ND^2}\,\alpha^*\Delta^2 T \qquad (4)$$

where the * superscript denotes the parameters which have been made dimensionless by the characteristic group α/ND^2. In this equation time, τ , is made dimensionless by the reciprocal of the pulse rate N, the incremental distance squared associated with the differential operator ∇^2 is made dimensionless by the diameter squared, D^2, and the thermal diffusivity α^* by a characteristic value of α . Equivalent performance will be obtained in a pulse tube if the value of the characteristic group, α/ND^2, is the same.

Different from sound, the length does not affect this optimum pulse rate. It does, however, indicate that any chamber where it is hoped the surface heat pumping would be a maximum should have a constant equivalent diameter so that

all of it can operate at the ideal pulse rate.

The fact there is an optimum speed which is quite small for large volumes is partially responsible for its not being noticed before. For example, a $1\frac{1}{2}$" tube would have an ideal speed of only about 8 pulses per minute, a rather uncommon frequency, and heat flow in such a case is very small per unit area. Therefore, not very large temperature differences would be built up to be noticed. There have probably been many unexplained hot spots in equipment involving gas under pressure where fluctuations occur which were due to this phenomenon.

Another interesting fact about the nature of the heat pumping phenomenon may be deduced from the simple picture of heat transfer to and from the gas. The <u>fraction</u> of the total gas in the tube which is effective in the heat transfer at a given value of α/ND^2 will be independent of tube diameter. Thus the refrigeration produced per cycle Q will be proportional to the diameter squared times the length, L,

$$Q = CD^2L \tag{5}$$

where C is the proportionality constant.

The net refrigeration rate, q, will be equal to the product of Q and n_o, the optimum pulse rate.

$$q = Qn_o \tag{6}$$

$$q = Cn_oD^2L \tag{7}$$

If operation is to be at the optimum value of the characteristic number, $C_o = (\alpha/ND^2)_o$, then

$$q = C\,\alpha\,L/C_o \tag{8}$$

This leads to the surprising conclusion that all tubes with equal total length and top length, but different diameters, produce the same amount of cooling if all the operating conditions are held the same except for the speed, which must be kept proportional to $1/D^2$. Thus, small diameter tubes operating at high speeds produce just as much cooling as large diameter tubes operating at low speeds.

3. TEST RESULTS

Figure 22 shows typical test results for a set of tests at the same operating condition with the heat load varied. The lower curve shows the relation between the applied heat load and the cold end temperature while the top curve shows the relation between the measured heat pumping rate and the cold end temperature.

Since radiation and conduction losses are negligible, the difference between the two curves is essentially the thermal loss in the regenerator. When both ends of the regenerator are at the same temperature, i.e., room temperature, then the regenerator losses are zero and the two curves intersect.

Extrapolating the test data to the condition for which the heat pumping rate is zero shows that the cold end temperature would be T_{co} as predicted by the model, Equation (3). All the test results substantiate this within reasonable limits. It is noted that the test points fall on straight lines. Since the heat pumping rate is proportional to the temperature difference between the gas and the walls it is to be expected that there would be a linear relationship between the cold end temperature and the heat pumping rate. The heat input data will also fall on a straight line because the regenerator thermal losses are directly proportional to the difference in temperature between the hot and cold end.

In order to see the relationship between the other variables more clearly the cooling capacity at a given cold end temperature is used to represent the entire curve. This is possible because all tubes with the same volume ratio have the same value of T_{co} and thus one point on the curve defines it if the hot end temperature is the same for all.

Figure 23 is a plot of the effect on cooling capacity of varying the pressure for pulse tube No. 25 operating at a speed of 40 RPM and a cold end temperature of $300^{\circ}R$. It shows that for a given pressure ratio the cooling capacity increases almost linearly with increasing pressure. If the high pressure is held constant and the low pressure decreased the cooling increases more rapidly at lower pressures.

Figure 24 shows the effect of changing the speed while holding the pressures constant for pulse tube No. 25 operating at a cold end temperature of $350^{\circ}R$. The cooling capacity increases linearly with speed at the very low speeds then approaches a maximum heat pumping rate assymptotically. If the pressure in the

tube reaches the high and low values in a square wave then the maximum amount of heat would be pumped even at very high speeds because heat is always flowing to the wall for half the time with the same initial temperature gradient. In actual practice pressure drop in the regenerator would prevent the pressures from changing completely and the cooling capacity would fall off at high speeds.

Figure 25 shows a comparison of three pulse tubes with the same top length and diameter but different total lengths having volume ratios of .10, .15 and .20. When operating at the same speed and pressures with the top at room temperature, it is seen that for each tube the curve through the test points extrapolates to the value of T_{co} for each tube as predicted by Equation (3). It is also interesting to note that the three curves are almost parallel. This is probably explained by the fact that the same mass of gas is pushed into the top of the tube with each pulse, and the temperature change in the gas is proportional to the difference in temperature between the hot and cold end of the tube. The higher heat pumping rate of the longer tubes is probably due to the fact that the gas is preheated to a higher temperature before entering the top in the longer tubes.

Figure 26 is the test correlation for test code 2 which confirms the fact that the heat pumping rate is directly proportional to length of the tube, everything else being equal. Test results for three tubes of different lengths with volume ratios of .15, diameter of 3/4" amd operating at the same conditions show that all of the data falls on a common line when the heat pumping rate/length is plotted against the cold end temperature.

The test results for test code 1 are shown in Figure 27. This is a plot of heat pumping rate vs. cold end temperature for three tubes of different diameter, $\frac{1}{2}$, $\frac{1}{4}$ and 3/4 inches. All three tubes have the same volume ratio, .15 and two of the tubes have the same length. The heat pumping rate for the other tube has

been adjusted in proportion to its length to be comparable to the other test data. Test results with the $\frac{1}{4}$" diameter tube were obtained with a different calorimeter which might explain some of the scatter of these points.

The results, however, do confirm Equation (8) which states that tubes of different diameters but the same lengths will pump the same amount of heat if they are operating at the same value of α/ND^2. For these tests α was held constant by operating at the same pressures and the speeds set such that the value of ND^2 was the same.

Test results for air show similar relations as the results for helium. The amount of test work done with air was limited because air directly from the air supply was too dirty and air in the compressor system caused two compressor burnouts.

Figures 28 and 29 are pictures of the tubes that were tested. Figure 28 shows pulse tube No. 27 mounted on the calorimeter described in this report and Figure 29 shows the $\frac{1}{4}$ inch diameter pulse tube, No. 33, mounted on a different calorimeter.

4. EMPIRICAL FORMULATION

The rather simple relationships between all of the pulse tube variables suggest the possibility of combining them into a general equation that will predict the heat pumping rate as a function of gas properties, geometric parameters, and operating conditions. It is realized that any such correlation of the test data based on such a general equation would be confirmation of its validity only for the range of the variables that has been covered in this test program.

Experimental evidence shows that tubes of different diameters operate best at the same value of ND^2. This seems to indicate that the Fourier number does in fact characterize the heat transfer in pulse tube refrigeration. Solutions to heat transfer problems that are similar to this are of the form

$$q = qm(1-e^{-CN_F}) \tag{13}$$

where qm is the heat pumping rate for N_F approaching infinity - i.e., very low pulse rates. If qm can be computed and q measured, then a plot of q/qm versus N_F should lead to the value of the constant C.

It has been observed too that the cold end temperature of a pulse tube refrigerator increases linearly with an increase in heat load, everything else being held constant. If qmh is used to denote the pseudo-maximum heat pumping rate when the cold end temperature T_c, is equal to the hot end temperature, T_h, and T_{co} is used to denote the cold end temperature when no heat is being pumped, then for everything else being held constant the following relation is observed;

$$qm = qmh\ (T_c-T_{co})/(T_h-T_{co}) \tag{14}$$

The model describing the heat pumping mechanism predicts that for the case when q = 0 then the cold end temperature is

$$T_{co} = T_h(L_o/L_t)^{\gamma-1} \tag{15}$$

The heat pumping rate is the product of the cooling per pulse, Q, and the pulse rate.

$$q = Q_n \tag{16}$$

$$qmh = Qmh\ n \tag{17}$$

The description of the heat pumping mechanism says that the cooling per pulse is equal to the heat deposited in the top by gas which has been pushed up from the lower part of the tube. Q is thus of the form

$$Q = m\ C_p\ \Delta T \tag{18}$$

in which m is the mass of gas that flows into the top from the lower part of the

tube and ΔT is the temperature change of the gas while it is in the top.

Consider the case when operation of the tube is first started and the tube is at temperature T_h throughout. As a result of isentropic compression the difference in temperature between the gas and the wall will be

$$\Delta T_{mh} = T_h \left(P_h/P_\ell\right)^{\frac{\gamma-1}{\gamma}} - T_h \tag{19}$$

The subscript m is used there because this is the maximum change that can occur in the gas temperature and the subscript h denotes the special case when the cold end is at the same temperature as the hot end.

The mass of gas that is involved is equal to the difference between the mass of gas in the top at the end of the low pressure period and the mass of gas in the top at the end of the high pressure period. For the case under consideration in which enough time is allowed for all the heat to flow from the gas to the wall the gas temperature at the end of each phase will be T_h and the mass of gas is thus

$$m = \left(P_h - P_\ell\right) V_o/RT_h \tag{20}$$

The top volume, V_o, can be expressed in terms of its length, L_o, and diameter, D,

$$m = \left(P_h - P_\ell\right) \pi D^2 L_o/4RT_h \tag{21}$$

As an approximation then, the maximum heat pumped per pulse when the tube is at the hot end temperature is

$$Q_{mh} = \frac{\left(P_h - P_\ell\right) \pi D^2 L_o}{4RT_h} C_p T_h \left[\left(\frac{P_h}{P_\ell}\right)^{\frac{\gamma-1}{\gamma}} - 1\right] \tag{22}$$

Equations (17) and (14) are used with (22) to give q_m for some other cold end temperature. When this is substituted into (13) the expression for the heat pumping rate is obtained.

$$q = \left(\frac{T_c - T_{co}}{T_h - T_{co}}\right) \frac{\pi n D^2 L_o}{4} \frac{C_p (P_h - P_\ell)}{R} \left[\left(\frac{P_h}{P_\ell}\right)^{\frac{\gamma-1}{\gamma}} - 1\right](1 - e^{-CN_F}) \qquad (23)$$

Preliminary analytic studies show that the Fourier number should be computed on the basis of gas properties that prevail during the high pressure period. The characteristic value of the Fourier number is thus computed on the basis of the gas properties at the hot end temperature and the high pressure.

The IBM 7070 computer at the Syracuse University Computing Center was used to compute the ratio of q/qm and N_F for all of the tests using Equation (23). There was a spread of data which seemed to be related to the pressures and also a difference for tubes of different length ratios. It was found that the pressure difference term has to be replaced by the term $P_h \ (P_h/345)^{.375}$. The correction for tubes with different length ratios is based on the observation from Figure 9 that tubes with a lower volume ratio pump more heat. This is attributed to the fact that the gas is preheated to a higher temperature before it enters the top. The correction factor for this is $(L_t/L_o)^{\gamma-1}$.

The final form of the heat pumping equation is

$$q = \frac{(L_t/L_o)^{\gamma-1}}{3.61} \left(\frac{T_c - T_{co}}{T_h - T_{co}}\right) L_o n D^2 \frac{C_p}{R} P_h \left(\frac{P_h}{345}\right)^{.375}$$

$$\left[\left(\frac{P_h}{P}\right)^{\frac{\gamma-1}{\gamma}} - 1\right] (1 - e^{-CN_F}) \qquad (24)$$

The constants in this equation apply for q in watts, L and D in inches, n in RPM and P_h in psia.

The test data for helium with a heat pumping rate greater than 3 watts is shown in Figure 30. From this plot the value of the constant C that gives best fit for Equation (24) is C = 26.6. Figure 31 shows the test results for air. There is not enough test data to evaluate the constants for air but the curve is seen to be substantially different than the helium data.

Air has a thermal diffusivity that is about seven times less than that for helium at given conditions, thus the performance of a given pulse tube with air is substantially less than the performance with helium. Being a diatomic gas Equation (15) also indicates that a tube operating with air will not get as cold.

This empirical relation, Equation (24), will be very useful in predicting the heat pumping rate of pulse tubes that fall within the region of the variables that were considered in this test program.

Acknowledgment

The computer work included in this report was supported in part by the National Science Foundation under Grant GP-1137.

Test Data for Pulse Tube No. 25 - Heat Pumping Rate, Wall Temperature, and Wall Temperature Change

Symbol	Meaning	Units
D	Tube Diameter	Inches
L	Total Length	"
LO	Top Length	"
PH	High Pressure	psia
PL	Low Pressure	psia
N	Pulse Rate	RPM
WI	Watts In, Cold End	Watts
WO	Watts Out, Top	Watts
T	Temperature of Wall	^{o}R
DT	Temperature Change of Wall During One Cycle	^{o}R

Subscripts

C	Cold End
H	Hot End
1,5	Wall Positions

5. MULTI STAGE PULSE TUBES

From the very start of the work on Pulse Tube Refrigeration it was realized that they could be staged together so that very low temperatures could be achieved. If there was not a possibility of multi staging, there would not have been a good reason for a great deal of work on pulse tubes. Whereas temperatures much lower than can be achieved with the freons can be obtained with single stage pulse tubes, there is not that much interest in that temperature range, -100 to -220°F. The cryogenic temperatures -300°F and colder are of much more interest.

The problem of the analysis of a multi-stage pulse tube is very much more complex than that of the single stage unit and it, of course, depends on the single stage analysis. Therefore, before multi-stage analytical work can be very valuable it is necessary to have very good confidence in our understanding of the basic single stage system. Although considerable progress has been made, there still is a great deal to be done.

As a result, our work on multi-stage pulse tubes has been limited and confined to two objectives:

a. Definite experimental confirmation of the fact that multi-staging can be accomplished.

b. Multi-stage units can attain cryogenic temperatures in small sizes which might be of interest in small spot coolers.

Both of these objectives have been accomplished. Two small two-stage pulse tubes were built and tested. The initial one achieved 95°K and a later one, which was slightly modified, achieved 79.5°K.

In addition to this, substantial time has been spent in attempts at multi-stage analysis and some worthwhile understanding has been attained. However, the condition of this work is not believed to be sufficiently well organized to be presented at this time.

V. REVERSIBLE PULSE TUBE REFRIGERATION

1. THEORY

A Pulse Tube Refrigerator operated with valves loses greatly in efficiency due to irreversible isenthalpic expansion through the valves. This basic method inefficiency can be eliminated by replacing the valves and compressor system with a piston and chamber which can be varied in size from zero to a maximum one by a motion of the piston. Figure 40 shows such a schematic reversible Pulse Tube Refrigerator.

It requires work to decrease the volume and push the gas through the regenerator and heat exchanger into the Pulse Tube, increasing the pressure. This work would come partly from the motor and partly from the flywheel by slowing it down slightly. When the piston, however, moves back the gas does work as the gas expands out of the pulse tube into the opening chamber made by the receding piston. This energy will be restored to the flywheel. In this way much of the irreversible loss by expansion through the valves is eliminated.

If a frictionless system with no pressure drop through the regenerator and heat exchanger is hypothesized, the net work done by the piston must be due to the cycle carried out by the total enclosed gas. The sum of all the little differential packets of gas which make up the enclosed volume will determine the net ideal work which will necessarily have to be supplied by the moving piston.

In order for a differential gas packet to cause a necessity for work on the moving face of the piston, it is necessary that its volume be greater during compression than during expansion so that more work is required for compression than is recovered during expansion. Cycles for a differential gas packet can be plotted on a PV diagram as shown in Figure 32. In such a cycle the volume being greater during compression than during expansion results in a work quantity from the moving piston of areas A + B of which only A is recovered. Therefore, the net work required by this differential packet is equal to area B.

If there is no volume difference during compression and expansion, then work received and recovered would be the same as shown in Figure 32 and no net work would be required from the moving face of the piston. Work for compression would come from the flywheel. However, the work returned would be of equal magnitude.

In Figure 32 is shown a differential gas packet cycle which would deliver energy to the moving face of the piston. Such a cycle would have an engine driving effect.

Consider now the actual reversible pulse tube operation. It is expected that compression would occur quite rapidly so that very little heat is transferred. Then a pause occurs during which heat is transferred to the walls of the tube giving half of the pulse tube refrigeration effect. This causes all the differential gas packets which are cooled to shrink and the total pressure to drop at constant total volume. Expansion then occurs quickly so that there is relatively little heat transfer. This is followed by a pause during which heat is transferred from the walls to the gas giving the other half of the pulse tube refrigeration effect. This heat transfer causes all the differential gas packets which are heated to expand, increasing the pressure in the whole system at constant volume.

The integrated effect for all the gas packets could be plotted as the PV diagram shown in Figure 33. The volume here includes the chamber volume by the piston, the regenerator volume, and the pulse tube volume. The compression and expansion are a mixture of isothermal compression in the regenerator, nearly isentropic compression in the piston chamber, and effectively a combination of the two in the pulse tube.

If compression were assumed isentropic the work of compression W_c can be approximated by

$$W_c = mc_v T_1 \left\{ \left(\frac{P_h}{P_\ell} \right)^{\frac{\gamma - 1}{\gamma}} - 1 \right\}$$

where

m = total mass of enclosed gas

c_v = constant volume specific heat

T_1 = temperature prior to compression

P_h = high pressure

P_ℓ = low pressure

The work recovered W_r would be

$$W_r = mc_vT_2 \left\{\left(\frac{P_h}{P_\ell}\right)^{\frac{\gamma-1}{\gamma}} - 1\right\}$$

The net W_n would be the difference between the two

$$W_n = mc_v (T_1 - T_2) \left\{\left(\frac{P_h}{P_\ell}\right)^{\frac{\gamma-1}{\gamma}} - 1\right\}$$

$$W_n = mc_vT_1 \left(1 - \frac{T_2}{T_1}\right) \left\{\left(\frac{P_h}{P_\ell}\right)^{\frac{\gamma-1}{\gamma}} - 1\right\}$$

An estimate of the net work requirement for the ideal no loss operation is just the problem of estimating T_2. If T_2 is .9 T_1 the net work requirements would be .1 of the isentropic constant volume work.

It is interesting to compare the work required for operation of a valved system. Considering again isentropic compression the W_i

$$W_i = m_c c_p T_1 \left\{\left(\frac{P_h}{P_\ell}\right)^{\frac{\gamma-1}{\gamma}} - 1\right\}$$

where

m_c = mass of gas leaving pulse tube to be compressed.

The mass of gas compressed will not, however, be equivalent to that in the reversible system as some will remain in the pulse tube and will be compressed by the returned gas m_c. The gas m_r remaining in the tube will be approximately equal to

$$m_r = \frac{P_\ell}{P_h} m$$

Thus

$$m_c = m(1 - \frac{P_\ell}{P_h})$$

Therefore the ideal work requirement W_i with a valved pulse tube would be

$$W_i = mc_p T_1 (1 - \frac{P_\ell}{P_h}) \{(\frac{P_h}{P_\ell})^{\frac{\gamma-1}{\gamma}} - 1\}$$

The ratio of work requirement of the reversible W_n to valved system W_i would be

$$\frac{W_n}{W_i} = \frac{mC_v T_1 (1 - \frac{T_2}{T_1}) \{(\frac{P_h}{P_\ell})^{\frac{\gamma-1}{\gamma}} - 1\}}{mC_p T_1 (1 - \frac{P_\ell}{P_h}) \{(\frac{P_h}{P_\ell})^{\frac{\gamma-1}{\gamma}} - 1\}}$$

$$\frac{W_n}{W_i} = \frac{C_v (1 - \frac{T_2}{T_1})}{C_p (1 - \frac{P_\ell}{P_h})}$$

Estimating rather possible values:

$$\frac{c_v}{c_p} = .6$$

$$\frac{W_n}{W_i} = \frac{.6 \times .1}{.66} = .09$$

$$\frac{T_2}{T_1} = .9$$

$$\frac{P_\ell}{P_h} = .33$$

In order to achieve the cycle diagrams shown in Figure 33 it is necessary for each little differential gas packet to give off heat after compression from its surroundings and receive heat after expansion from its surroundings. If we assume no heat transfer during the compression and expansion (and this may be a tolerable approximation if compression and expansion occur rapidly) the differential gas packet is carried through a Brayton Cycle. Figure 34 shows a TS diagram for the Brayton Cycle.

Individual differential gas packets would go through different Brayton Cycles. Packets near the wall would transfer more heat with the walls, but the temperature T_n and T_L would not be very different. Gas nearer the center of the tube would probably transfer less heat with the walls. However, the temperatures would be farther apart.

The efficiency of the ideal reversible pulse tube would be the sum of the efficiency of all the gas packets. It is, therefore, of interest to see what range

of efficiencies is possible so that a good educated approximation might be made.

The work of compression 1 to 2 would be

$$\delta W_{1-2} = \delta m_1 C_v T_1 \{(\frac{P_h}{P_\ell})^{\frac{\gamma-1}{\gamma}} - 1\}$$

The work of expansion

$$\delta W_{3-4} = \delta m_1 C_v T_4 \{(\frac{P_h}{P_\ell})^{\frac{\gamma-1}{\gamma}} - 1\}$$

Therefore, the net work W_n

$$\delta W_n = \delta m_1 C_v (T_1 - T_4) \{(\frac{P_h}{P_\ell})^{\frac{\gamma-1}{\gamma}} - 1\}$$

$$T_4 = T_h (\frac{P_\ell}{P_h})^{\frac{\gamma-1}{\gamma}}$$

$$\delta W_n = \delta m_1 C_v T_L (1 - \frac{T_h}{T_L} (\frac{P_\ell}{P_h})^{\frac{\gamma-1}{\gamma}} \{(\frac{P_h}{P_\ell})^{\frac{\gamma-1}{\gamma}} - 1\}$$

The heat pumped from T_ℓ to T_h would simply be

$$\delta Q_{\ell-h} = \delta m_1 C_v (T_1 - T_4)$$

$$\delta Q_{\ell-h} = \delta m_1 C_v (T_\ell - T_h (\frac{P_\ell}{P_h})^{\frac{\gamma-1}{\gamma}})$$

$$\delta Q_{\ell-h} = \delta m_1 C_v T_\ell [1 - \frac{T_h}{T_\ell} (\frac{P_\ell}{P_h})^{\frac{\gamma-1}{\gamma}}]$$

$$\frac{\delta W_n}{\delta Q_{\ell-h}} = \frac{\delta m_1 C_v T_\ell \left[1 - \left(\frac{T_h}{T_\ell}\right)\left(\frac{P_\ell}{P_h}\right)^{\frac{\gamma-1}{\gamma}}\right]\left\{\left(\frac{P_h}{P_\ell}\right)^{\frac{\gamma-1}{\gamma}} - 1\right\}}{\delta m_. C_v T_\ell \left[1 - \left(\frac{T_h}{T_\ell}\right)\left(\frac{P_\ell}{P_h}\right)^{\frac{\gamma-1}{\gamma}}\right]}$$

$$\frac{\delta W_n}{\delta Q} = \left\{\left(\frac{P_h}{P_\ell}\right)^{\frac{\gamma-1}{\gamma}} - 1\right\}$$

It is interesting to note that the work required per unit of heat pumped is independent of the two temperatures and only dependent on the pressure ratio.

The overall $\frac{W_n}{Q}$ would just be the integrated effect for all the differential gas packets.

$$\frac{W_n}{Q} = \left\{\left(\frac{P_h}{P_\ell}\right)^{\frac{\gamma-1}{\gamma}} - 1\right\}$$

The efficiency relative to the Carnot cycle E_c may be determined by simply dividing the $\left(\frac{W}{Q}\right)_c$ for a Carnot cycle by $\frac{W_n}{Q}$.

$$\left(\frac{W}{Q}\right)_c = \frac{T_h - T_\ell}{T_\ell}$$

$$E_c = \frac{T_h - T_L}{T_L \left\{\left(\frac{P_h}{P_\ell}\right)^{\frac{\gamma-1}{\gamma}} - 1\right\}}$$

$$E_c = \frac{[\frac{T_h}{T_L} - 1]}{\{(\frac{P_h}{P_\ell})^{\frac{\gamma-1}{\gamma}} - 1\}}$$

In the case of the pulse tube the problem is slightly more complex in that whereas a differential gas packet may operate between temperatures T_h and T_ℓ, there must be a temperature differential between the packet through other differential gas packets to transfer heat to the wall. As a result, though the differential gas packet will operate between temperatures T_h and T_ℓ it will actually pump heat between temperatures $T_h' < T_h$ and $T_L' > T_L$. Thus in our efficiency expression the primed temperatures really should be used.

$$E_c = \frac{[\frac{T_h'}{T_L'} - 1]}{\{(\frac{P_h}{P_\ell})^{\frac{\gamma-1}{\gamma}} - 1\}}$$

The problem then is to estimate the effective average temperatures between which heat is pumped. If the temperature ratio between which heat is pumped is at all close to that which is achievable with the pressure, the efficiency will be quite good.

2. PULSE TUBE REFRIGERATOR IDEAL VOLUME RATIO

It has been shown that the refrigeration achievable with a pulse tube refrigerator may be represented quite closely by the following equation.

$$Q_r = C_1 V_1 \frac{T - T_s (\frac{V_1}{V_t})^{\gamma-1}}{T_s - T_s (\frac{V_1}{V_t})^{\gamma-1}}$$

Where

Q_r = Ideal refrigeration available

V_t = Total volume of tube

V_1 = Volume of top constant temperature cap

T = Temperature of refrigeration load

T_s = Top temperature of the sink.

A sample plot is shown in Figure 35. There is a question of what part of the tube should be made V_1 as making it bigger makes the refrigeration available at higher temperatures increase but decreases it at lower temperatures. Thus there must be some ideal volume ratio for every temperature T. This may be derived as follows

$$Q_r = C_2 V_r \frac{[\frac{T}{T_s} - (V_r)^{\gamma-1}]}{[1 - (V_r)^{\gamma-1}]}$$

To differentiate, let

$$u = C_2 V_r \left(\frac{T}{T_s} - V_r^{\gamma-1}\right)$$

$$du = C_2 \frac{T}{T_s} - C_2 \gamma V_r^{\gamma-1}$$

$$v = \frac{1}{1 - V_r^{\gamma-1}}$$

$$v = \frac{1}{z}$$

$$z = 1 - V_r^{\gamma-1}$$

$$dv = \frac{(\gamma - 1)V_r^{\gamma-2}}{z^2}$$

$$= \frac{(\gamma - 1)V_r^{\gamma-2}}{[1 - V_r^{\gamma-1}]^2}$$

$$duv = C_2 V_r \left(\frac{T}{T_s} - V_r^{\gamma-1}\right) \frac{(\gamma - 1)V_r^{\gamma-2}}{[1 - V_r^{\gamma-1}]}$$

$$+ \frac{1}{1 - V_r^{\gamma-1}} \left[C_2 \frac{T}{T_s} - C_2 \gamma V_r^{\gamma-1}\right]$$

The diffe ential will be zero for an optimum, therefore

$$0 = (\gamma - 1)V_r^{\gamma-1} \left[\frac{T}{T_s} - V_r^{\gamma-1}\right] + [1 - V_r^{\gamma-1}]\left[\frac{T}{T_s} - \gamma V_r^{\gamma-1}\right]$$

$$= .66V_r^{.66} \left(\frac{T}{T_s} - V_r^{.66}\right) + [1 - V_r^{.66}]\left[\frac{T}{T_s} - 1.66V_r^{.66}\right]$$

$$= .66\frac{T}{T_s} V_r^{.66} - .66V_r^{1.33} + \frac{T}{T_s} - 1.66V_r^{.66} - \frac{T}{T_s} V_r^{.66} + 1.66V_r^{1.32}$$

$$= V_r^{1.32} - 1.66V_r^{.66} + \frac{T}{T_s} - .33\frac{T}{T_s} V_r^{.66}$$

$$\frac{T}{T_s}(1 - .33V_r^{.66}) = 1.66V_r^{.66} - V_r^{1.32}$$

$$\frac{T}{T_s} = \frac{1.66V_r^{.66} - V_r^{1.33}}{1 - .33V_r^{.66}}$$

This then gives the ideal volume ratio for any temperature of operation. A plot of this equation is given in Figure 36.

3. OBJECTIVES OF TEST PROGRAM

Basic objectives of the test program were to determine the general performance characteristics of the reversible pulse tube refrigerator and then draw some comparisons with standard pulse tube systems. Parameters to be observed and varied were selected to yield the most complete operating curves and to allow easy correlation of data with previously observed valved pulse tube results.

To determine the most characteristic performance data for the reversible system a procedure of comparing the refrigeration load with cold end temperature was used. The parameters varied were:

a. The cylinder pressures

b. The operating speed of the compressor

c. The applied heat load on the cold heat exchanger

Along with these results, a complete record of pressure-time variations in the cylinder was recorded by an oscillograph. These traces were used to determine actual compression ratios in the refrigerator.

The determination of actual power used in the refrigeration process was also a prime objective. To help make this evaluation, a series of tests were run on the basic test unit to find all system losses excluding the pulse tube refrigerator. Tests were run to find bearing, motor and flow losses in the unit. From these values, a comparison of power readings under load would reveal actual pulse tube power consumption.

A detailed description of the apparatus follows which gives a complete picture of the means employed to obtain the variation of parameters and observation of variables required to carry out the desired test program. Diagrams and photographs appear in the report which give overall and detailed illustrations of the apparatus.

Not included in the analysis, but appearing in the illustrations, are some related items which proved to require further refinement before completion of a test program on them. In the photograph, Figure 37, the long cylinder extending from the section beneath the regenerator is a variable volume extension to the cylinder area. By moving a piston in this tube, a variable compression ratio could be achieved through effectively increasing the cylinder volume. Use of this concept proved unsatisfactory in its present form by virtue of excessive heating of the gas which entered the long cylinder, and was compressed to a high pressure. All tests in the series were therefore run with the extension volume shut off from the system.

In Figure 38 a pulse tube configuration of nineteen tubes with no regenerator or flow straighteners can be seen. This unit was constructed to evaluate the possibility of transporting large quantities of heat through a small temperature difference while doing away with the regenerator and operating directly from a piston. The unit could pump large quantities of heat, as shown, but ineffective heat transfer at the cold end rendered it unable to carry a refrigerated load. Further work on the principle, which proved sound, is hoped for the future.

4. DESCRIPTION OF EXPERIMENTAL APPARATUS

The test unit used for these experiments was designed and constructed expressly for reversible operation. Basically, it consists of four parallel one-quarter inch diameter pulse tubes with common hot and cold end heat exchangers. Directly beneath the tube is a two-and-one-half inch long regenerator, three-quarters of an inch in diameter. This regenerator is packed with over four hundred 200 mesh bronze screens. Sintered metal plugs at the base of the four tubes serve to help straighten and smooth gas flow. Under the regenerator is a section containing a water jacket which serves to hold gas entering the regenerator at a reasonably constant temperature. An overall view of the system, as well as a view of a standard pulse tube configuration, can be seen in Figures 39, 40 and 41.

Instrumentation provided on the refrigerator includes copper-constantan thermocouples at both heat exchangers and a calibrated resistance heater on the cold end to apply known refrigeration loads. Also seen in the diagram mentioned above are the cooling coils at the hot end and the mounting arrangement for the strain gauge pressure transducer.

Driving the gas into and out of the system is a specially designed aluminum piston operating in a stainless steel liner with heavy duty sealing to prevent oil from entering the regenerator and fouling it. The piston is activated by a single cylinder compressor which is attached to the piston rod. A calibrated electric motor drives the compressor through a variable ratio pulley system and a large flywheel. Power flow to the motor is registered on a wattmeter.

To provide adequate insulation, a vacuum system was installed over the refrigerator and the unit was wrapped in mylar super insulation. The vacuum pot was held down by a continuously operating fore pump to prevent convection losses, while the mylar wrapping cut radiation heat transfer. This arrangement along with a view of the overall apparatus set-up can be seen in the photograph, Figure 42.

Supporting instrumentation included a Brush oscillograph which recorded pressure-time diagrams, and two microvoltmeters to display thermocouple output voltages. A variac supplied a continuous range of voltages to the resistance heat load on the cold heat exchanger. Motor and compressor speeds were checked by a Hasler hand tachometer and a Strobotach light.

Helium was used in all tests as the refrigerant. Charging of the system took place with the piston located one-half way between top and bottom dead center. At this level, both the area above the piston and the area below, which connected to the compressor base, were pressurized equally. In this manner, excessive pressure differentials across the piston were prevented and motor torque requirements were smoothened considerably. Some system power loss was introduced, however,

because of pumping work required on the gas in the compressor base area. These losses were included in the system power requirements mentioned earlier.

Tests were performed by allowing conditions to stabilize at zero refrigeration load and then to apply increments of power to the heater and observe cold temperature variation. Some tests were made of cooling time for various pressure values and of temperature ratios with the top uncooled. These are mentioned briefly in the results which follow in the next section.

5. RESULTS OF REVERSIBLE PULSE TUBE TEST PROGRAM

This section deals with interpretation of the curves shown in Figures 43, 44 and 45, and is intended to give an overall qualitative picture of reversible pulse tube performance. Comparison of reversible and valved pulse tube data was facilitated by use of the following characteristic and similarity relations:

a. Available refrigeration is directly proportional to tube length.

b. Optimum operating speeds can be found by using equal Fourier numbers: α/ND^2 = constant, for various tube diameters.

c. Regenerator losses can be estimated as inversely proportional to the length of the regenerator.

Examination of the curves plotted on these assumptions yields the following conclusions:

(1) Corrected for regenerator length difference in Figure 43, ($3\frac{1}{2}$ inches on the valved to $2\frac{1}{2}$ on the reversible), the reversible unit is able to attain a nearly equal minimum temperature. Refrigeration load attainable at higher cold temperatures, however, drops off for the reversible unit until at the top heat sink temperature of 520°R, the valved unit carries 50% more load. A partial explanation of this decreased refrigerating ability is due to the slightly higher operating pressures in the valved unit. Previous pulse tube data shows available refrigeration to be a function of the high pressure. The zero regenerator loss curves are shown to illustrate how the unit should work between the

ideal minimum square wave pressurization pattern. In the reversible system, it appears that more pulses per minute are necessary to allow for equal heat transfer to take place at the high pressure end of the cycle. This conclusion also helps explain the gap in load carrying ability displayed in the first curve referred to.

(2) The family of curves in Figure 44 illustrates the dependency of refrigeration availability on operating pressures. All the curves represent compression ratios of approximately 4.2 = 1 at a constant speed of 370 RPM. The increased available refrigeration can be seen to be a nearly linear function of the high pressure achieved in the pulse tube. These results help fortify the explanation of why the reversible unit could not carry as great a load as the valved unit in the previous curve; these units also operated at equal compression ratios of 4.2 = 1.

(3) Figure 45 is very interesting since it shows that the reversible unit performs better at a higher speed than predicted by the Fourier number approach. The similarity relation when applied to the reversible unit gives an optimum speed of 360 RPM from a valved optimum of 40 RPM. All this data is presented for compression ratios of nearly 4.2 = 1 in each case. Examination of Figure 29 gives an indication of why such behavior might be expected. The pressure-time trace shown displays a nearly sinusoidal pressure variation with sharp spikes at the high pressure end. From this fact, it can be seen that the high pressure is actually in effect for a much shorter time than on normal valved pulse tubes. The valved pressure-time diagram exhibits a nearly square wave pressurization pattern. In the reversible system, it appears that more pulses per minute are necessary to allow for equal heat transfer to take place at the high pressure end of the cycle. This conclusion also helps explain the gap in load carrying ability displayed in the first curve referred to.

At the time of this writing, only limited test work has been completed, not allowing a highly detailed analysis of the data to have been carried out. From

the data seen in this report, however, many interesting general conclusions can be drawn.

The primary fact to be seen from these results is that reversible pulse tubes do compare very favorably with valved units. Observed data and indicated corrections for pressures and regenerator losses give very good correlation of load carrying and general performance characteristics. Further consideration of the altered pressurization pattern, which points toward new optimum operating speeds, gives even greater agreeability. Although a new operating speed criterion is indicated, the proportionality of heat pumping and tube length should not be altered, since this is not influenced by the pulses per minute applied. This fact allows the use of data from different tube lengths to be accurately compared when scaled down.

Further work is indicated to more fully evaluate the reversible concept. Tests with varying compression ratios should be performed along with more compressor speed ranges. A new single tube model of comparable dimensions to valved units may prove best for further correlation work. Extensive investigation of the pressurization pattern should lead to new optimization relations for reversible systems. Improvement of the apparatus such as better oil seals, and improved vacuum insulation would also prove a great aid in future tests.

This initial investigation of the reversible system has shown the principle to be extremely sound and to obey expected performance parameters. Agreement with predicted efficiency values is discussed in the next section.

6. REVERSIBLE PULSE TUBE EFFICIENCY

In the preceding section, it was shown that reversible action of a pulse tube does not impair performance of the system, but actually compares favorably with valved operation. This section attempts to determine whether the expected increases in efficiency predicted were actually realized in operation.

Because of the small refrigeration loads, any power input changes could not

be noted as loads were varied. The necessarily large wattmeter scale was not sensitive enough to observe these changes. For this reason, the efficiency comparison is carried out at zero load conditions. Since refrigeration loads are in actuality quite small, this computation gives a quite accurate picture of efficiency throughout the majority of the operating range.

The method of approaching an efficiency comparison in this report is an approximation of valved pulse tube work input by means of computing isentropic compression work from P_ℓ to P_h. This approximation is, of course, lower than actual compressor work, and the efficiency results will represent a minimum. Calculations are made at different points to determine relative increases in efficiency by operating in the reversible mode.

Actual reversible power input is determined by taking the steady state wattmeter reading and subtracting system power losses mentioned in Section IV of this report. A curve of these losses versus the high cylinder pressure is shown in Figure 47. Calculations are done on the following page.

Measurements of electric power required to run the reversible pulse tube test rig were made in such a way as to measure the total power used for compressing the gas into the tubes. The total power when the test section was running at 470 RPM between pressures of 45 and 185 psia was 335 watts. Of this 265 watts was involved in electric motor losses, test rig friction, etc. Therefore, total power required for the pulse tubes was only 70 watts. An estimate of the improved efficiency of the reversible pulse tubes can be made by computing the ideal power required to operate the same pulse tubes with a valved system.

This is done by first computing the gas requirements

$$SCFM = VN \left(\frac{P_h - P_\ell}{P_{atm}}\right) \frac{T_h}{T_L}$$

where

$$T_L = \frac{1}{3} (T_h - T_c) + T_c$$

$T_h = 520^\circ R$

T_c = pulse tube cold end temperature

$T_L = 300^\circ R$

$P_{atm} = 14.7$ psia

V = pulse tubes and regenerator volume

From this

SCFM = 6.50

The ideal work W_k to compress this gas is

$$W_k = mC_p T_h \left[\left(\frac{P_h}{P_\ell} \right)^{\frac{\gamma-1}{\gamma}} - 1 \right]$$

Computing for our case

$W_k = 1570$ Btu/hr

$W_k = 460$ watts

Thus the power actually experimentally measured is only $\frac{70}{460} = 15.2\%$ of the ideal power which would be required with a valved system and a 100% efficient isentropic compressor and electric motor. If these had a combined efficiency of 65% as they might at best have, the reversible system would demonstrate a work consumption of only 10% of the requirement of a valved system with actual compressor.

The greatly improved efficiency possible from reversible systems has therefore been confirmed.

It is interesting to note also that most of the 70 watts power requirement can be shown to be due to pressure drop through the regenerator and flow smoothing heat exchanger at the bottom of the tubes. Therefore, great improvements are still possible if better regenerators can be made.

The following table gives similar calculations and measurements for other specific cases. (W_r is actual experimental pulse tube work)

Calculations of Reversible and Isentropic Work Requirements for a Pulse Tube Refrigerator

RPM	P_h	P_ℓ	Rev. Power	Isentropic Power	$\frac{W_r}{W_k}$
470	185	45	70	460	.152
370	185	45	40	352	.1135
370	315	75	110	680	.162

VI. COMPACT CRYOGENIC THERMAL REGENERATORS

1. INTRODUCTION

All gas-operated cryogenic refrigerators require highly efficient heat exchange means to cool the feed, high pressure gas with the exhausting low pressure gas. Though this heat exchange means may operate across a temperature range ($T_1 - T_2$) as great as 200°K or more, the ΔT (temperature difference between entering and leaving gas) must be 10°K or smaller. An inefficiency I_e is defined as follows.

$$I_e = \frac{\Delta T}{T_1 - T_2}$$

ΔT = Temperature difference between entering and exhausting gas

T_1 = Hot end temperature

T_2 = Cold end temperature

For good cryogenic refrigerator efficiency, it is necessary to make these heat exchange inefficiencies 1 - 3%. In general cryogenic refrigerator design, this will be found to be true.

In large cryogenic refrigerator design it is not too difficult to achieve this with heat exchangers 3 to 12 feet long. These may be either counter flow heat exchangers or thermal regenerators. Recently there has arisen a need for miniature cryogenic refrigerators where the lengths available are only 3 to 5 inches.

Some of the most successful of these miniature refrigerators use the Stirling cycle, Gifford-McMahon cycle, or Pulse Tube refrigeration. All of these use very short thermal regenerators and their success is in considerable part due to the high efficiency which may be achieved with such small thermal regenerators (99+%). The small size of these thermal regenerators complicates the problem of their performance in three ways.

a. To achieve the order of the efficiencies required, the flow passage equivalent diameters must be small as compared with that used in other heat exchange systems.

b. End to end conduction heat transfer, due to the short length, will be relatively large and cannot be neglected as frequently is done with larger systems.

c. The boundary effects, due to heat transfer to and from the regenerator walls, are correspondingly much larger for these small regenerators and cannot be neglected, as thelosses introduced in this way may be of the same order of magnitude as the matrix heat transfer losses.

Condition C, which shall be referred to as the wall effect, results from the difference between the mass of the wall and the mass of the matrix material. The wall, which is usually a metal such as stainless steel, has a much greater mass and a higher specific heat per unit of area than the matrices and can, therefore, store more heat per unit of temperature than the matrices. Thus the wall does not experience as large a warming temperature from the entering gas as the matrices, and similarly it is not cooled as much as the matrices by the exiting gas during the warming blow period. This means that in each regenerative cycle the gas near the walls will not be cooled or warmed as much as the gas passing through the matrix material and the mixing of these two gas streams will either raise the temperature of the gas leaving the regenerator at the cold end or lower the temperature of the gas leaving at the warm end.

This is a report on experimental tests on small thermal regenerators of a size of interest to these small refrigerators. The regenerators were all 3/4" in diameter and 4" long. The regenerators were filled with fine wire mesh screens. Details are given in the table on page 77.

The tests were carried out with the equipment shown schematically in Figure 65. Two regenerators were operated between room temperature ($72^{\circ}F$) and liquid nitrogen temperature. Gas from a compressor flowed through one thermal regenerator then through an excellent heat exchanger bonded to a first liquid nitrogen bath well shielded by a second liquid nitrogen bath, and thence out through the other thermal regenerator. The flow was reversed 60, 100, and 150 times per minute by reversing the valve set. The total flow rate was varied by by-passing gas from compressor exhaust to suction.

In this way all losses due to the regenerator manifested themselves in time average ΔT's of the gas flowing and conduction through the regenerators. Due to the radiation shielding, this represented all the heat transfer to the first liquid nitrogen bath. Thus the boil off of liquid nitrogen represented a measure of the total heat losses. This boil off, after being warmed to room temperature, was measured with a gas meter capable of measuring .001 standard cubic feet.

The compressor was a hermetically sealed freon unit which was evacuated and filled with helium gas for the tests. Helium flow rates were measured with an orifice flow meter which had been calibrated against a standard orifice.

The valve was actually one rotary disc valve which assured accurate flow period timing. It was driven by a variable speed motor. The RPM was determined by a counter-timer method with a precision error less than .5 RPM.

Regenerator inefficiency tests were conducted by randomly stacking wire screens into two .750 inch phenolic tubes, as shown in Figure 65 . These regenerators were then placed in the rig, andliquid nitrogen was poured into each of the reserviors while a vacuum was drawn on the system. After the initial boil off of the liquid nitrogen ceased, the vacuum pump was turned off and the system was pressurized. The helium flow was set by starting the compressor and adjusting the low pressure, through the helium supply, and the manometer reading. The manometer reading was controlled by adjusting the pressure ratio across the compressor. By these two adjustments, using a .143 inch diameter calibrated orifice plate, the helium flow rate could be controlled within $\pm$ .2 (SCFM) between 9 (SCFM) and 20 (SCFM). The regenerator inefficiency was calculated from the boil off of theliquid nitrogen, measured from the Precision Wet Test Meter, and the helium flow rate with an accuracy of more than $\pm$ .03%.

The tests performed consisted of setting the regenerator length and then varying either the valve speed, that is the blow time, for a fixed (14 SCFM) helium flow rate, or the flow rate for fixed valve speeds. In each case the regenerator length was established by calculating the number of screens required to give a

minimum packing density. Thus for 150 mesh screens, 335 screens were used for a 2 inch long regenerator, 503 for 3 inch, and 670 for 4 inch.

The effect of end to end conduction was investigated by varying the packing density and the screen material. Packing density effects were determined by adding more screens to the regenerator while holding the length constant, and by varying the length while holding the number of screens constant. In the first case, with the length fixed, the increase in the thermal conductivity due to the increased packing density will be the only factor contributing to a possible decay in performance. On the other hand, the addition of screens will increase the heat transfer area, and if the end to end conduction effect is small, the increase in area will produce an increase in the regenerator performance. This testing was employed to indicate whether the end to end conduction can be overcome by the convective heat transfer area, and at what point the end to end conduction becomes too large to be overcome.

In the second case, holding the number of screens constant and varying the packing density by varying the length occupied by the screens, the heat transfer will remain constant and the conduction parameter

$$\frac{K_s \cdot A_{fr}}{L}$$

will increase. Since the end to end conduction will be amplified by the decrease in L, as well as the increase in K, an increase in inefficiency will necessarily indicate the order of magnitude and the importance of just the end to end conduction effect.

The effect of screen material was studied by using both bronze screens in tests of the first case. In addition the influence of the boundary condition on the end to end conduction was investigated by using a .020 inch perforated copper plate on either end, a $\frac{1}{2}$ inch copper block, and by leaving the ends free with only a thin wire "S" slip on either end to hold the screens in place. The large mass of the copper blocks and the perforated plates will prevent them from swinging through as large a temperature change as the screens and, therefore, the condition of a constant boundary temperature near T_h and T_R will be achieved. In the case of the "S" clips, the two

end screens will have one end thermally free, and therefore, the temperature swing of the end screens will not be restricted by the boundaries. In this case, if the end screen is taken to represent the boundary, then the boundary temperature will vary with time in accordance with the swing of the regenerator. It was felt that through these three end conditions, the difference between a constant boundary temperature and a variable boundary temperature could be evaluated.

The wall effect was investigated by changing the wall material and the screen material. For these tests 150 mesh screen were packed into a .750 inch I.D. x 1.000 inch O.D. phenolic tube to give a minimum packing density. The regenerator length was varied from 2 to 4 inches, the helium flow set a 14 SCFM, and the valve speed varied between 40 and 180 RPM. These tests enabled data to be gathered that could be plotted to give the regenerator inefficiency as a function of the capacity ratio $(M_s C_{ps}/\dot{m} C_{pg} \cdot \Theta_H)$ and the number of heat transfer units $(hA_s/\dot{m}C_{pg})$.

Tests run to determine the over-all regenerator inefficiency with the wall effect were:

Reg. length (inches)	No. of Screens	NTU	Screen Mat'l.	Wall Mat'l.
4.00	670	389	Bronze	Cotton base phenolic
3.00	503	272	"	"
2.00	335	193	"	"
1.34	225	129	"	"
4.00	670	389	"	.020" thick S.S. steel
3.00	503	272	"	"
2.00	335	193	"	"
4.00	670	385	Stainless steel	"
3.00	503	272	"	"
2.00	335	192	"	"

Reg. Length (inches)	No. of Screens	NTU	Screen Material	Wall Material
3.00	503	272	Stainless steel	Cotton base phenolic
4.00	-	-	.015-.018 dia. lead balls	"
3.00	-	-	"	"
2.00	-	-	"	"
4.00	-	-	.006-.009 dia. lead balls	"
3.00	-	-	"	"
2.00	-	-	"	"

The regenerators used to test the stainless steel wall were made by boring out the phenolic tube and press fitting in a .020 inch thick stainless steel tube.

In all the tests run, two or three consecutive runs on succeeding days were made to establish the precision of the data. On several occasions the tests were repeated after the rig was warmed up to room temperature, the regenerators removed from the rig, the screens removed from the regenerator, and after repacking the regenerators, placing them back into the rig and cooling the rig down to liquid nitrogen temperature again. If the data was consistent within an efficiency of $\pm$ .04 after consecutive runs, the data was recorded and plotted. If the data was not consistent the testing procedure was always started over again after the complete procedure of warming up the system and repacking the regenerators was first carried out.

2. TEST RESULTS

The details of all the worthwhile tests run are plotted in Figures 48 and 49. Figure 48 represents the total heat loss and Figure 49 the inefficiencies

The data as can be seen is accurate to about $\pm$ .02 - .03%. It is interesting to note that the inefficiency is relatively independent of flow rate for the range

of flows of interest to cryogenic refrigeration. At low flow rates the loss is a greater part end to end heat leak and at high flow rates the loss is due more to matrix heat exchange and the wall effect.

It is interesting to note that the inefficiency is greatly affected by the pulsing rate at high flow rates. The critical factor is the amount the matrix temperature changes per cycle. If it is large it increases the inefficiency. Interestingly, the smaller equivalent diameters and larger areas gave a substantial reduction in inefficiency between 100 mesh and 150 mesh. However, there was a relatively small improvement with further reduction to 200 mesh.

The results of this experimental investigation also revealed that the regenerator length, that is the NTU

$$NTU = \frac{hA}{\dot{m}C_p}$$

h = heat transfer coefficient

A = heat transfer area

$\dot{m}C_p$ = helium mass flow rate and specific heat

The wall effect, the regenerator end conditions, and the capacity ratio

$$C_r/C_y = \frac{(MC_p)\ \text{matrix}}{mC_p \cdot \Theta_H}$$

where Θ_H = blow time

all have an influence on the regenerator performance.

The results for the test run at a constant (14 SCFM helium flow rate are shown in Figures 50 through 55 . Figure 50 and 52 show that for two identical 3 inch long 150 mesh bronze screen regenerators, the regenerator with the stainless steel wall was .130% more inefficient at a capacity ratio of 20 than the regenerator with the phenolic wall. Since all other properties of the two regenerators were held constant, the decrease in performance is directly attributable to the wall material, that is the wall effect.

These two figures also show how important the capacity ratio is on the regenerator performance and especially on the wall effect. The wall effect, as shown, was more detrimental at lower capacity ratios; at a capacity ratio of 5 the stainless steel wall regenerator was .460% more inefficient than the phenolic wall regenerator. This indicates that it is the relative magnitudes of the wall temperature swing and the screen temperature swing that controls the wall effect. Any change in the variables M_s , C_{ps}, $\dot{m}$, C_{pg}, and Θ_H that produce a corresponding decrease in the capacity ratio will increase the wall effect. For long blow times, increasing the mass flow rate is especially harmful to the regenerator performance because it reduces the capacity ratio as well as the number of NTU's. This is shown in Figures 56 through 59 where at long blow times (1/150 min.), a valve speed of 75 RPM, the inefficiency is greatly affected by the flow rate.

The use of stainless steel screens helped to reduce the wall effect at low capacity ratios, Figure 53 . For this case the stainless steel regenerator was .290% more inefficient than the phenolic wall regenerator at a capacity ratio of 5. This reduction in efficiency at the lower capacity ratios can be attributed to the increased specific heat of the stainless steel screens. For a larger specific heat necessarily means that at the same capacity ratio the temperature swing of the wall will be increased for the stainless steel screen regenerator while the temperature swing of the screens will be identical to the swing of the bronze screens. This is seen by considering what effect the specific heat has on the capacity ratio. Since the mass of bronze screens and the stainless steel screens is approximately equal, the increase in the specific heat means that the flow time must also be increased to maintain the capacity ratio constant. A larger blow time means that a larger amount of heat must be transferred from the gas to both the wall and the screens, and a larger flow of heat to the wall will produce a larger wall temperature swing. However, the increased specific heat will keep the screen temperature swing from increasing, and thus the temperature of the gas

near the walls will be closer to the temperature of the gas passing through the screens. The smaller temperature difference between these two gas streams will in turn lower the inefficiency because their continual mixing will not reduce the total gas temperature as much for this case as compared to the bronze screen regenerator.

Further support for this wall effect theory is found by comparing the bronze screen-stainless steel wall regenerator's inefficiency at a capacity ratio of 6.1 and the all stainless steel regenerator's inefficiency at a capacity ratio of 5. The capacity ratio of 6.1 is used because it represents the difference in specific heats. At a capacity ratio of 6.1 the bronze screen regenerator had an inefficiency of 1.560% for a 3 in. length and 1.500% for a 4 in. length, as compared to 1.742% and 1.720% at a capacity ratio of 5. At a capacity ratio of 5 the stainless steel regenerator had an inefficiency of 1.565% for a 3 in. length and 1.413% for a 4 in. long regenerator.

Figures 60 through 63 show that the end to end conduction effects are less detrimental to the regenerator performance than the wall effect. For the conduction tests run by increasing the number of screens while holding the length constant, the heat transfer area increased more than the heat leak so that an improvement rather than a decrease in performance was found. This improvement was approximately .1% for both the stainless steel screens and the bronze screens.

For the conduction tests run by decreasing the length while holding the number of screens constant there was an increase in the regenerator inefficiency, but as shown in Figures 62 and 63 this increase becomes significant only at the shorter regnerator lengths. These two tests also revealed that the end to end conduction is affected only slightly by the blow time.

The effect of the end condition is shown in Figure 64 . From this diagram it is seen that the increased mass at the ends does help to reduce the inefficiency, but that for each of the end conditions the wall effect is not reduced. The stainless steel wall regenerator continued to have the same increased inefficiencies that were given above.

The above results have shown that by increasing the length, the wall effect and the end to end conduction are both decreased. In fact, it was thought that since the wall effect and end to end conduction becomes smaller, while the heat transfer area and the mass are increased by increasing the length, doubling the length would decrease the inefficiency by more than a factor of 2. However, it was noted that doubling the length does not cut the inefficiency in half. The decreases found experimentally were :

Screen material	Wall material	Inefficiency for 4 in. at $C_r/C_g = 20$	Decrease in inefficiency from 2 in. and $C_r/C_g = 10$
Bronze	Cotton base phenolic	.80%	42.8%
Bronze	.020 in. thick stainless steel	.93%	45.8%
Stainless steel	.020 in. thick stainless steel	.93%	43.8%

From the experimental work performed it is evident now that the originally proposed thermal losses do contribute significantly to the inefficiency of small regenerators, and that while these losses can be reduced by increasing the length, after 4 inches additional length will not substantially decrease the inefficiency. This necessarily means that to further reduce the inefficiency wall materials will have to be selected which reduce the wall effect.

In addition to the bronze and stainless steel screens tested, .015 - .018 in. diameter and .006 - .009 in. diameter lead spheres were tested also. The results given in Figures 54 and 55 show that inefficiences of the same order as obtained from the screens can be obtained with the small diameter spheres.

Regenerator Matrix Data Table

Test number	1	2	3
Length, in.	4.0	4.0	4.0
Diameter, in.	0.75	0.75	0.75
Mesh, wires/in.	100	150	200
Number of screens	400	670	890
Weight, grams	73.2	66.5	77.7
Weight, lbs.	.1615	.147	.1715
Porosity, P	.712	.738	.694
(1 - P)	.288	.262	.306
Wire diameter, D_w, in.	.0045	.0026	.0021
Equivalent diameter, $D_e = \frac{P\ (D_w)}{1 - P}$	.0111	.00732	.00477
Density of screen material, $lb_m/in.^3$	.318	.318	.318
V screen, $in.^3$	.508	.463	.540
A screen, $in.^2$	452	712	1025

FIG. 1

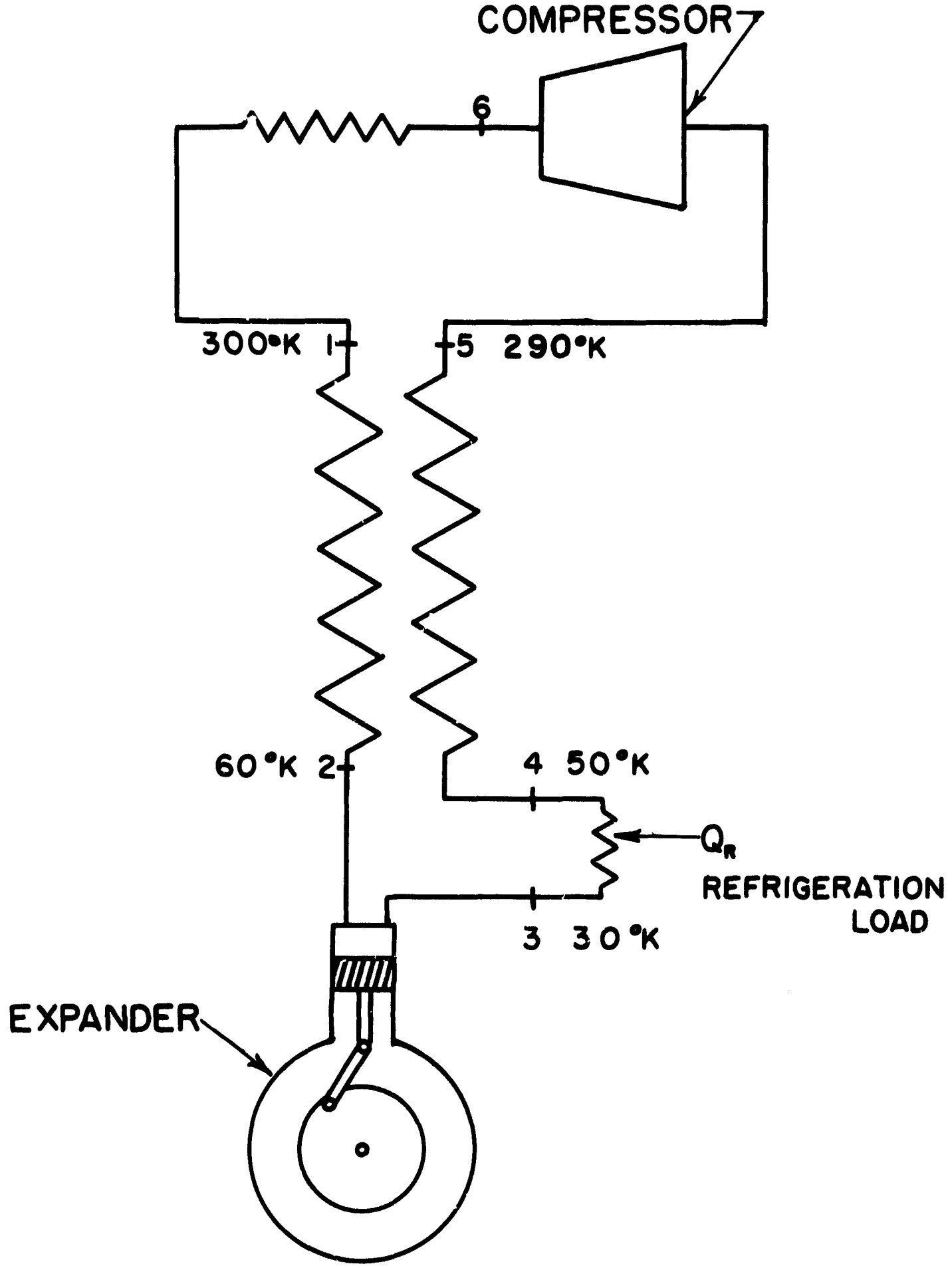

BASIC CRYOGENIC REFRIGERATOR SCHEMATIC

FIG. 2

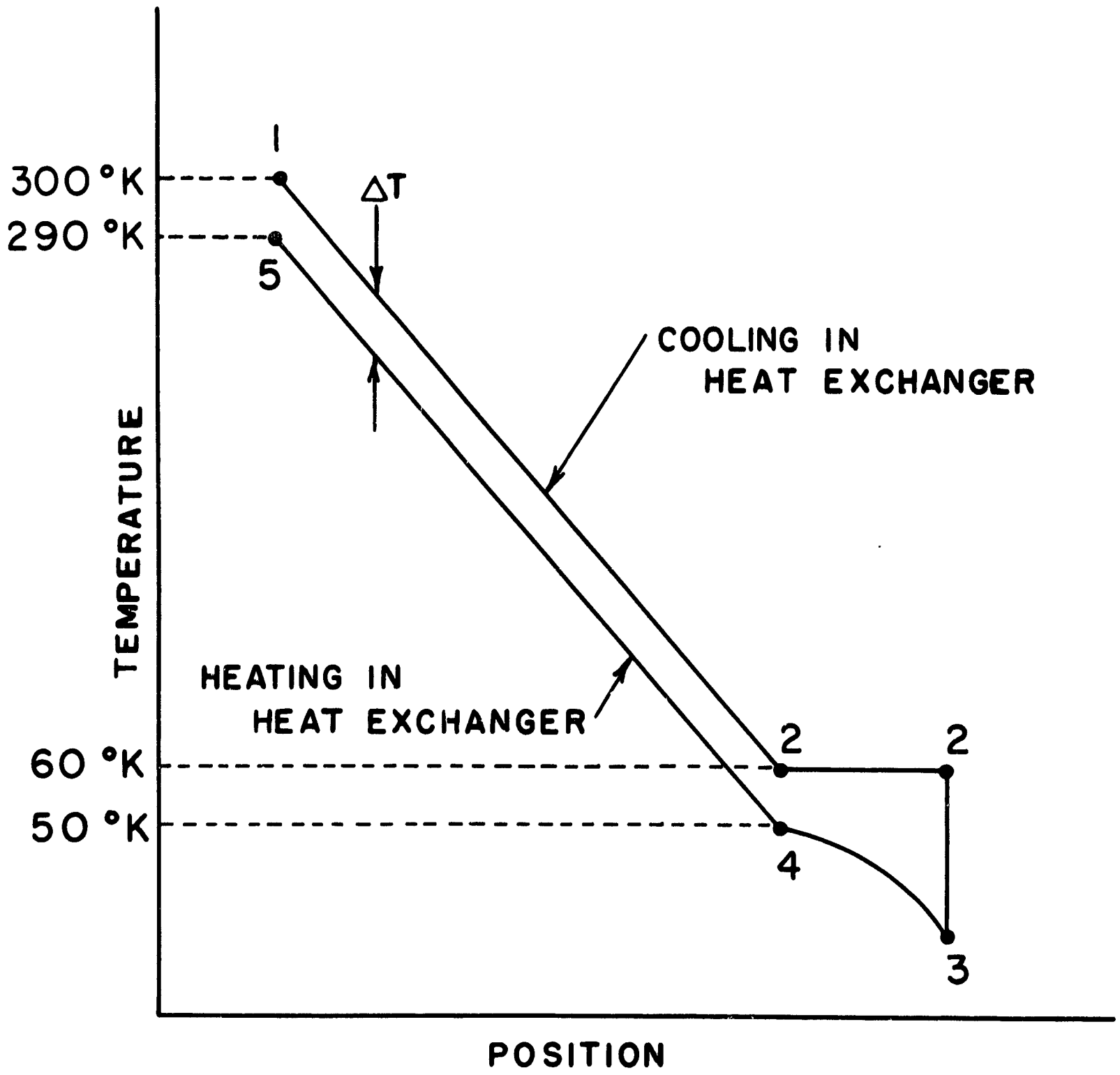

BASIC REFRIGATION TEMPERATURE PATTERN

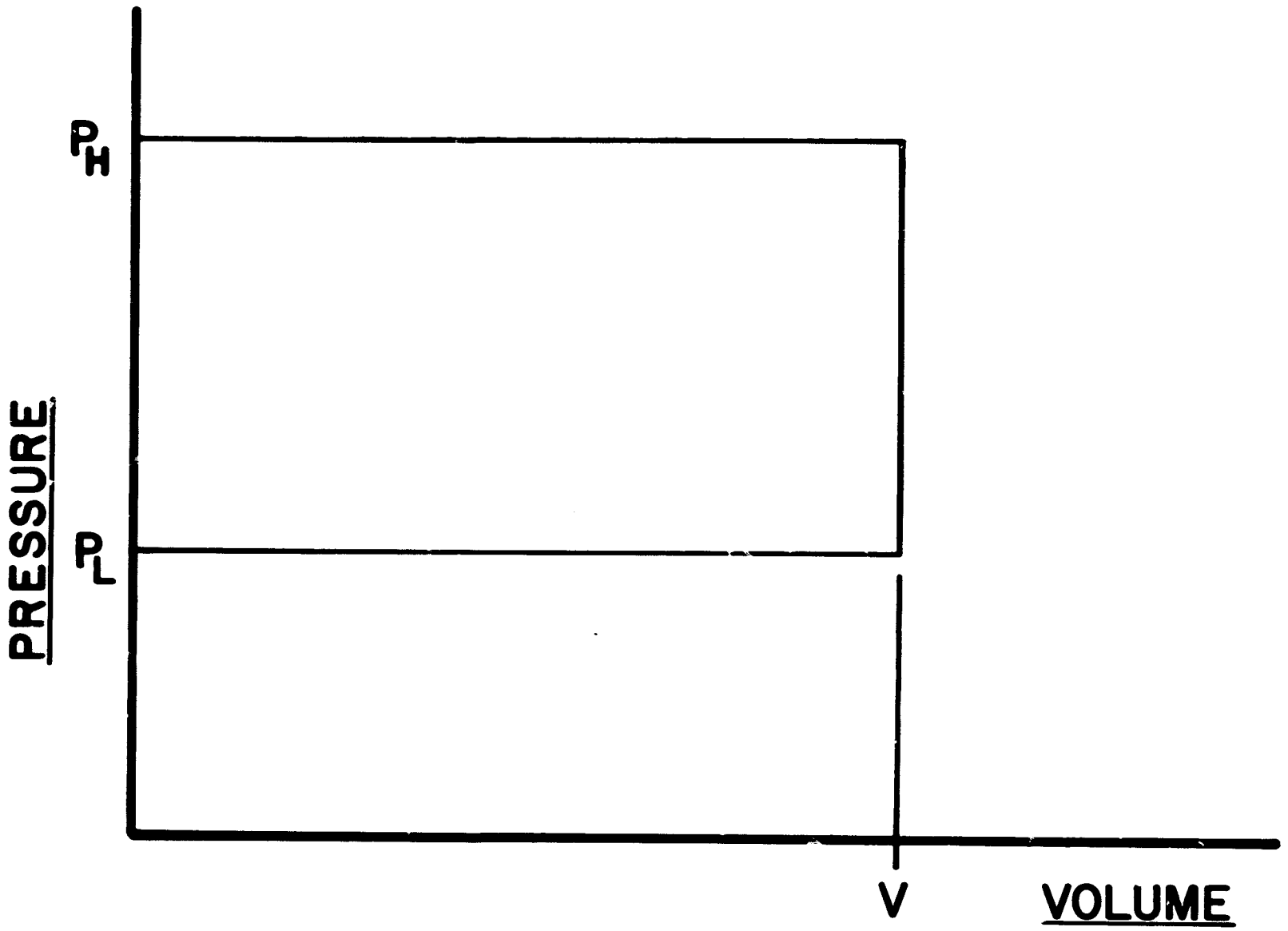

FIG. 3 PRESSURE - VOLUME DIAGRAM FOR A GAS BALANCING REFRIGERATOR

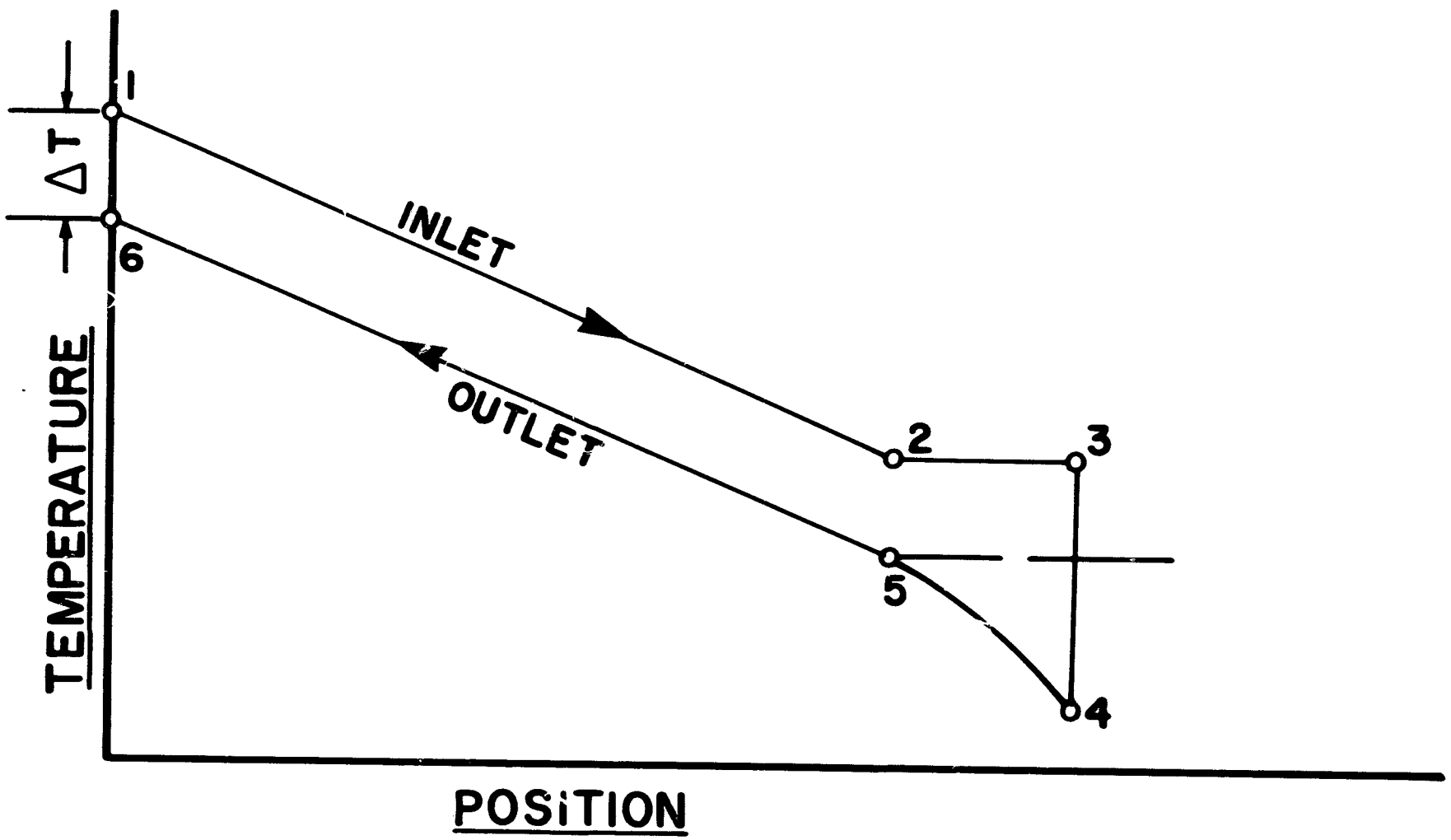

FIG. 4 TEMPERATURE POSITION DIAGRAM FOR A THERMAL REGENERATOR

FIG. 5

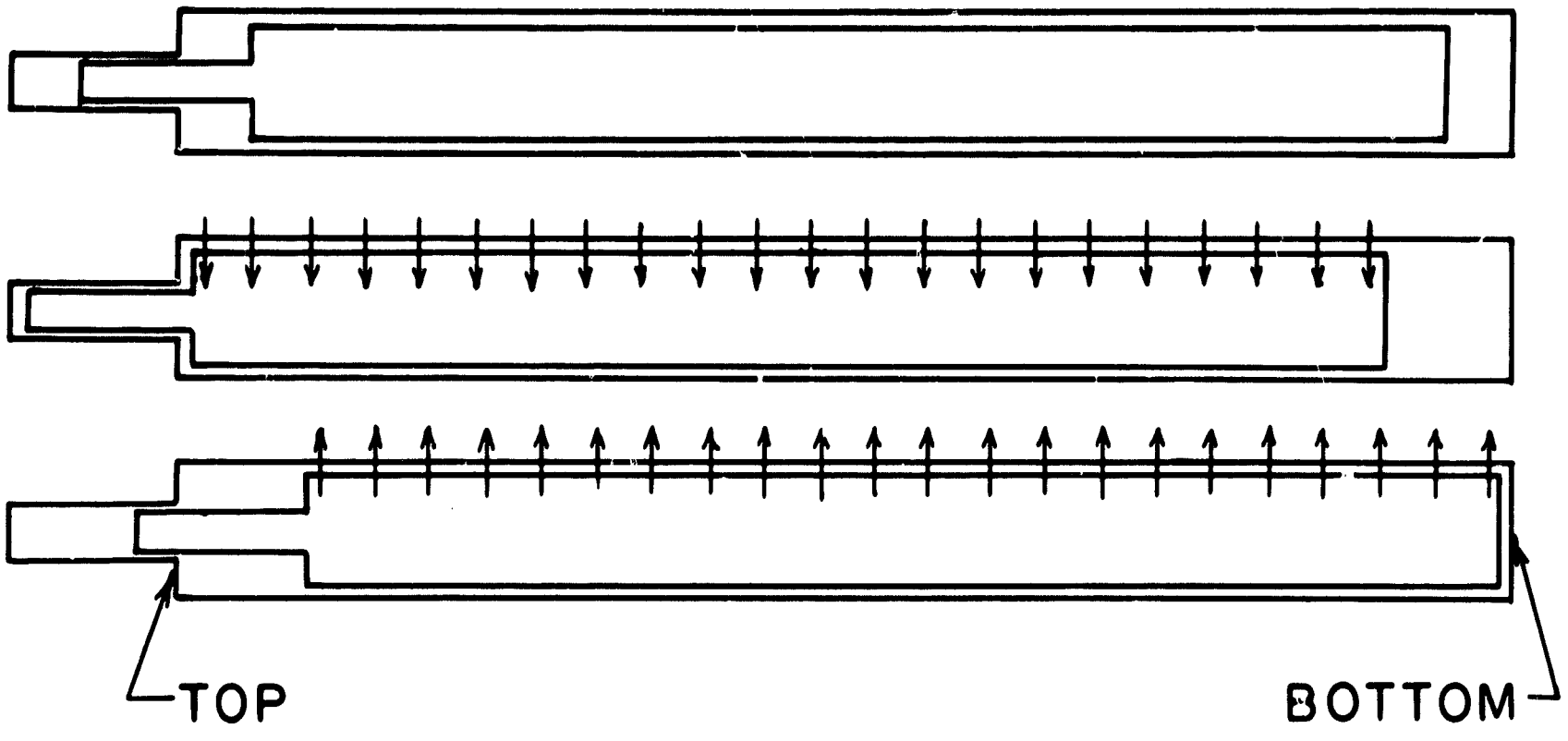

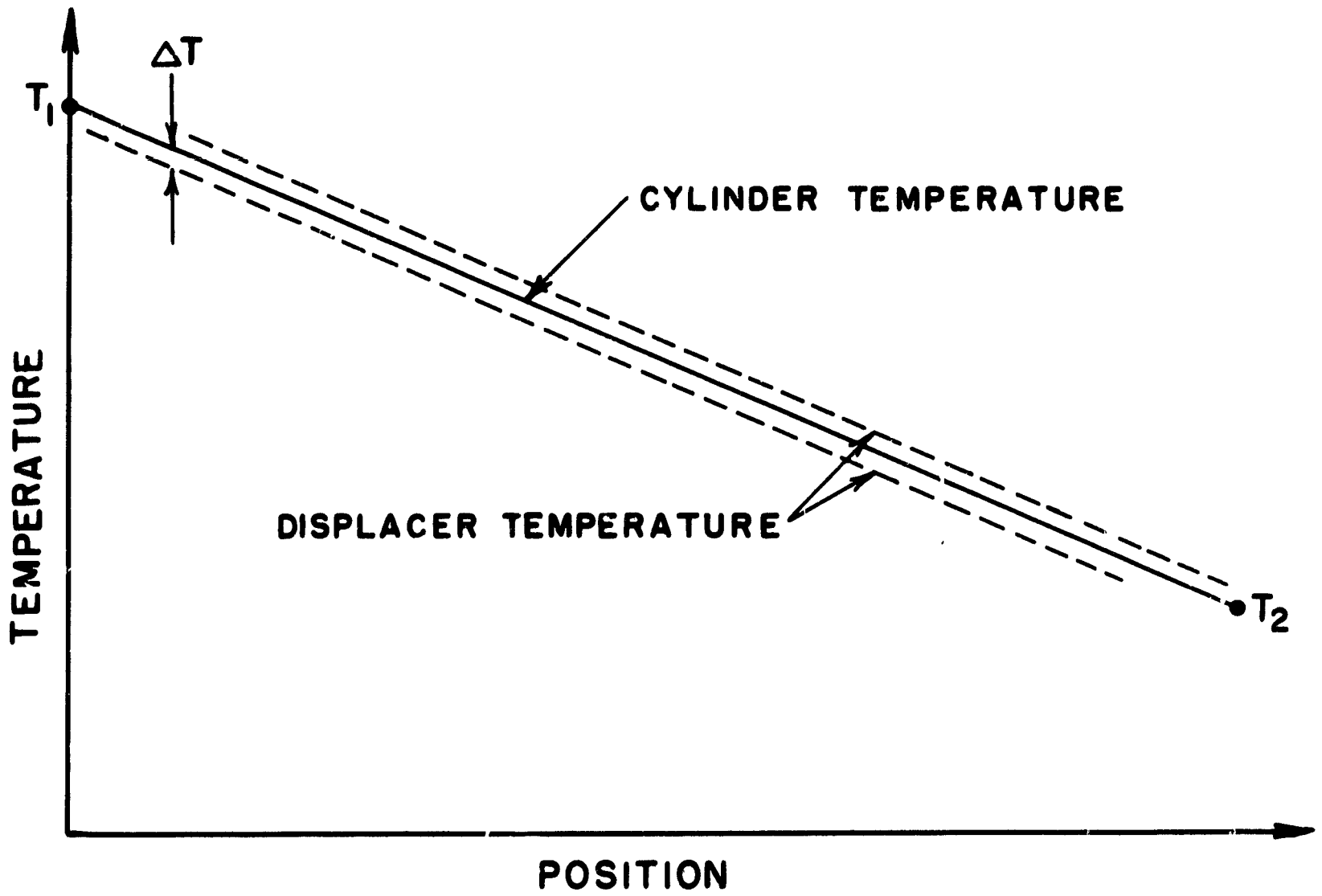

MOTIONAL HEAT TRANSFER TEMPERATURE PATTERN

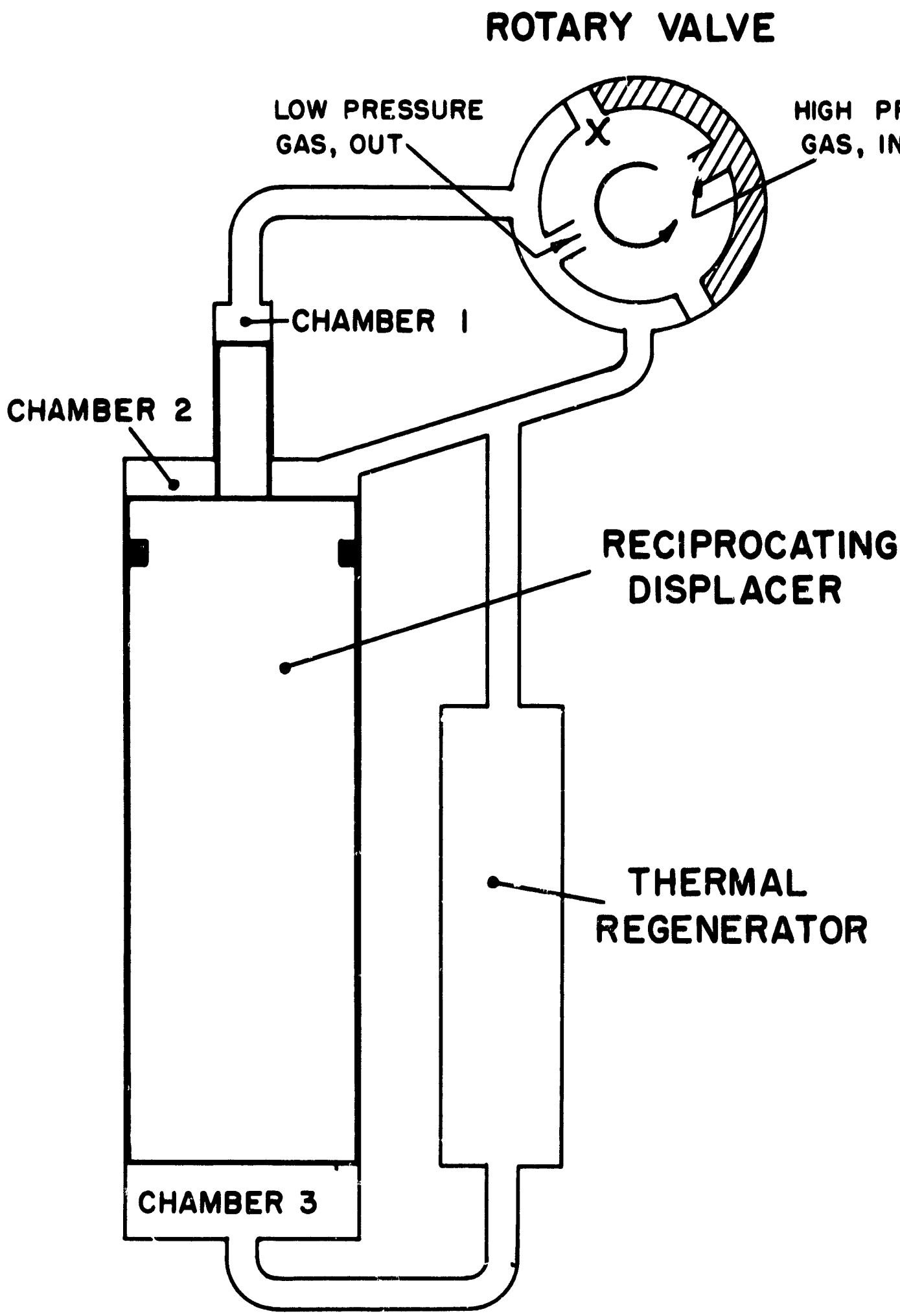

FIGURE 6 Single Stage Cryomatic Gas Balancing Refrigerator, Schematic Diagram

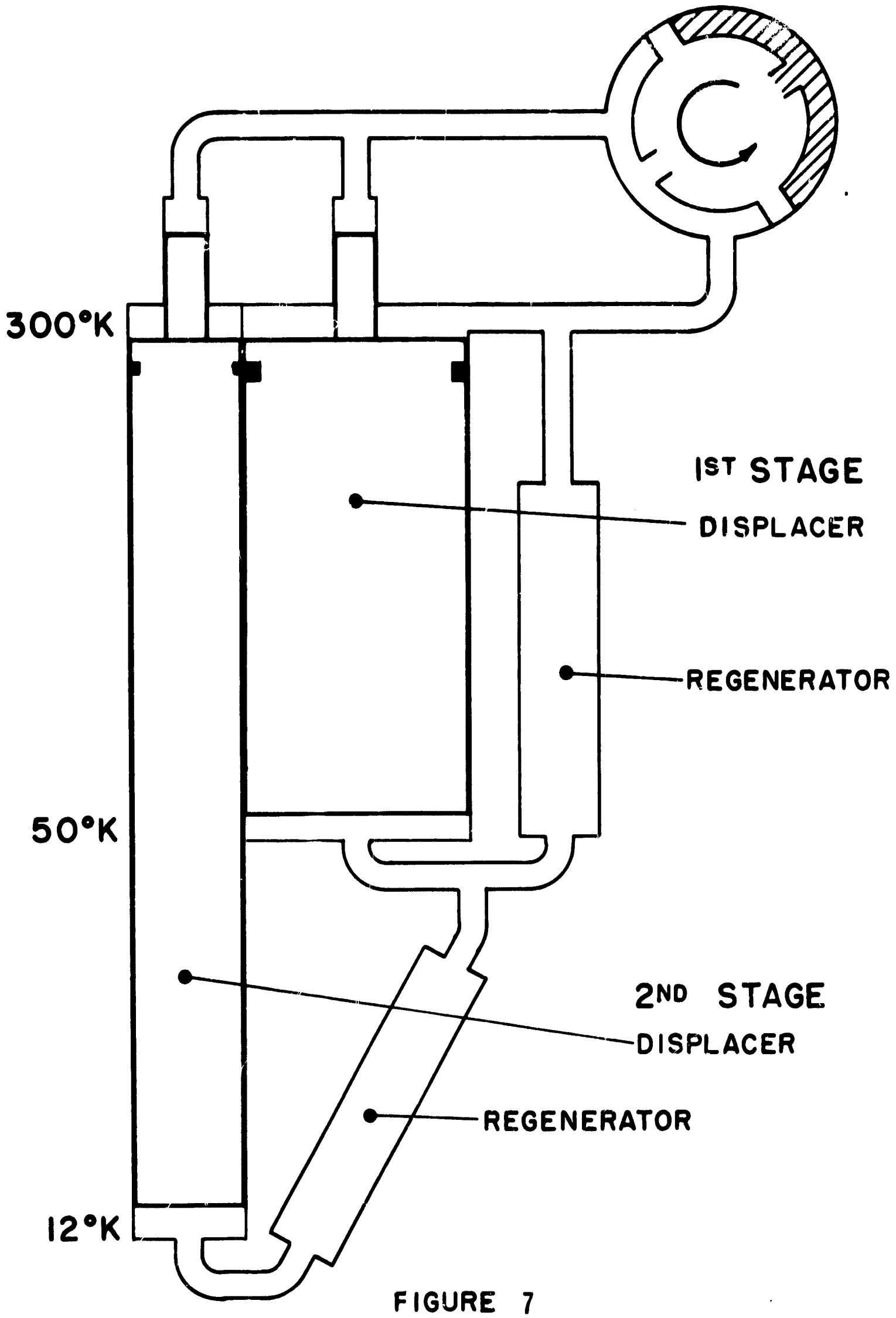

FIGURE 7

Two Stage Cryomatic Gas Balancing Refrigerator,
Schematic Diagram

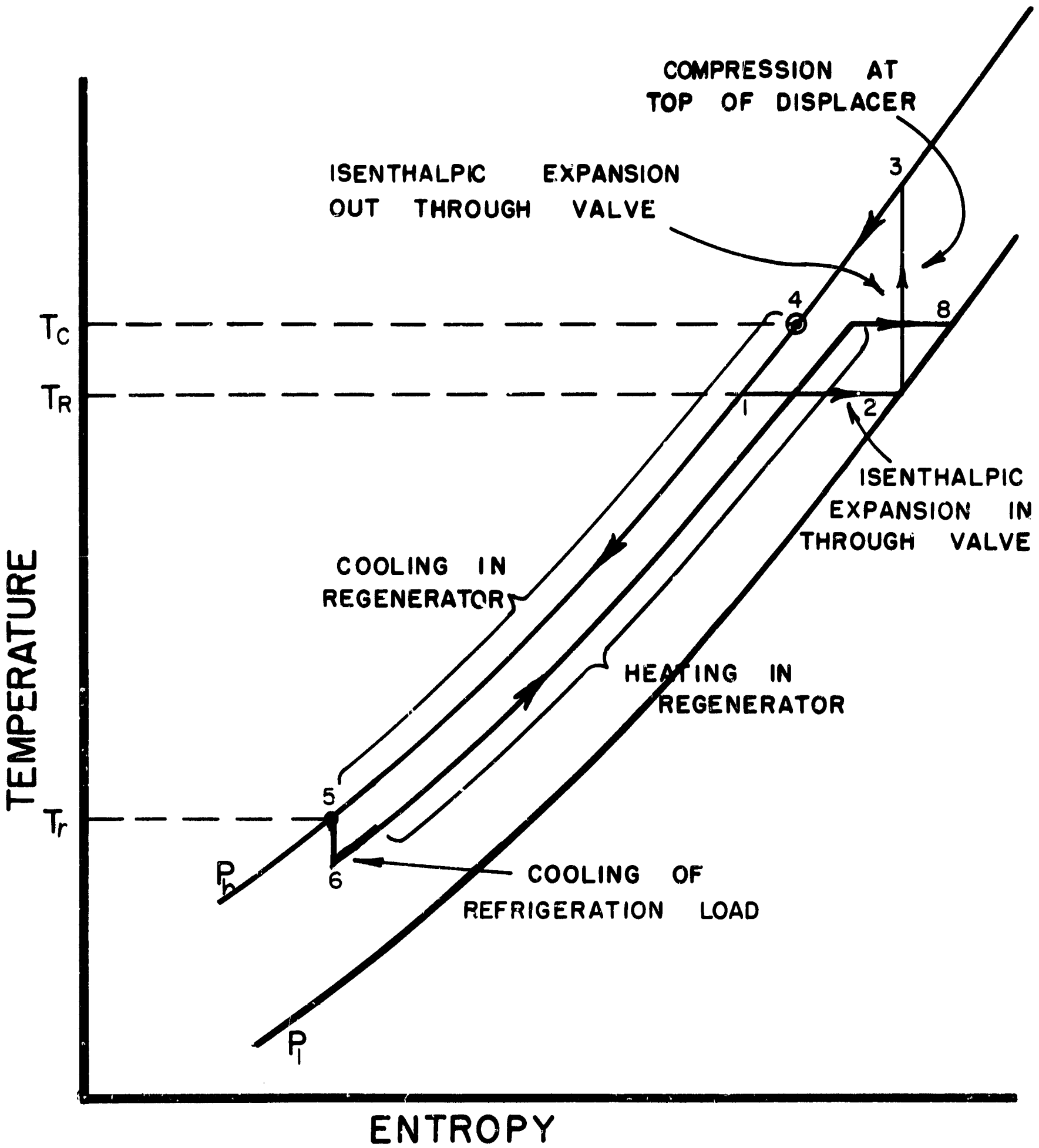

FIGURE 8. TEMPERATURE - ENTROPY DIAGRAM FOR FIRST BATCH OF GAS TO ENTER REFRIGERATOR

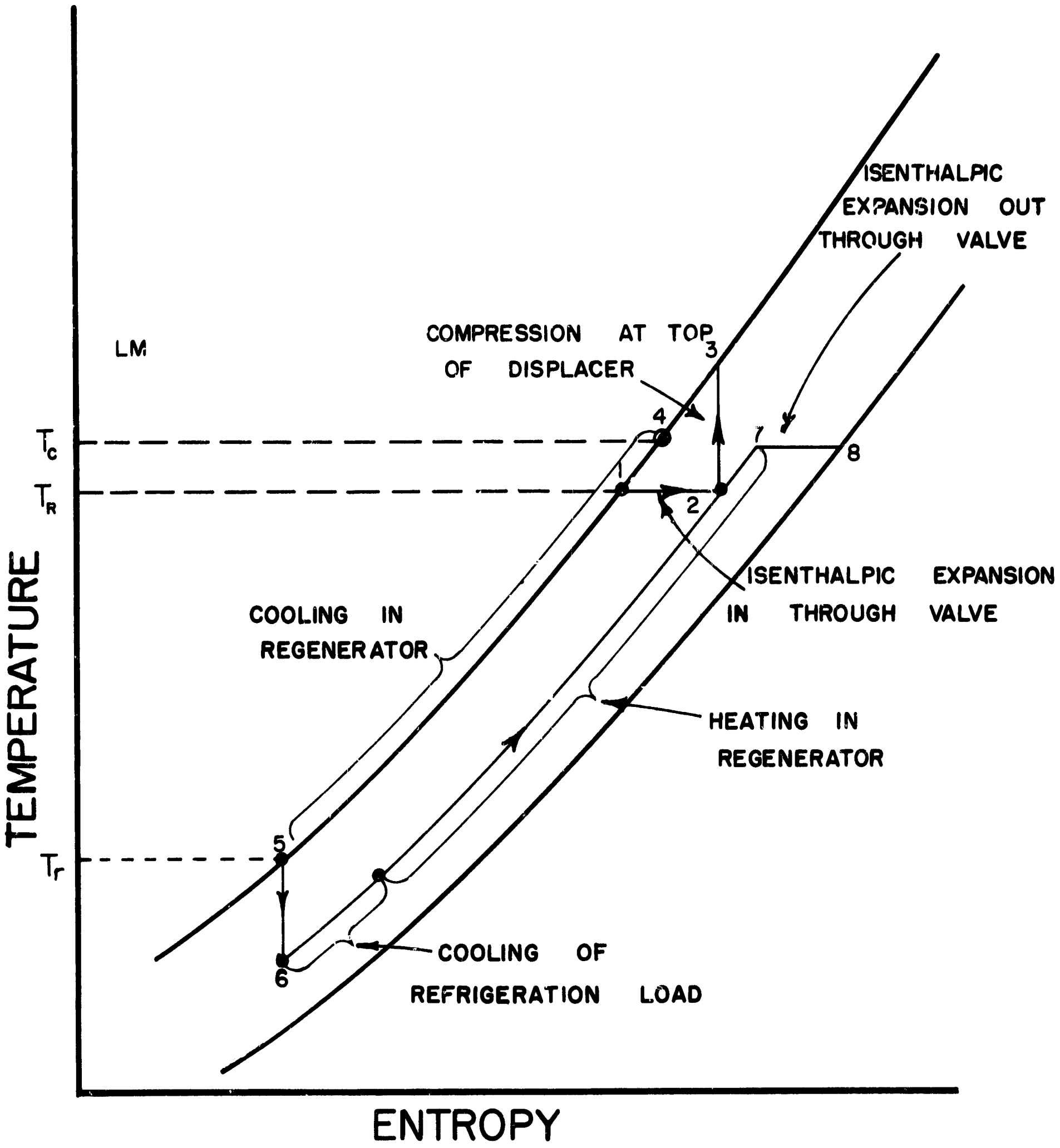

FIGURE 9 TEMPERATURE - ENTROPY DIAGRAM FOR BATCH OF GAS ENTERING THE REFRIGERATOR WHEN THE PRESSURE HAS BEEN BUILT UP HALF WAY.

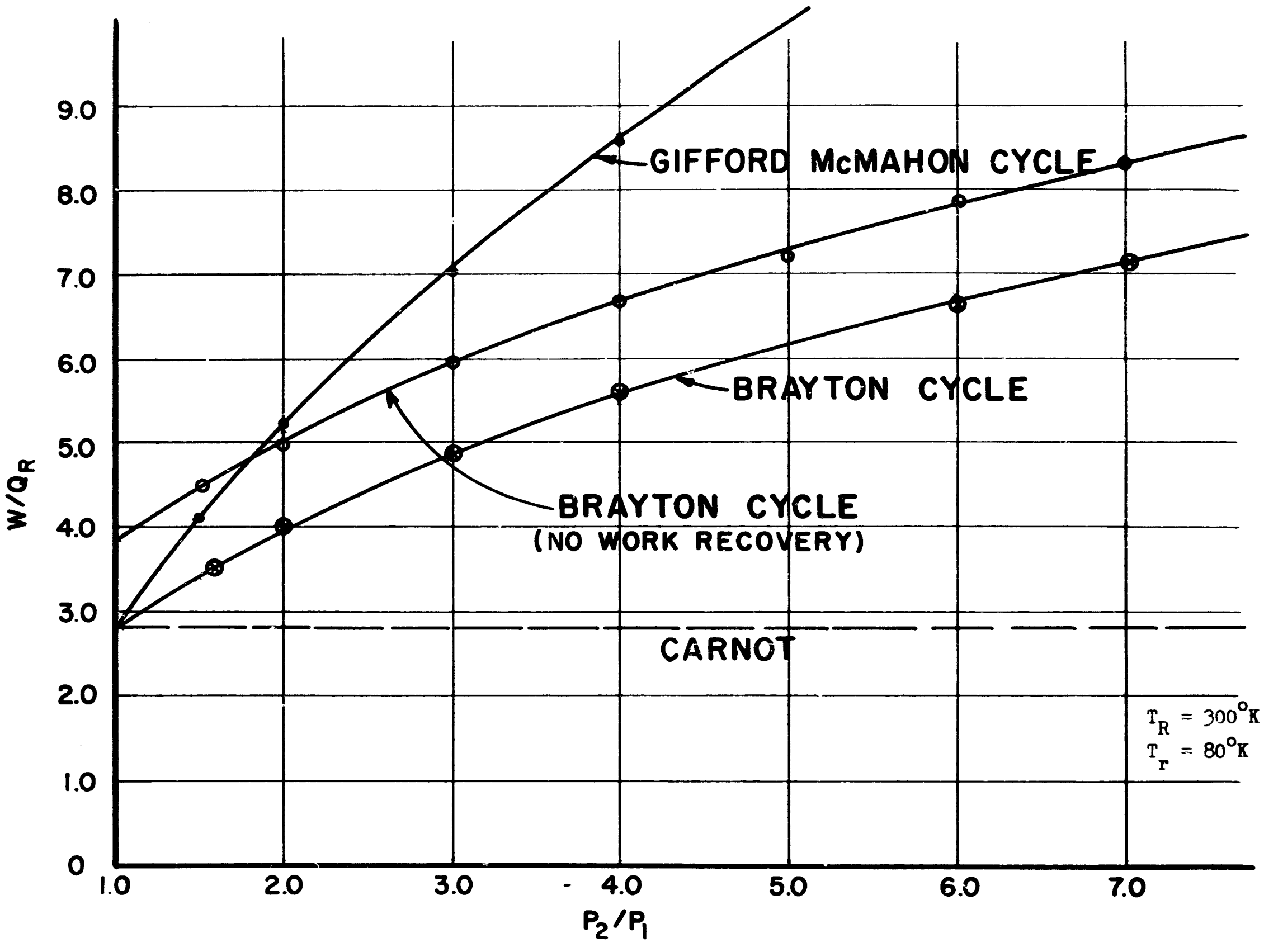

FIGURE 10 Refrigeration Cycle Performance Curves

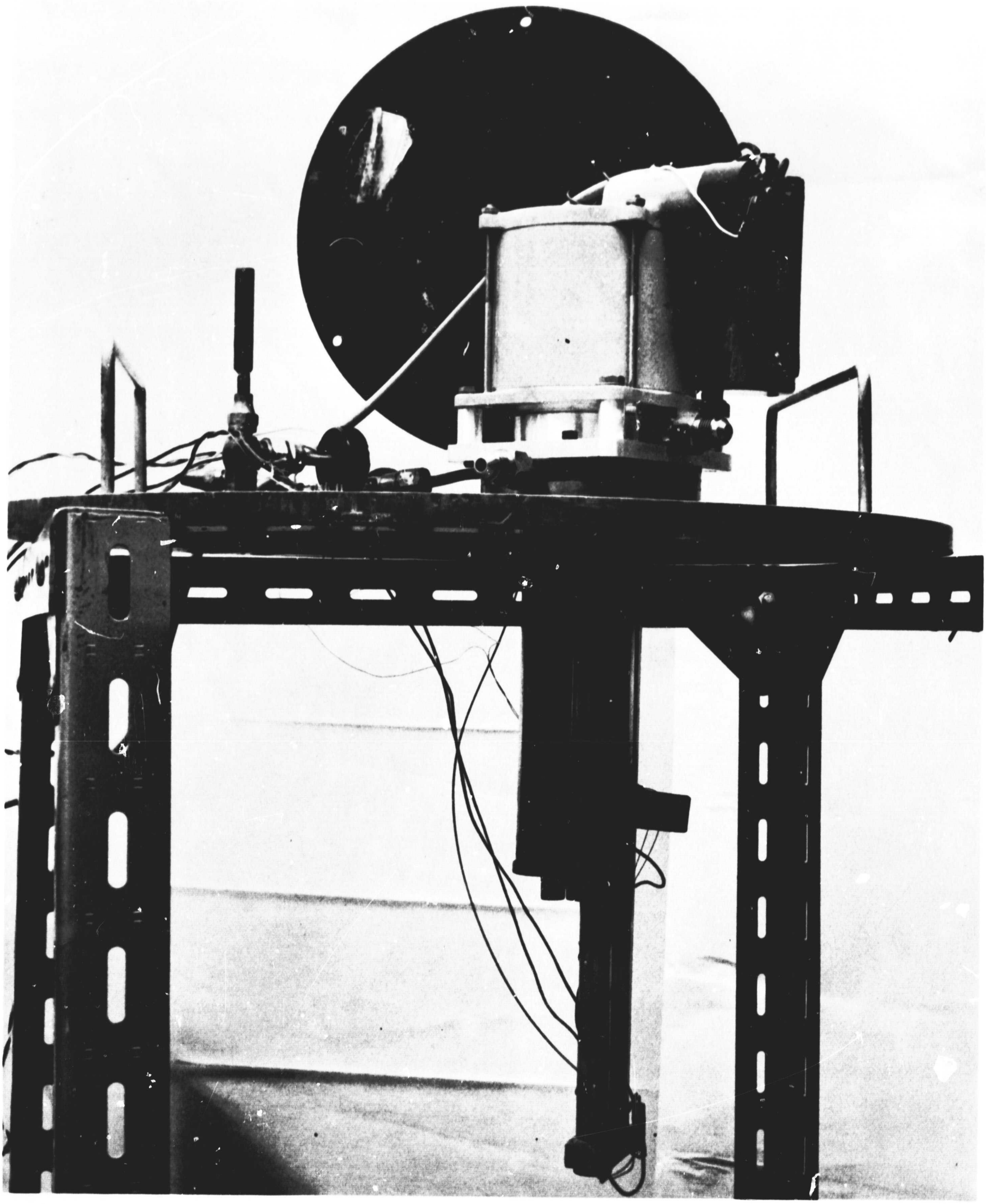

Figure 11 Two Stage Gas Balancing Refrigerator Model

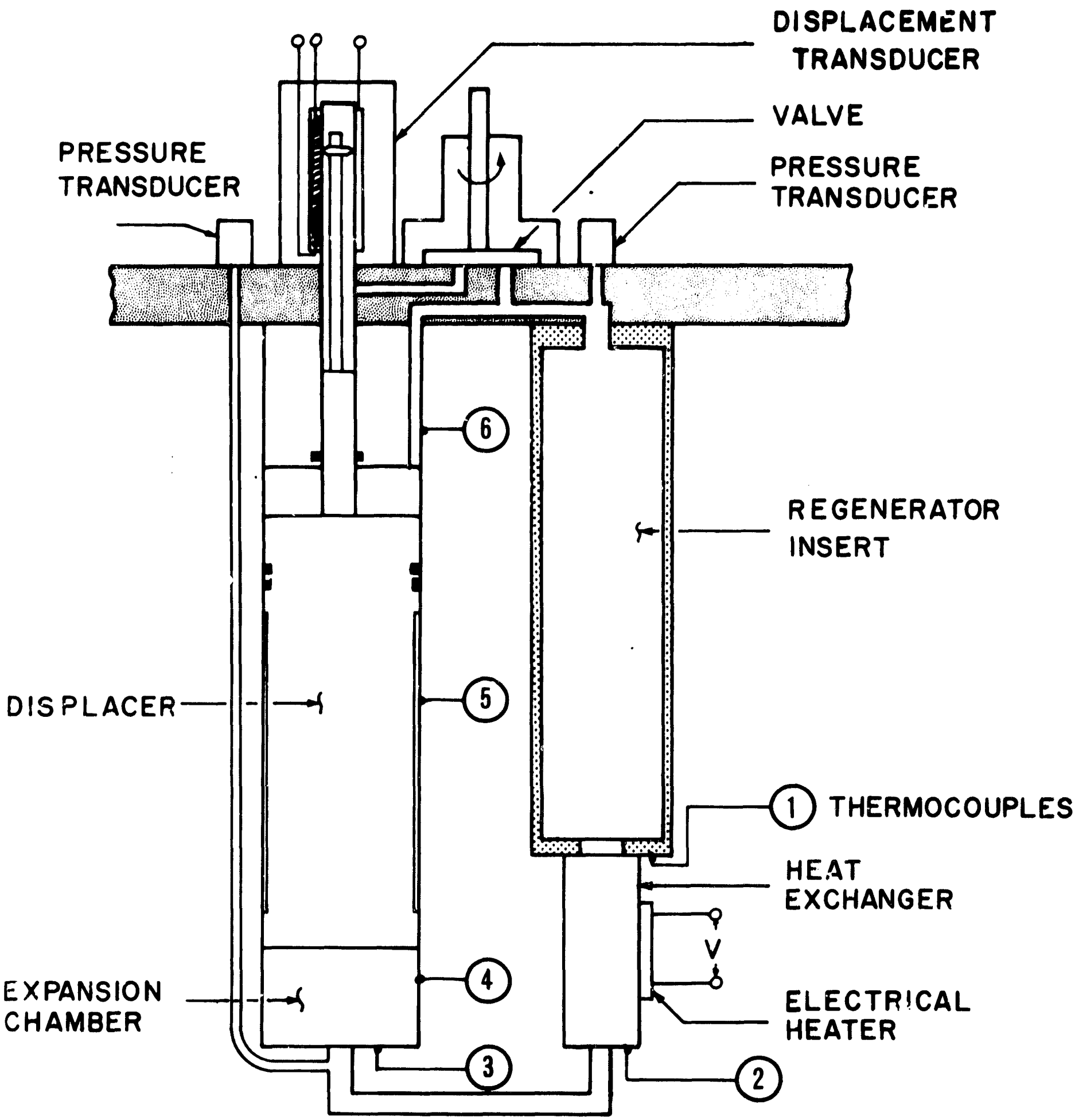

FIG 12 SINGLE STAGE GAS BALANCING TEST REFRIGERATOR

FIG 13 TEST APPARATUS SETUP

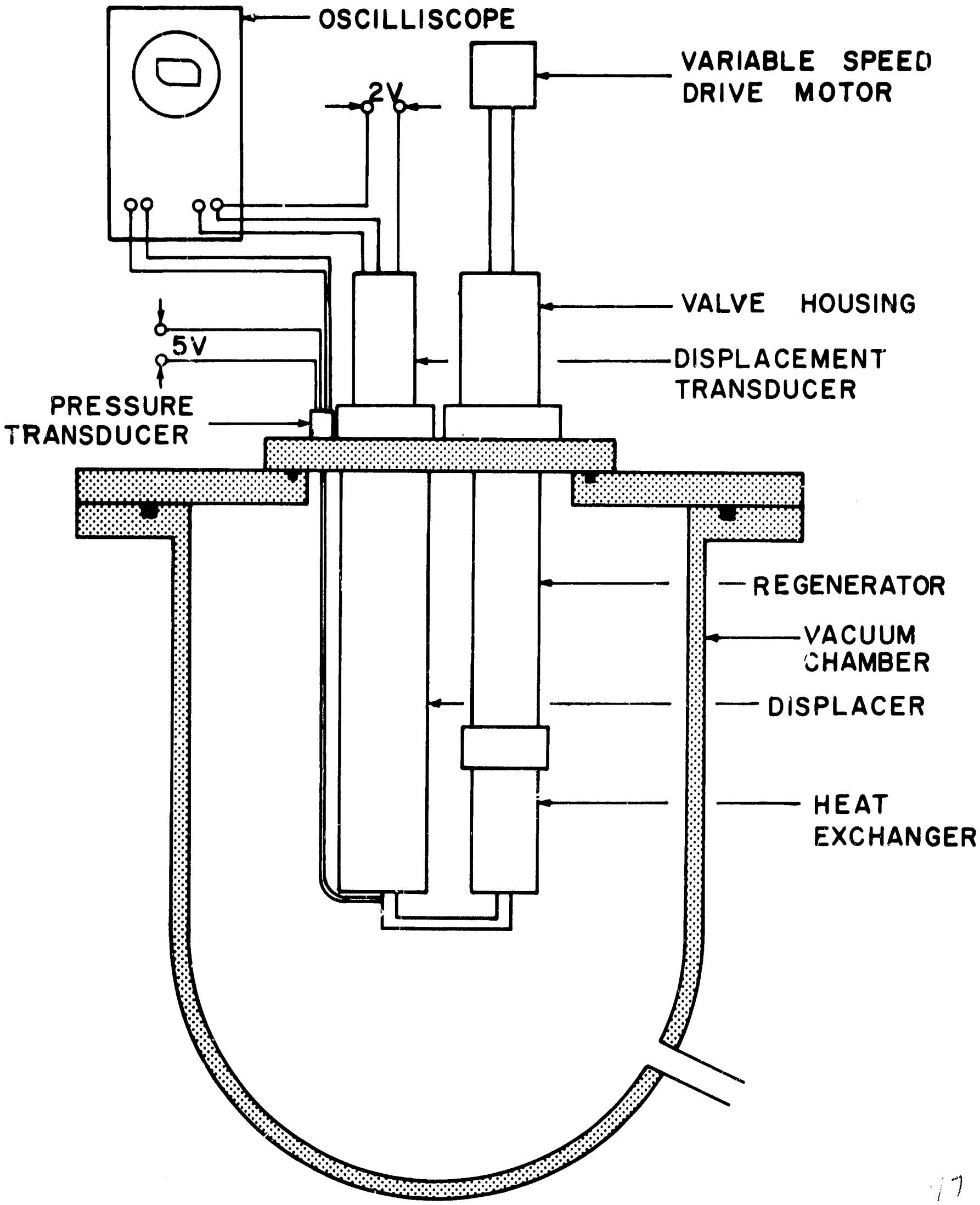

FIG 14 PRESSURE VOLUME DIAGRAM

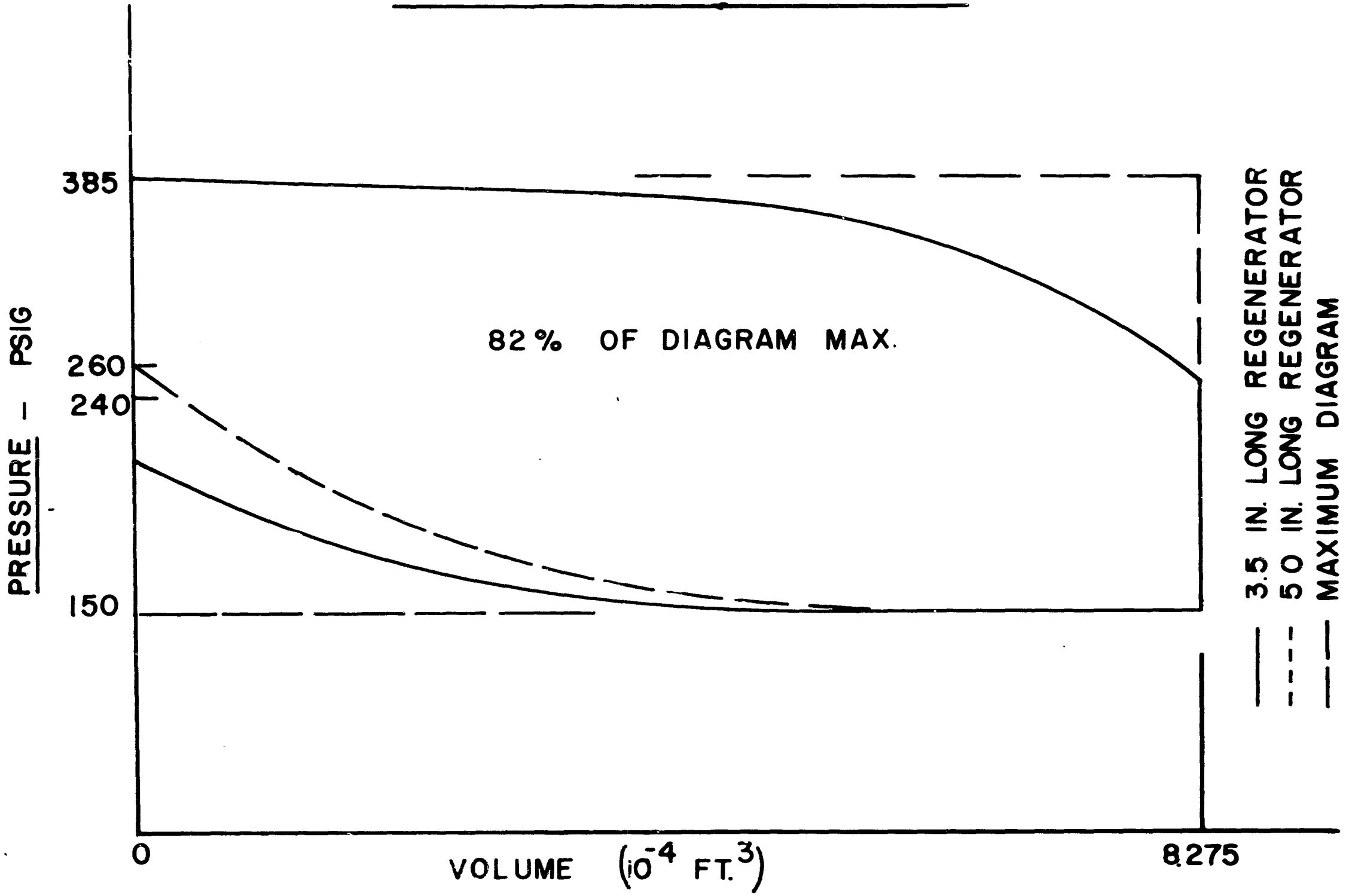

FIG 15 VARIATION OF AVAILABLE REFRIGERATION AS A FUNCTION OF DISPLACER SPEED

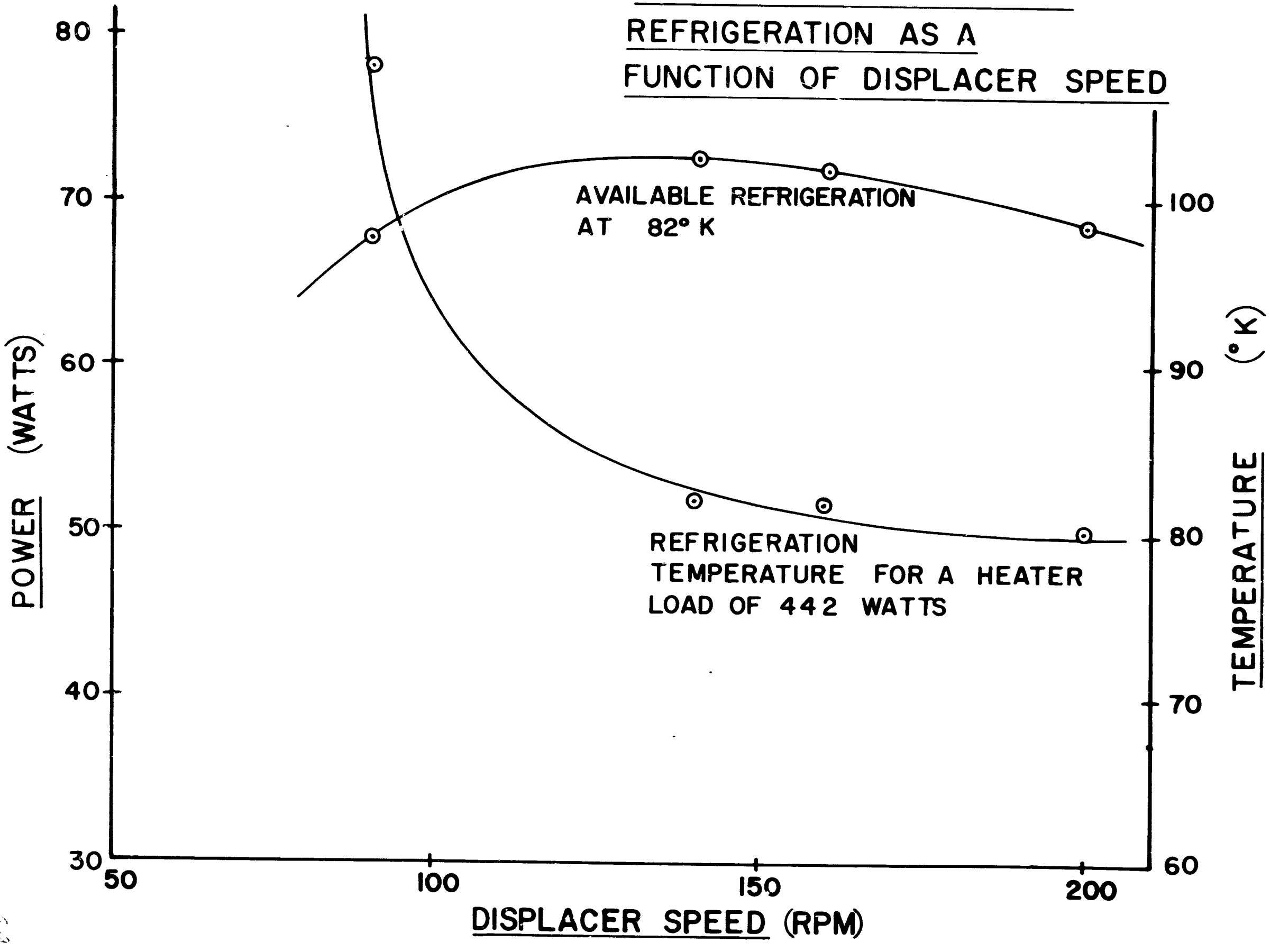

FIG 15 VARIATION OF AVAILABLE REFRIGERATION AS A FUNCTION OF DISPLACER SPEED

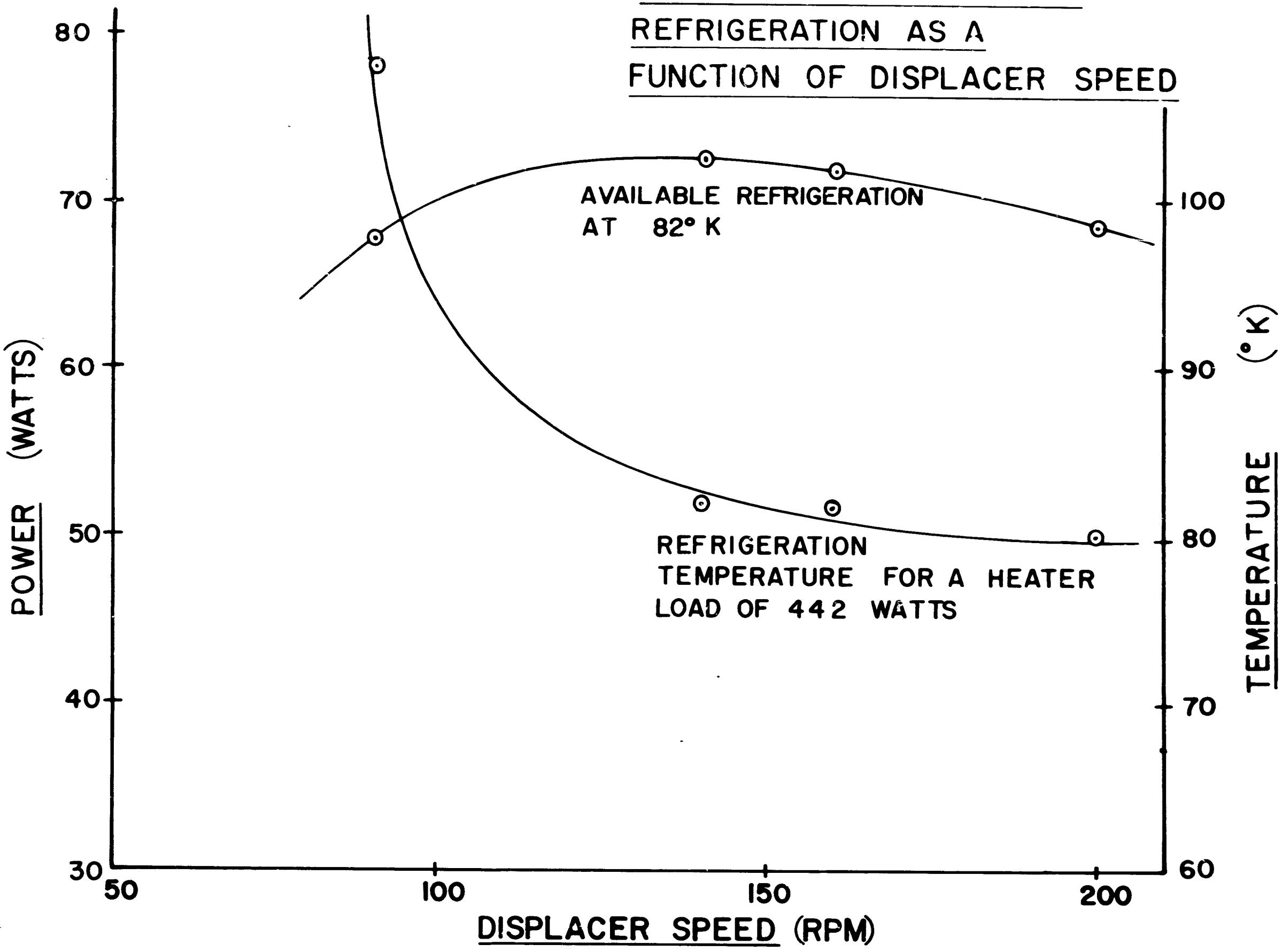

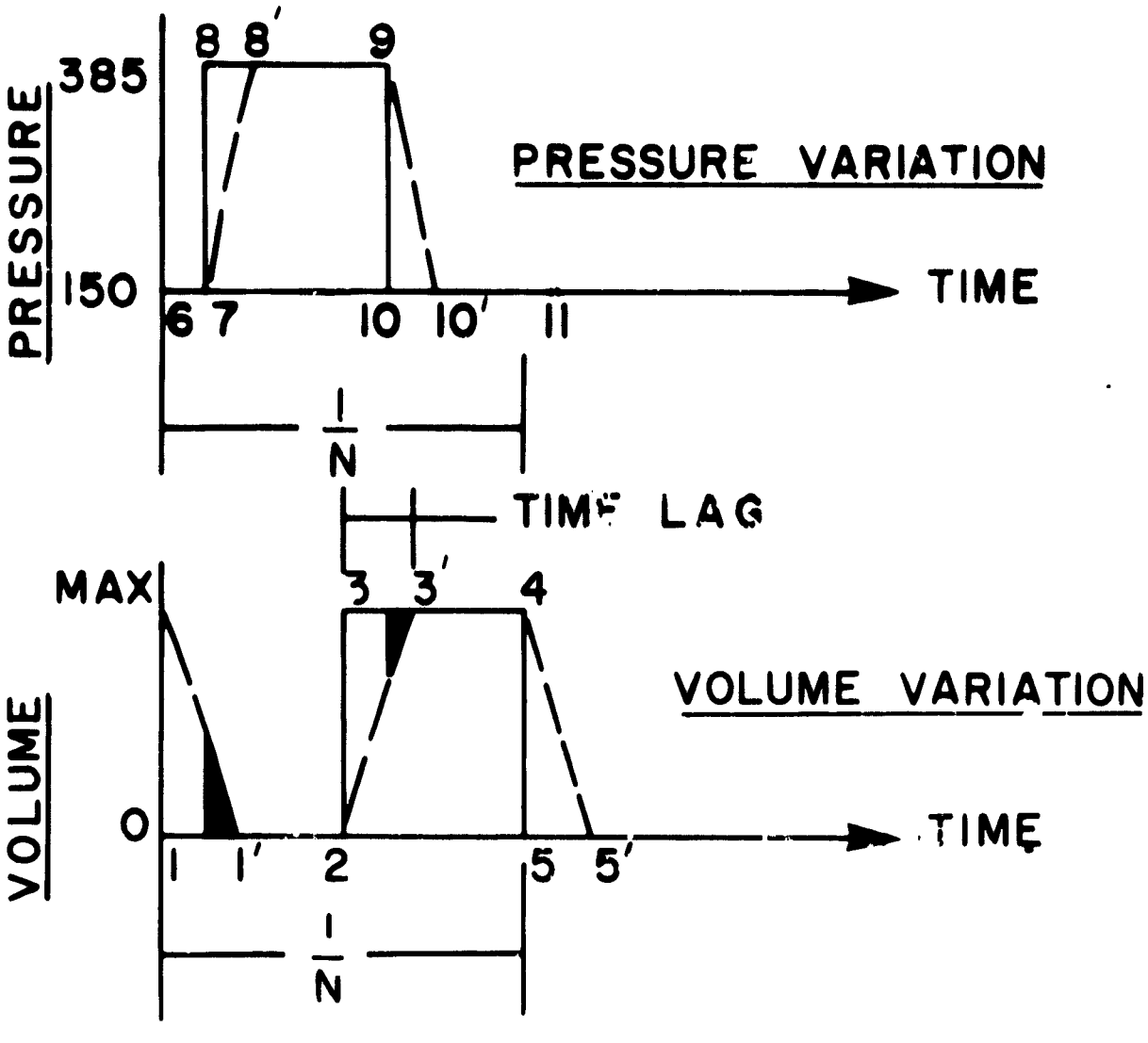

(a) PRESSURE & VOLUME TIME VARIATIONS

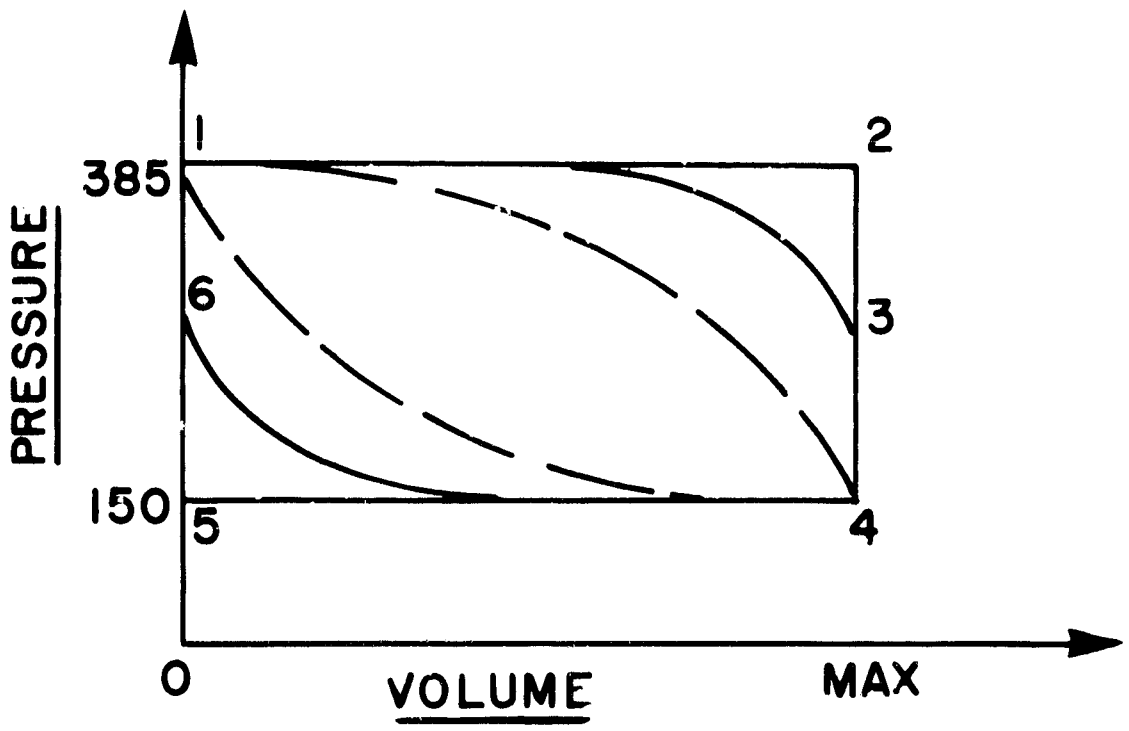

(b) PRESSURE VOLUME DIAGRAM

FIG 16

Pressure and Volume Changes with Time

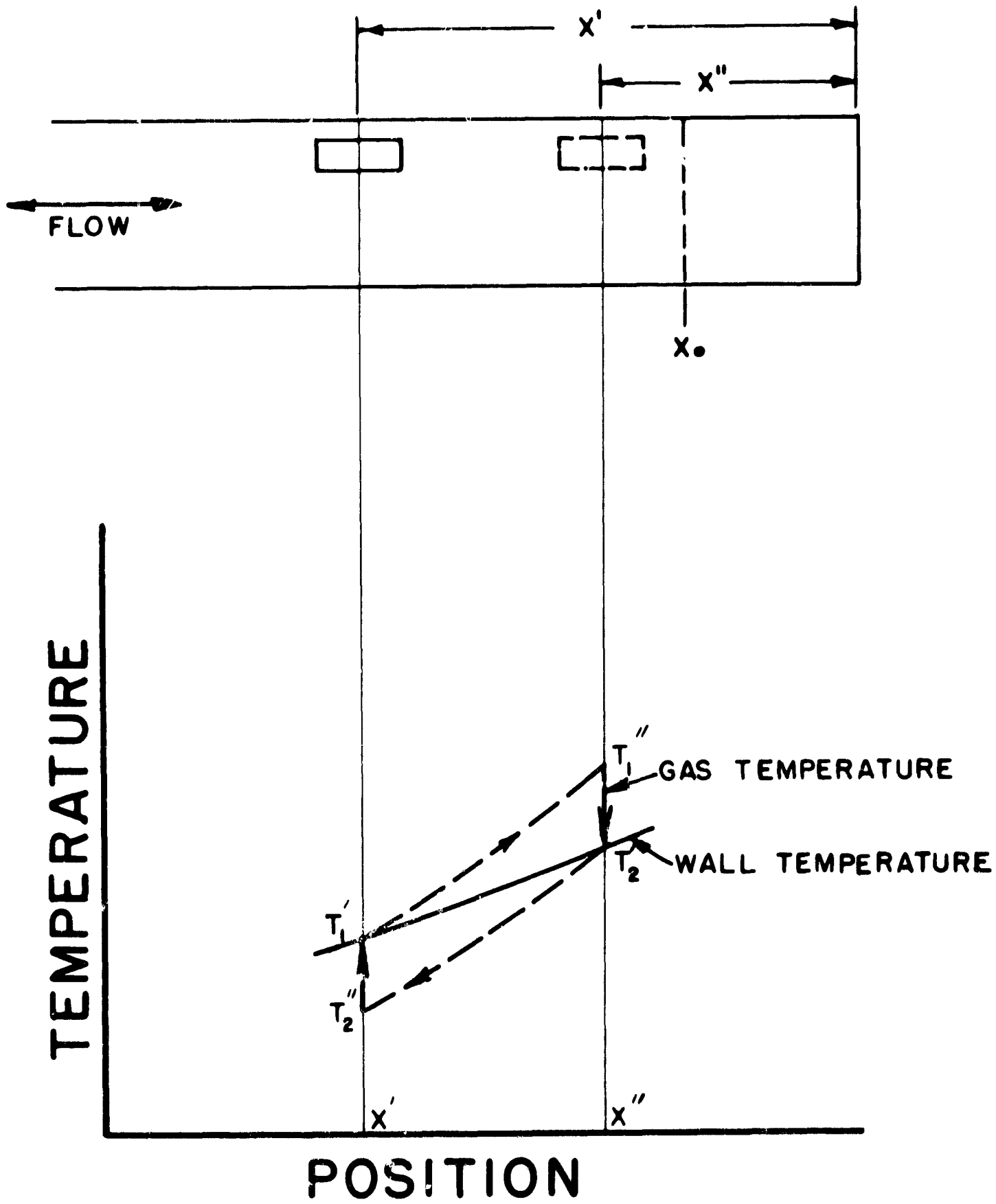

FIG. 17 GAS AND WALL TEMPERATURE vs. POSITION FOR SURFACE HEAT PUMPING CYCLE

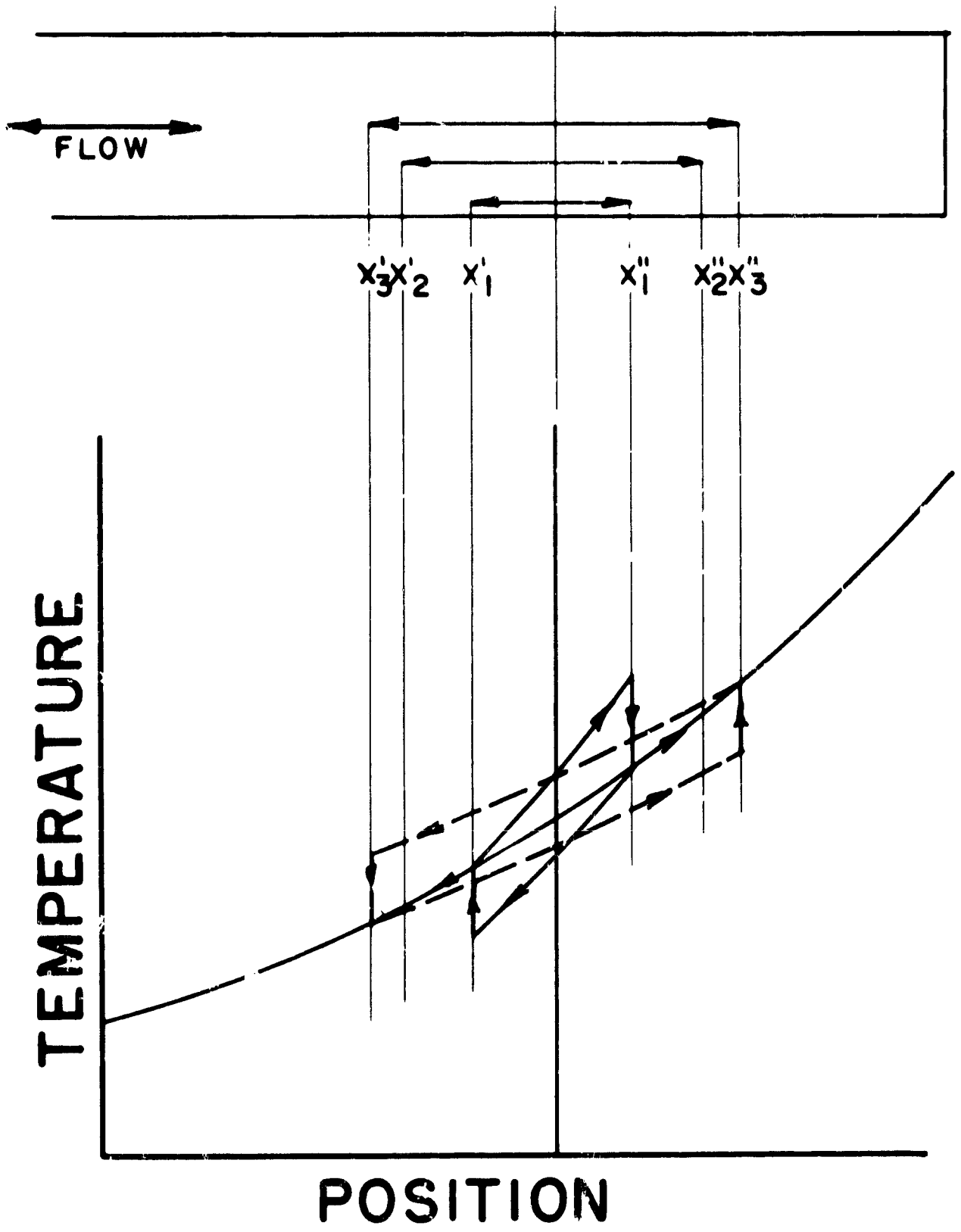

FIG. 18 GAS AND WALL TEMPERATURE vs. POSITION FOR ELEMENTS AT DIFFERENT RADII WITH VISCOUS EFFECTS

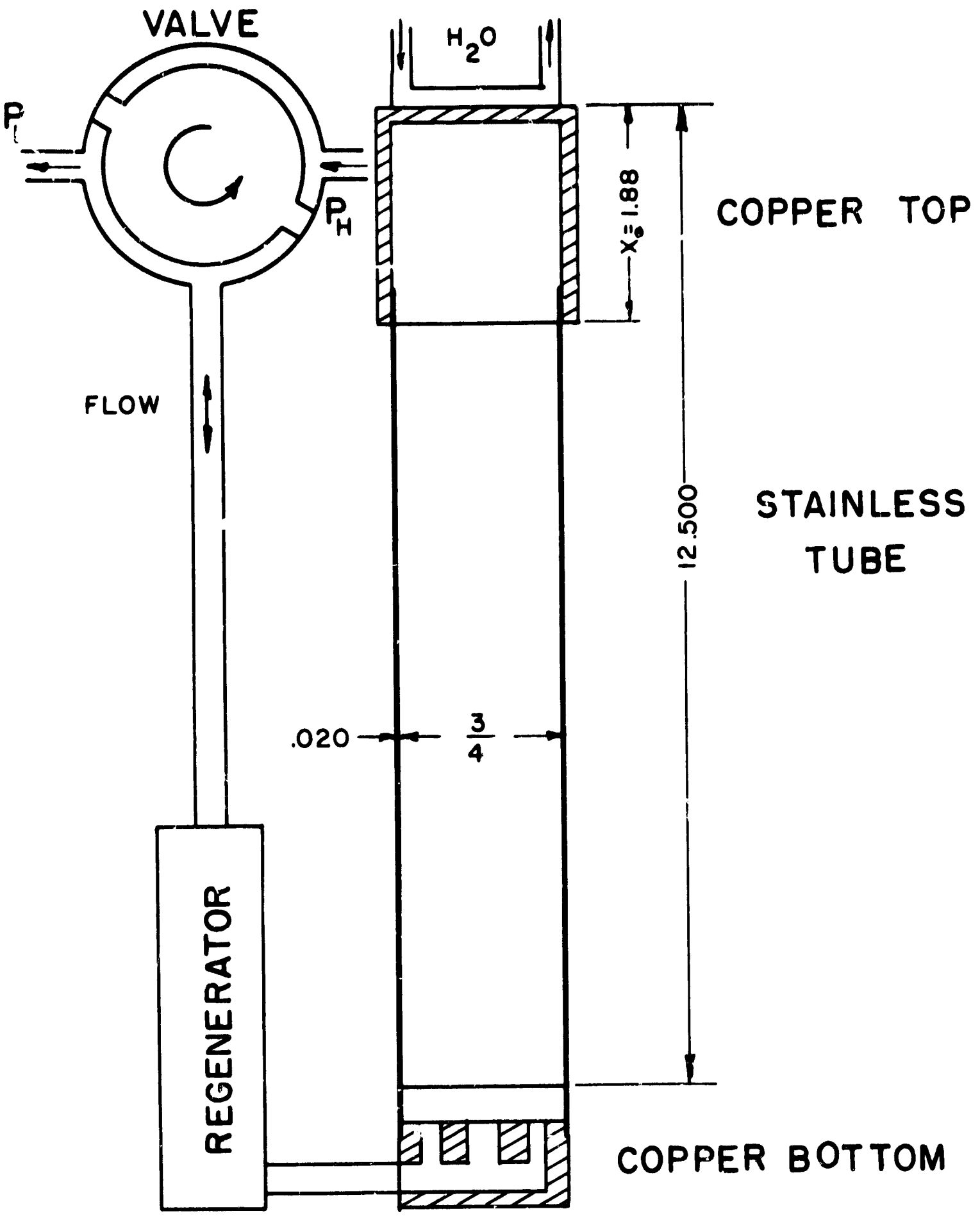

FIG. 19 PULSE TUBE REFRIGERATOR CONFIGURATION

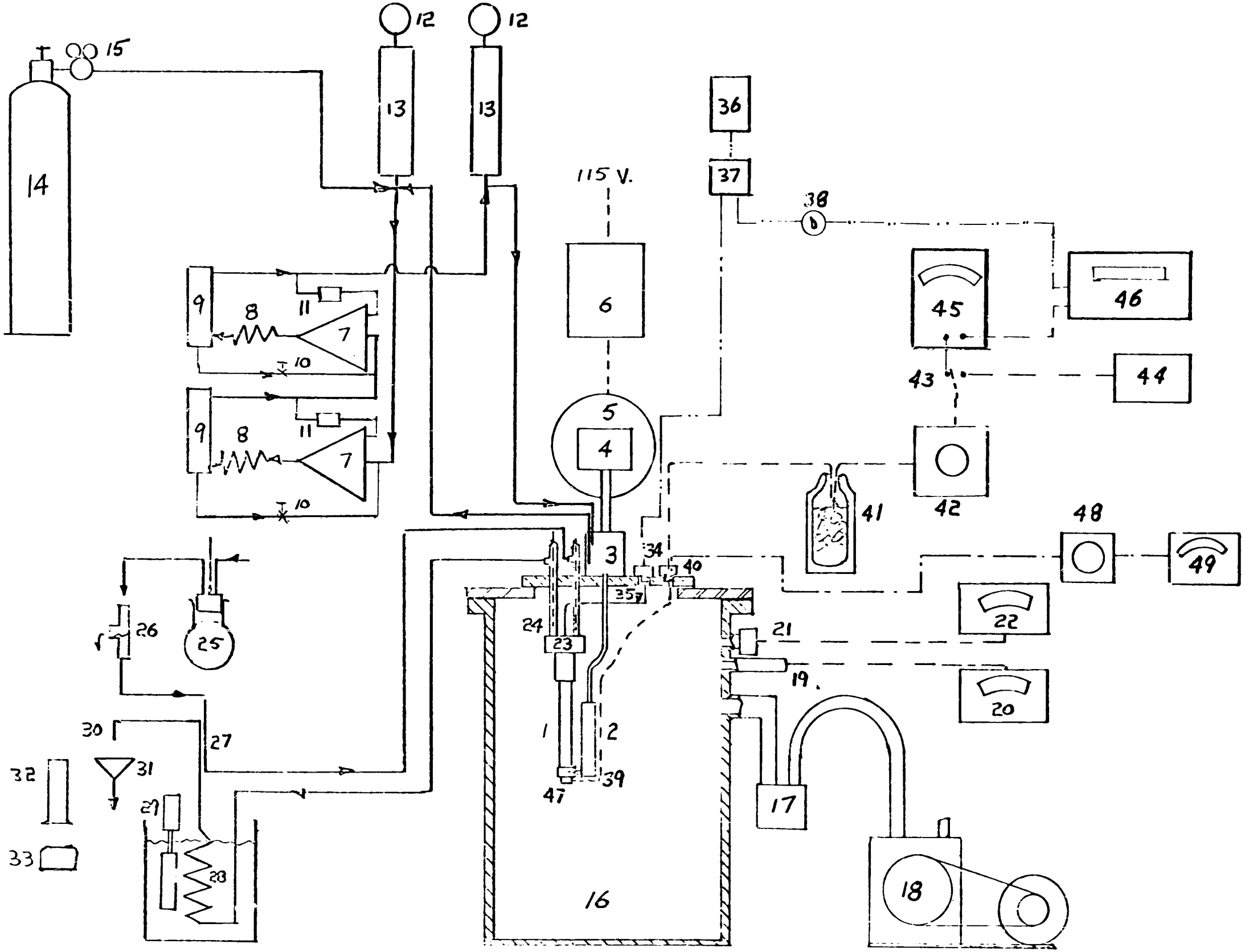

FIG. 20 **TEST SET UP**

TEST SET UP COMPONENTS (Figure 20)

Pulse Tube Refrigerator

1. Pulse tube
2. Regenerator

Variable Speed Drive

3. Valve
4. Speed reducer
5. D.C. Motor
6. Speed controller

Compressor System

7. Compressors
8. Aftercoolers
9. Oil separators
10. By-pass valves
11. Pressure cutouts
12. Pressure gauges
13. Surge tanks
14. Helium supply
15. Pressure regulator

Vacuum System

16. Vacuum pot
17. Diffusion pump
18. Fore pump
19. Discharge gauge tube
20. Discharge gauge
21. Parani gauge tube
22. Parani gauge

Calorimeter

23. Heat sink
24. Thermocouples
25. Water de-aerator
26. Constant head overflow
27. Heat exchanger
28. Temperature equalizer
29. Stirrer
30. Adjustable head
31. Drain
32. Burette
33. Timer

Pressure Transducer

34. Transducer
35. Connecting tube
36. Power supply
37. Bridge balance
38. Calibrating resistance

Temperature measurement

39. Thermocouple wire
40. Vacuum lead through
41. Ice bath
42. Switch box
43. Knife switch
44. Millivolt meter
45. Millivolt meter - Amplifier
46. Oscillograph

Heater

47. Resistance heater
48. Transformer
49. Voltmeter

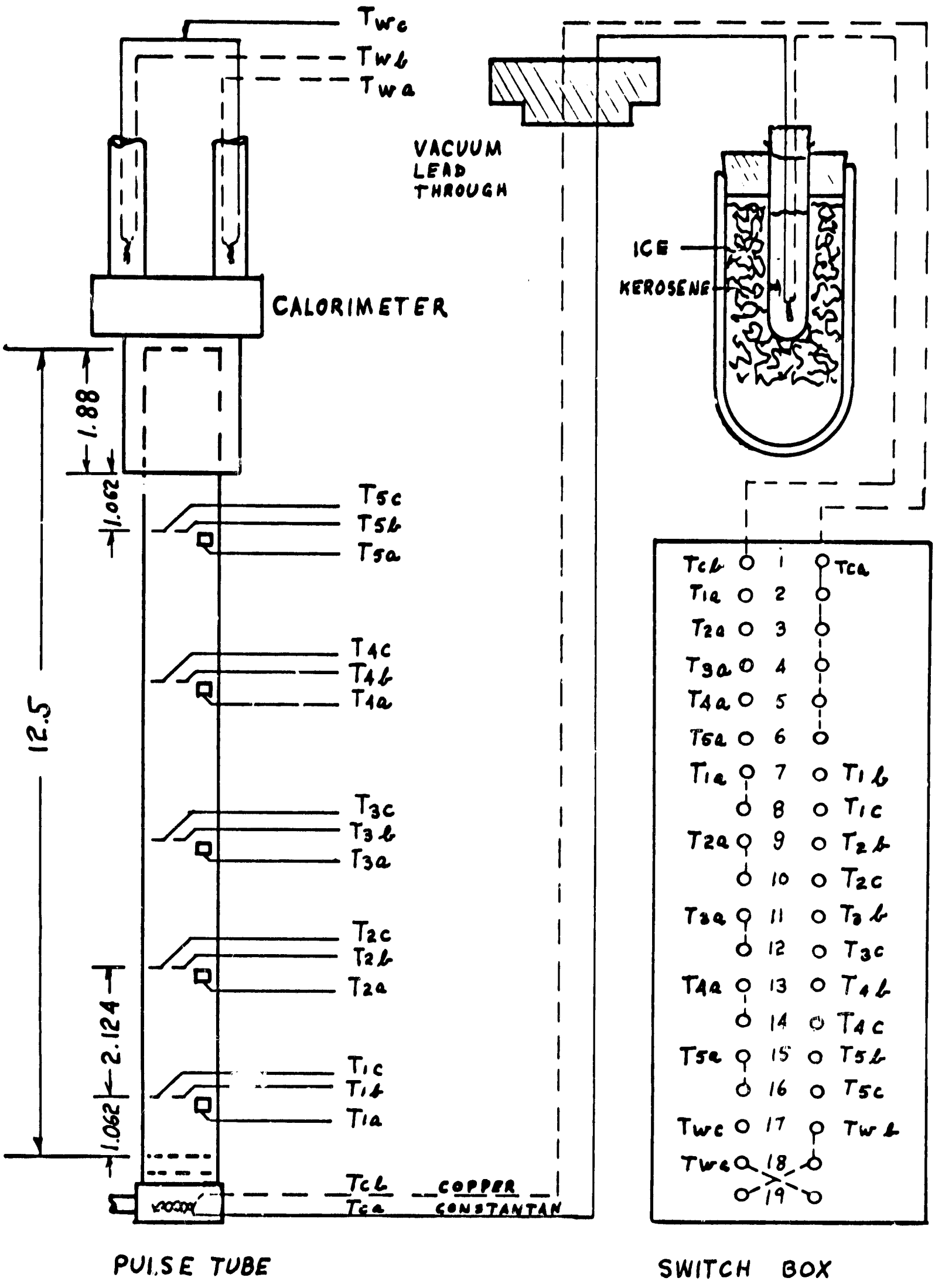

Figure 21 Schematic Diagram of Thermocouple Circuit

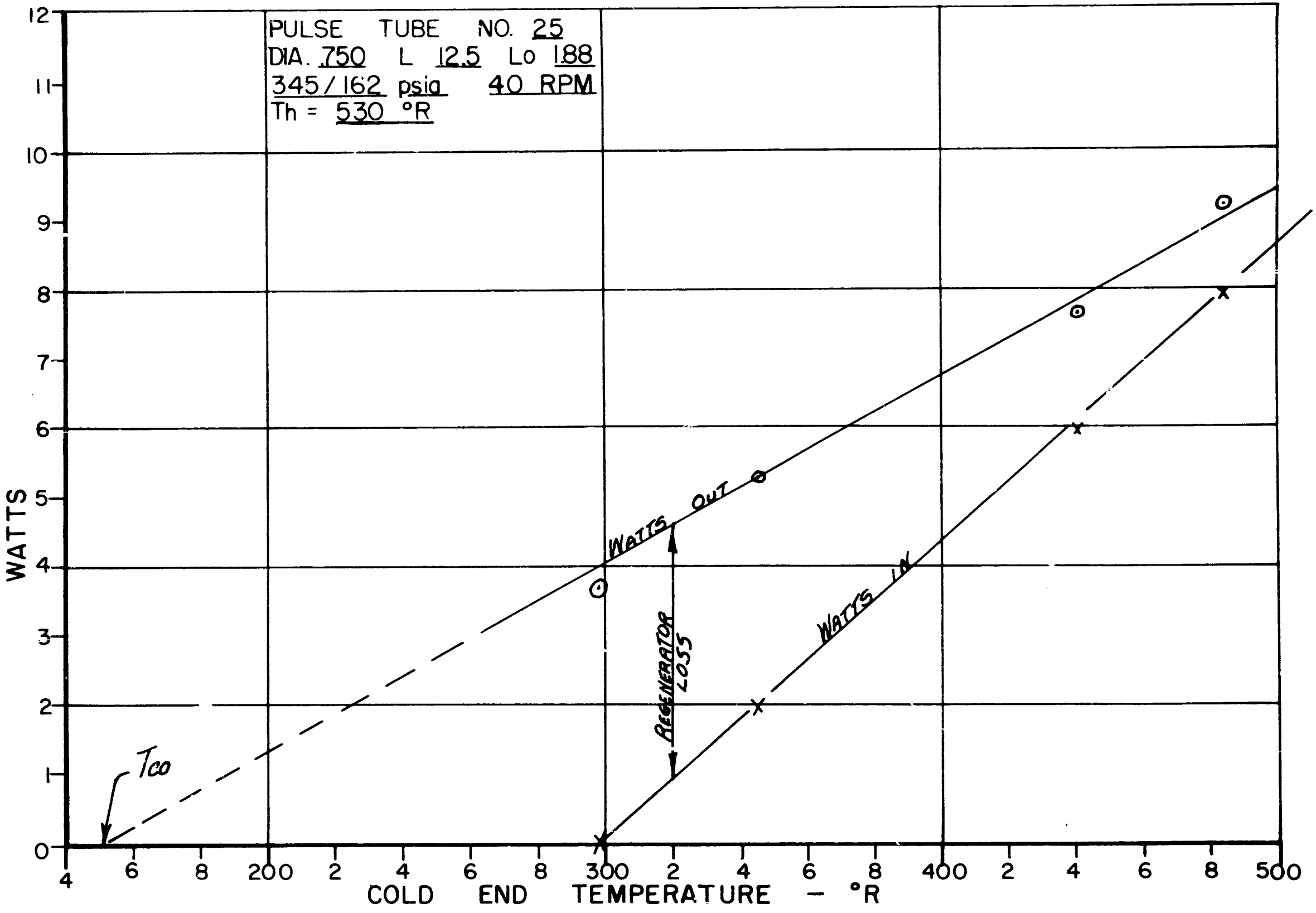

FIGURE 22 HEAT PUMPING RATE Vs. COLD END TEMPERATURE

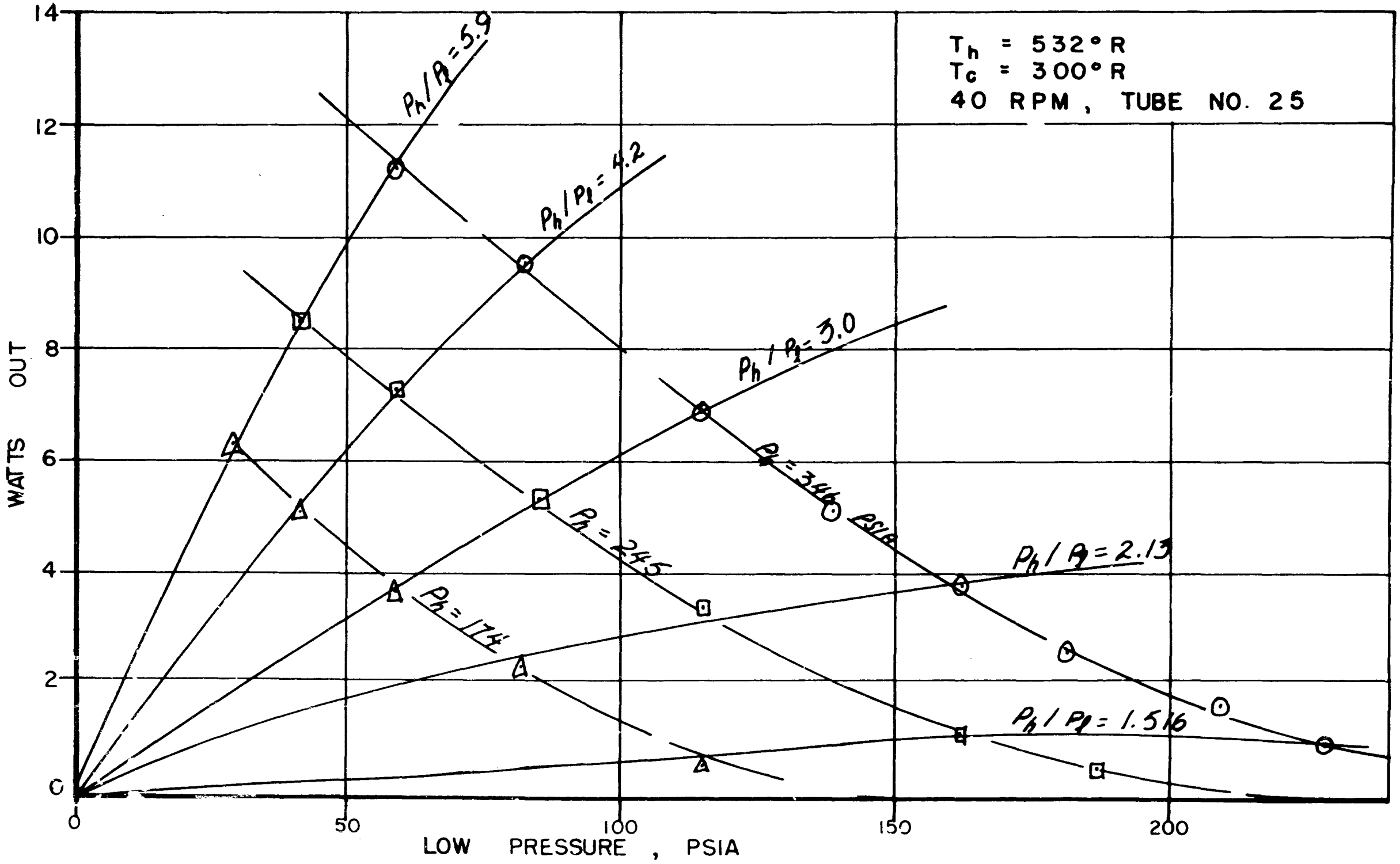

FIGURE 23 HEAT PUMPING RATE Vs. LOW PRESSURE AT CONSTANT HIGH PRESSURE AND PRESSURE RATIO

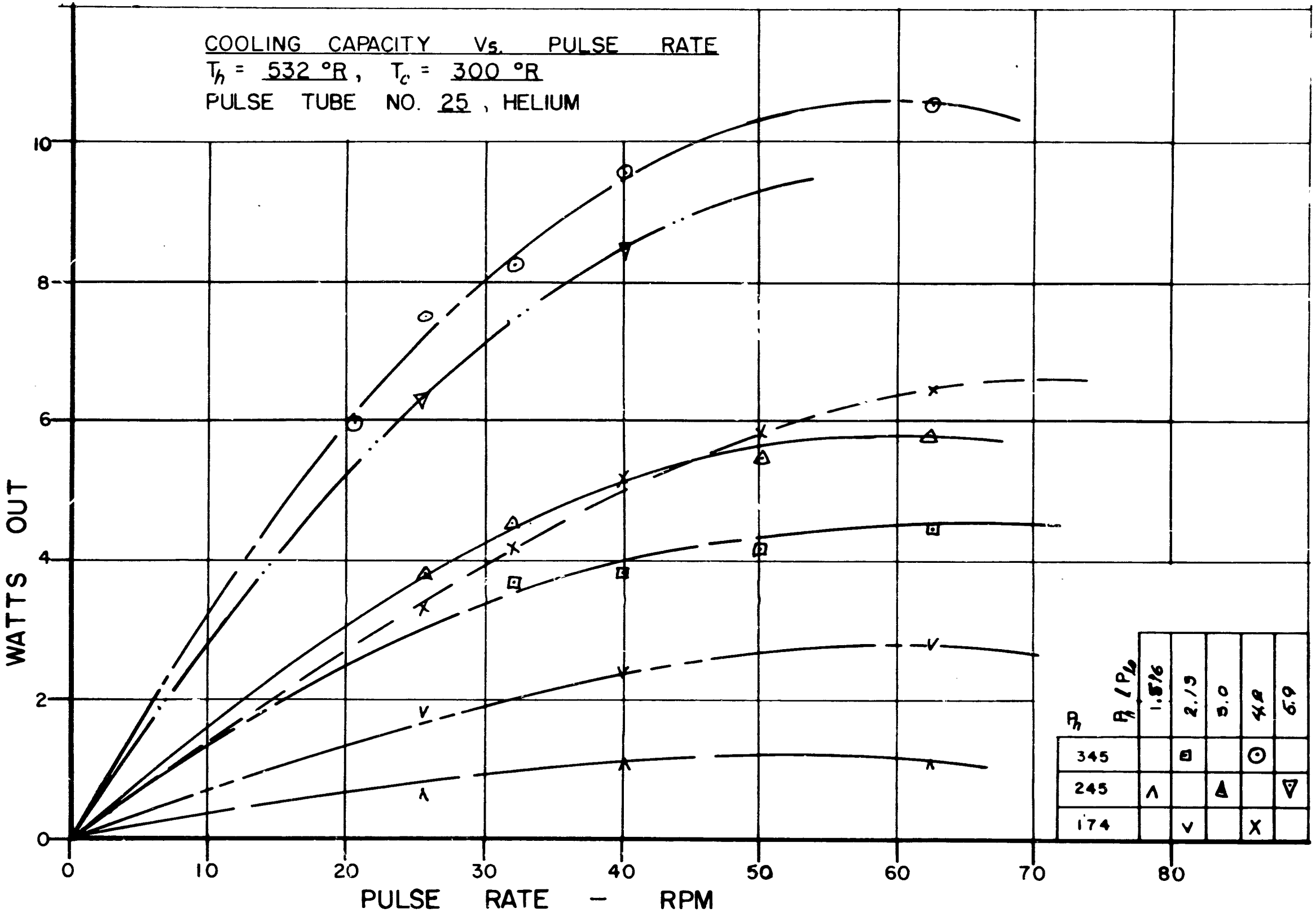

FIGURE 24 HEAT PUMPING RATE Vs. SPEED FOR CONSTANT PRESSURES

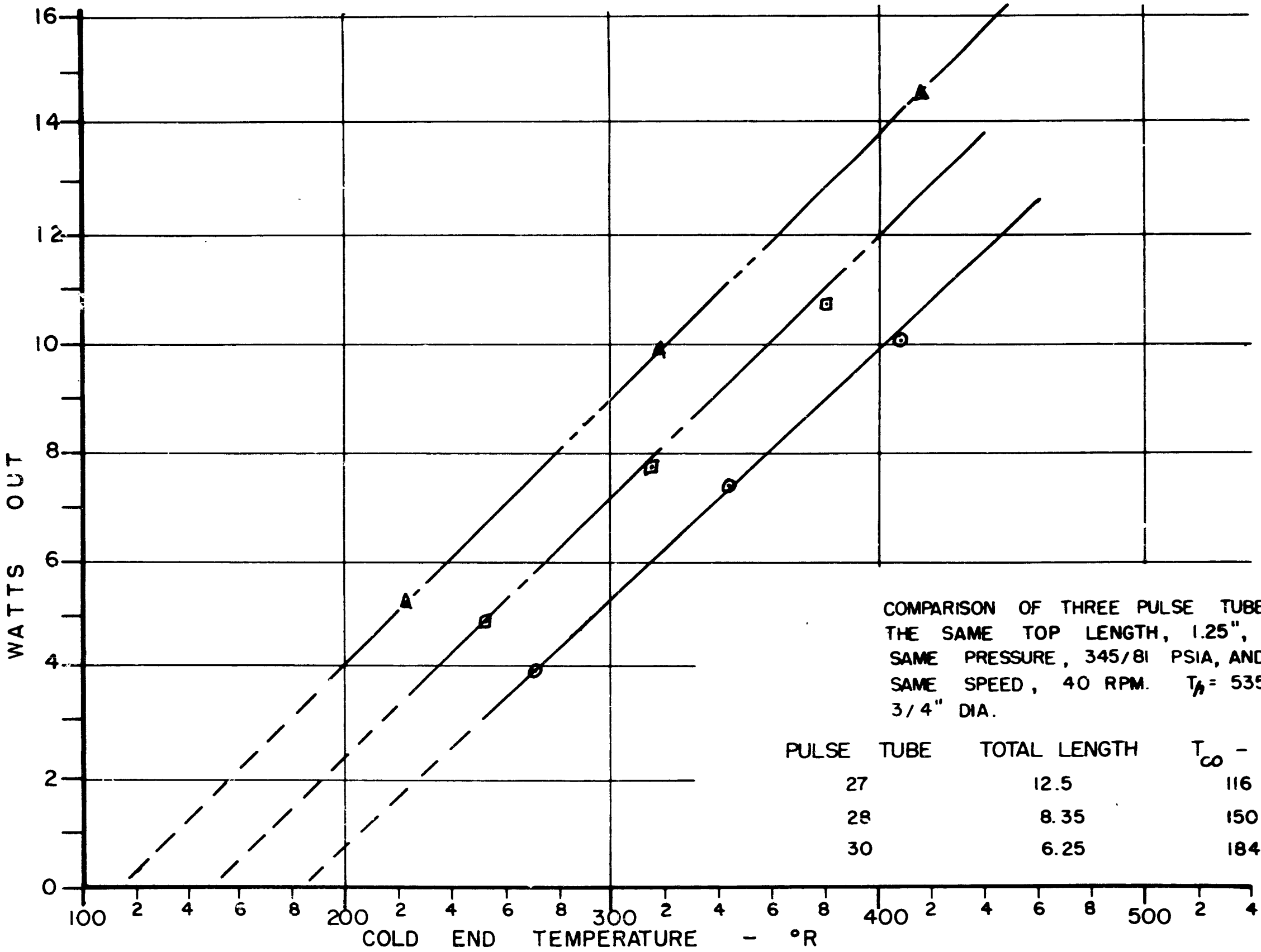

FIGURE 25 : HEAT PUMPING RATE Vs. COLD END TEMPERATURE FOR TUBES OF DIFFERENT LENGTH RATIOS

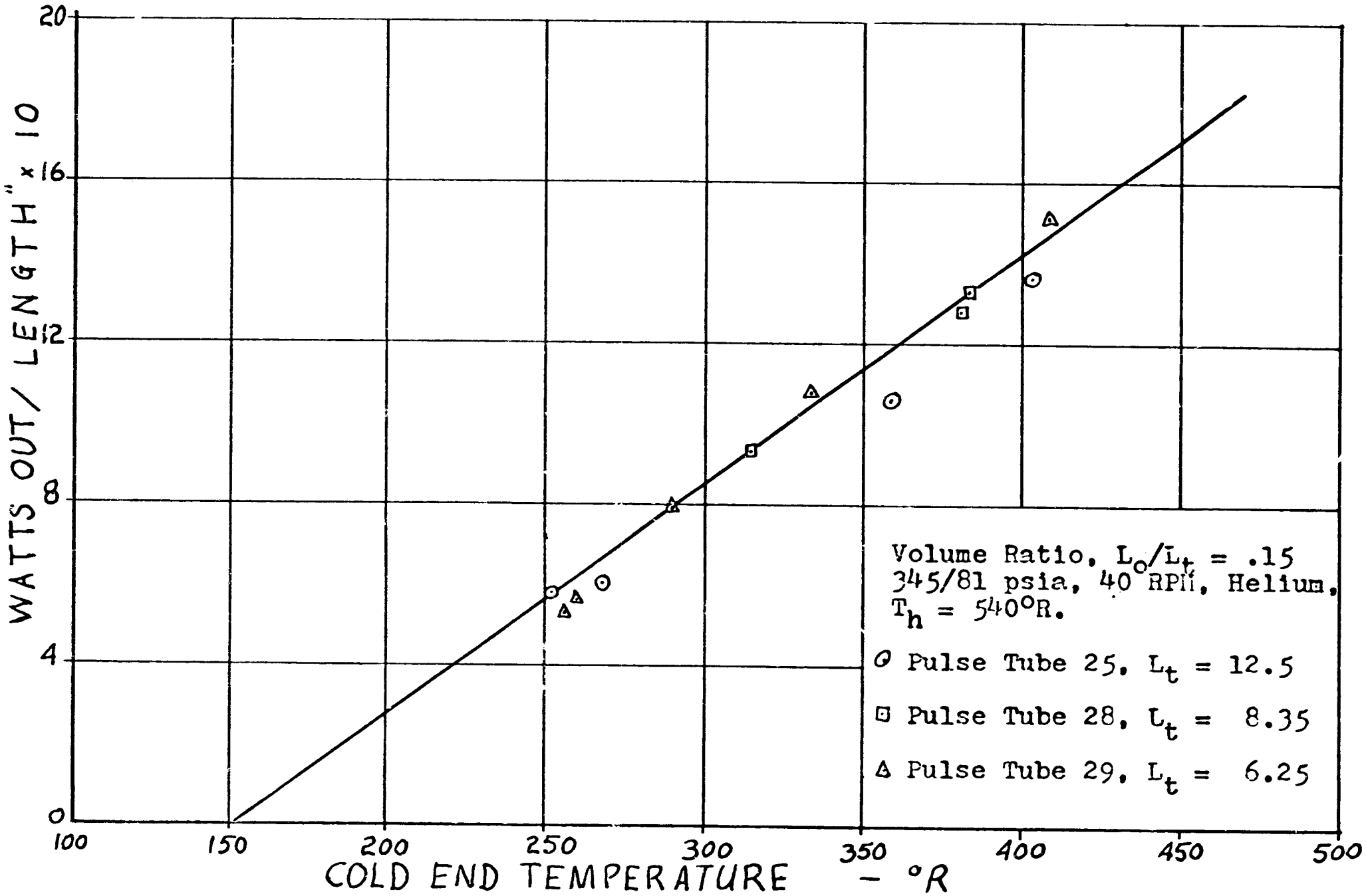

Figure 26 **Watts Out/Length vs. Cold End Temperature for Three Different Length Pulse Tubes**

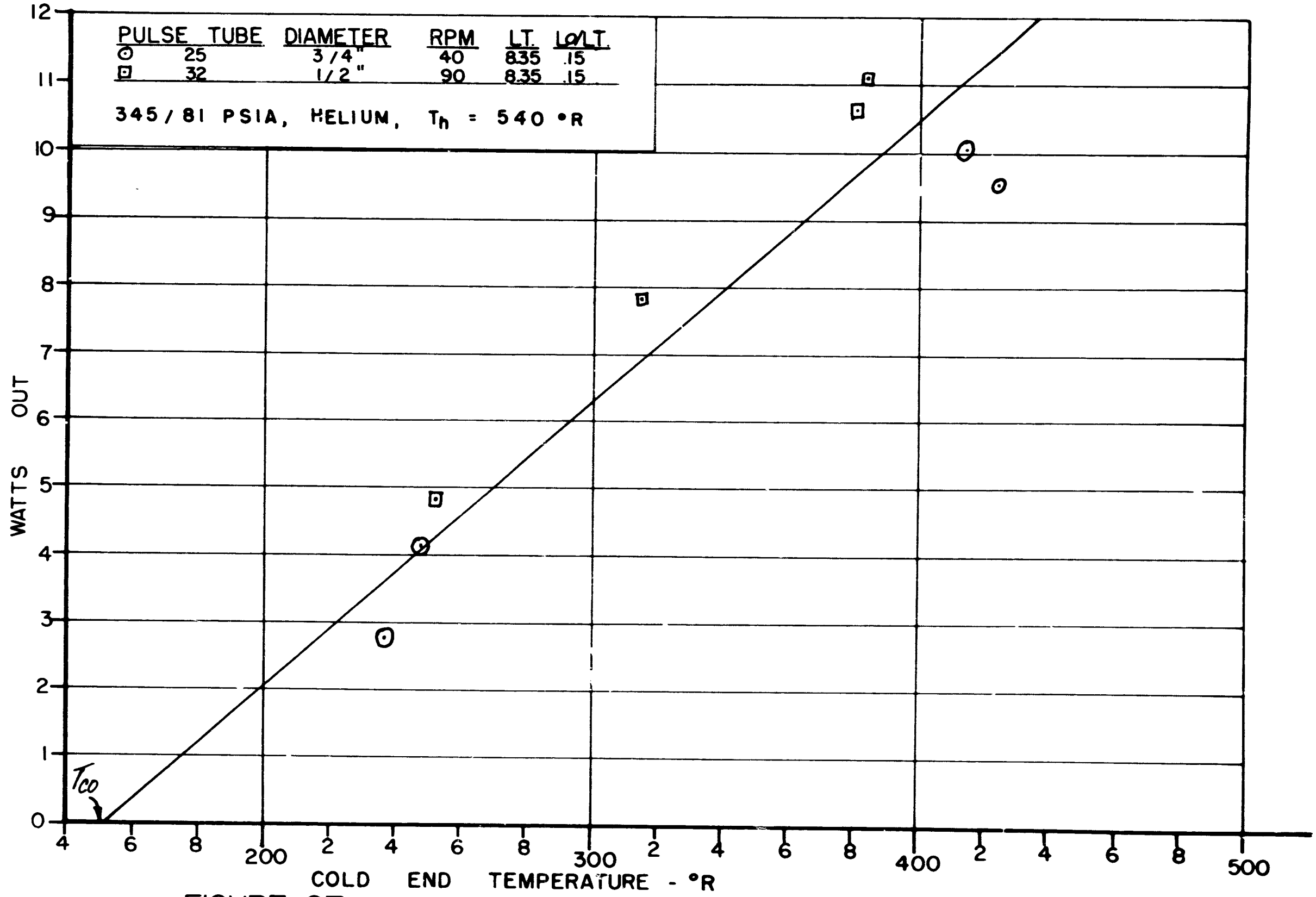

FIGURE 27 HEAT PUMPING RATE Vs. COLD END TEMPERATURE FOR DIFFERENT DIAMETER TUBES AT SAME VALUE OF ND^2

Figure 28 Photograph of Pulse Tubes 25, 27, 28, 29, 30 & 31

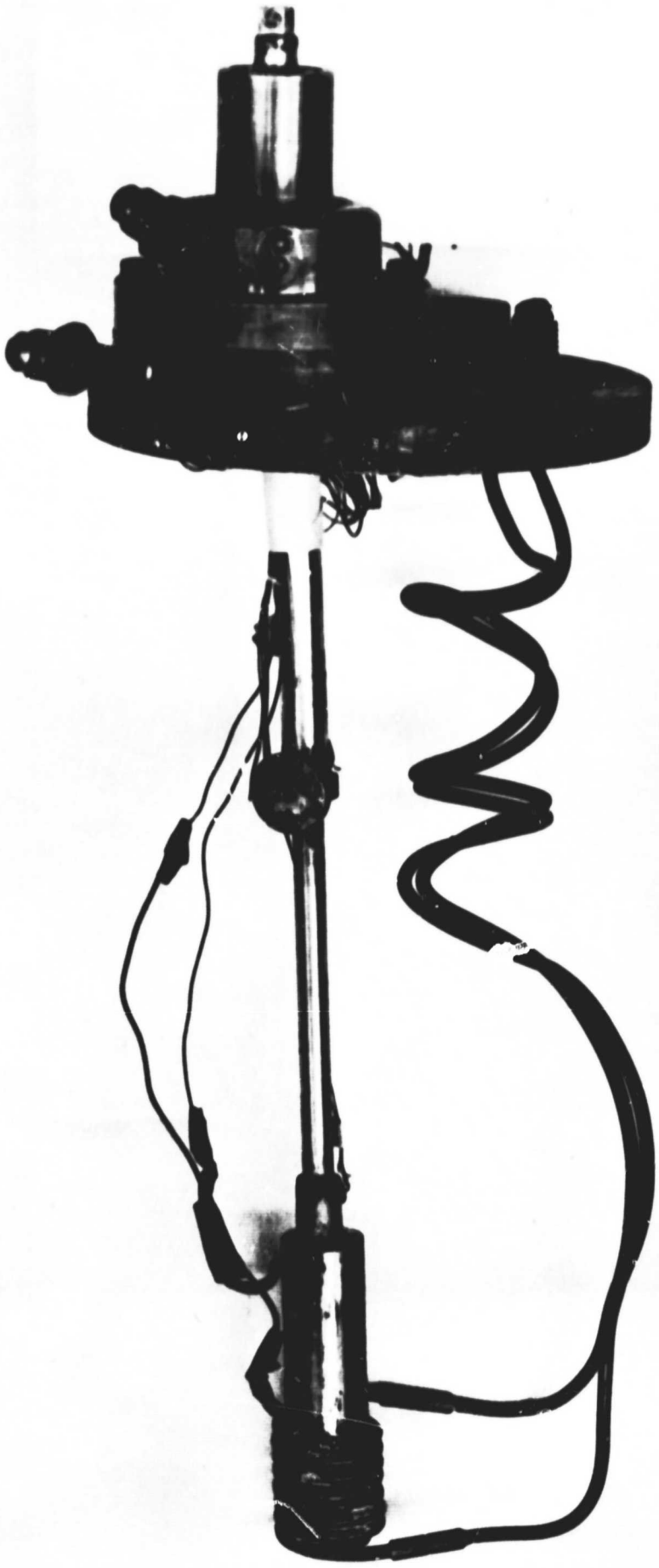

Figure 29 Photograph of $\frac{1}{4}$" Diameter Pulse Tube Mounted on Conduction Type Calorimeter

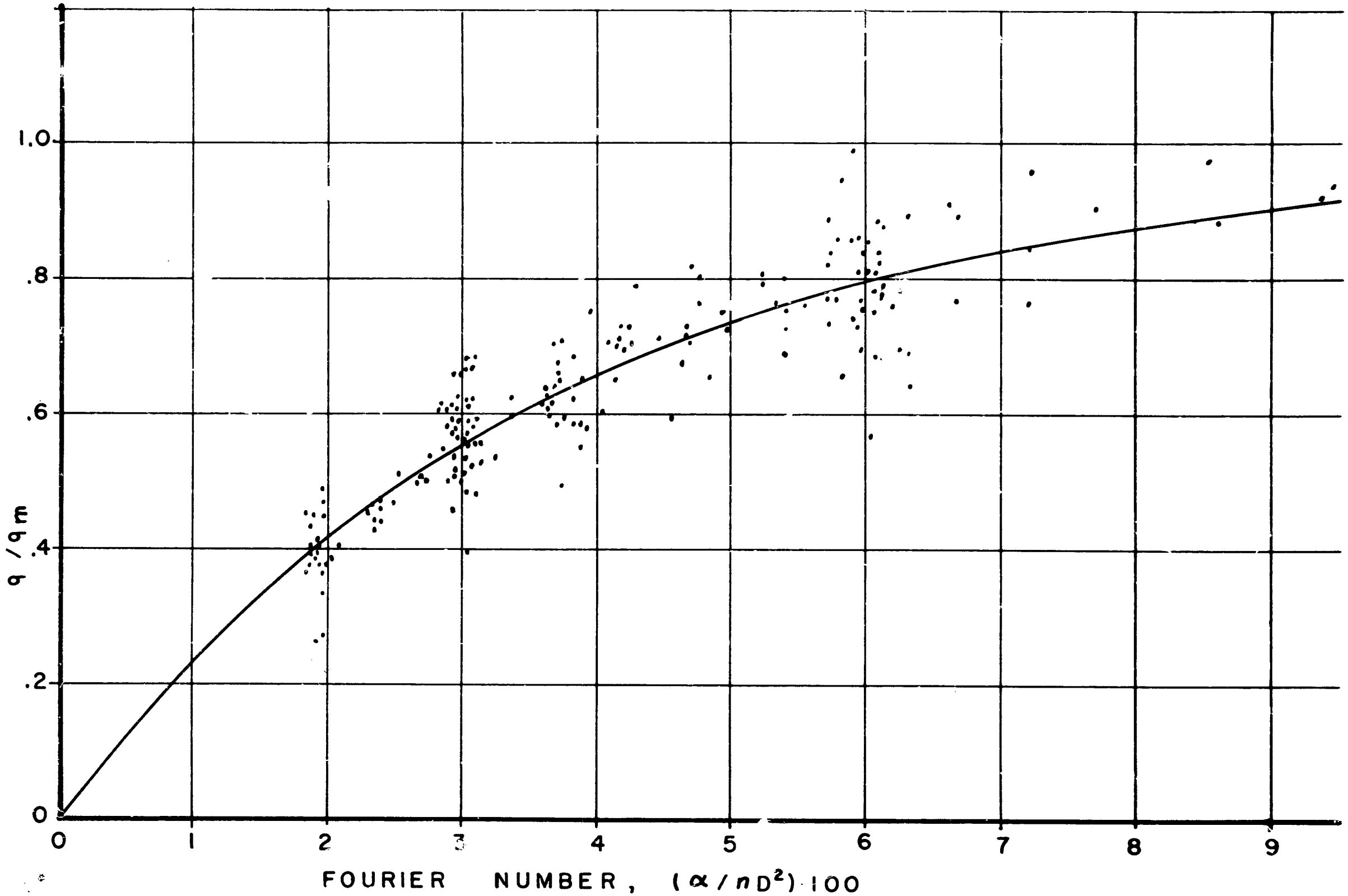

FIGURE 30 : CORRELATION OF TEST DATA WITH HELIUM

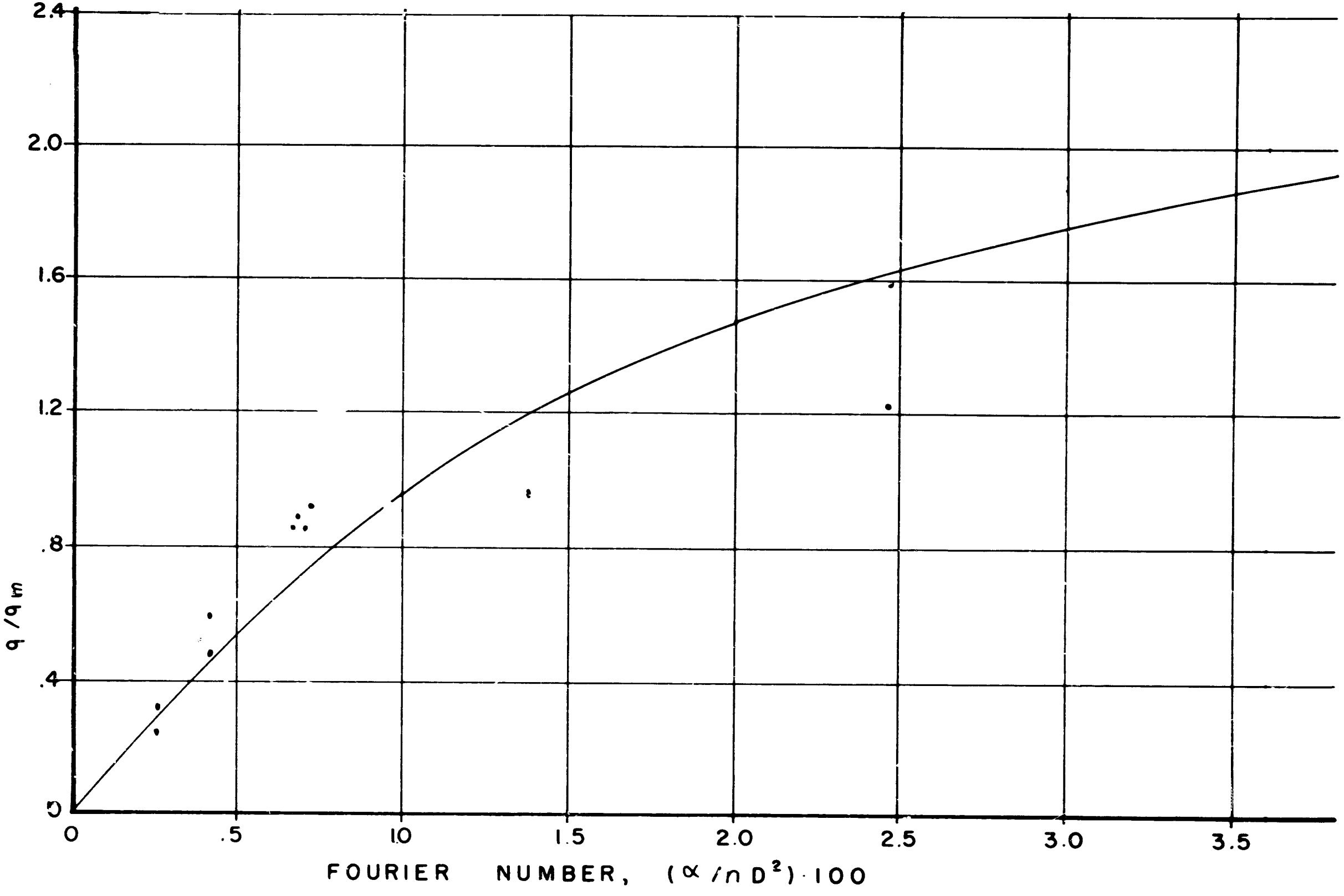

FIG. 31 CORRELATION OF TEST DATA WITH AIR

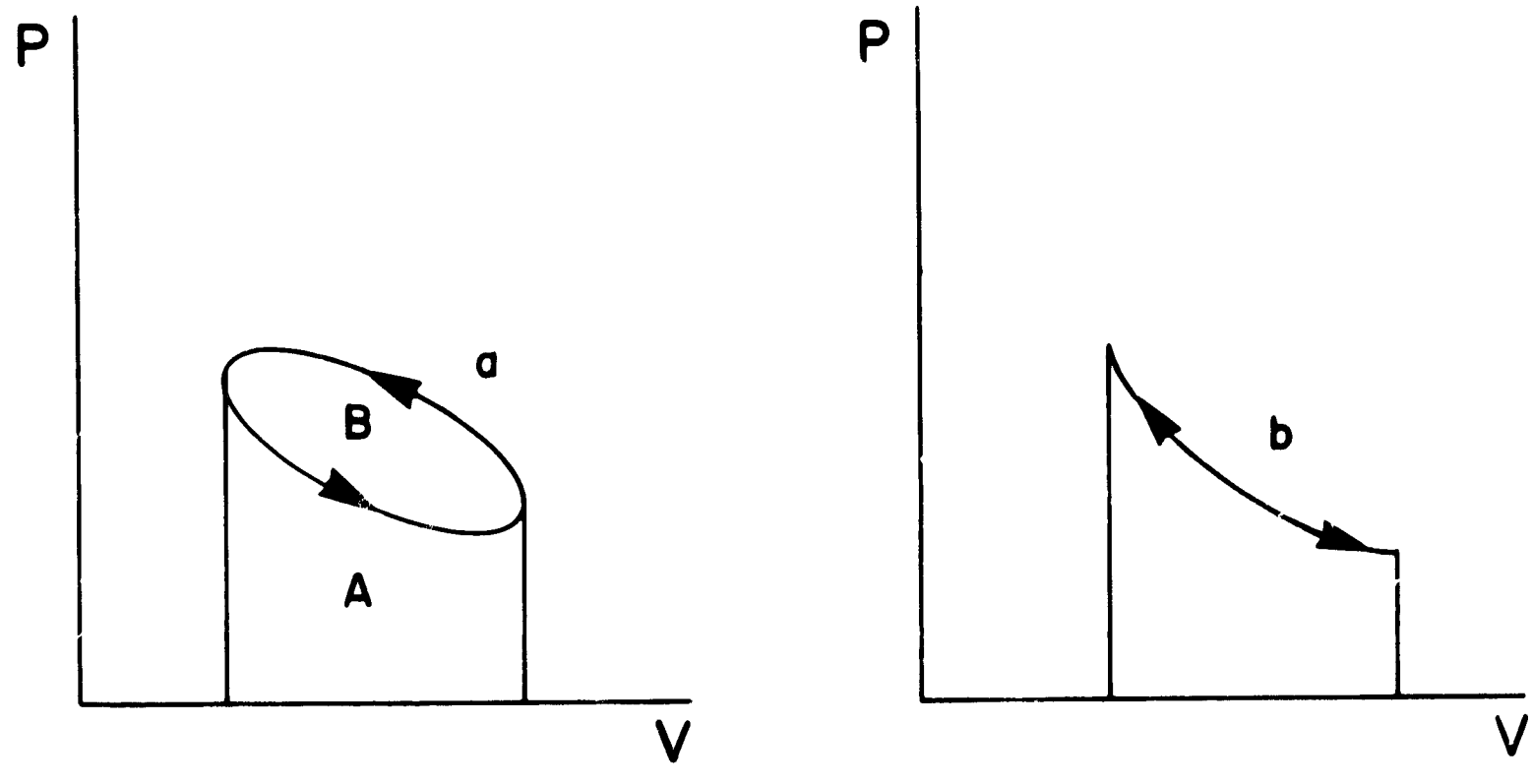

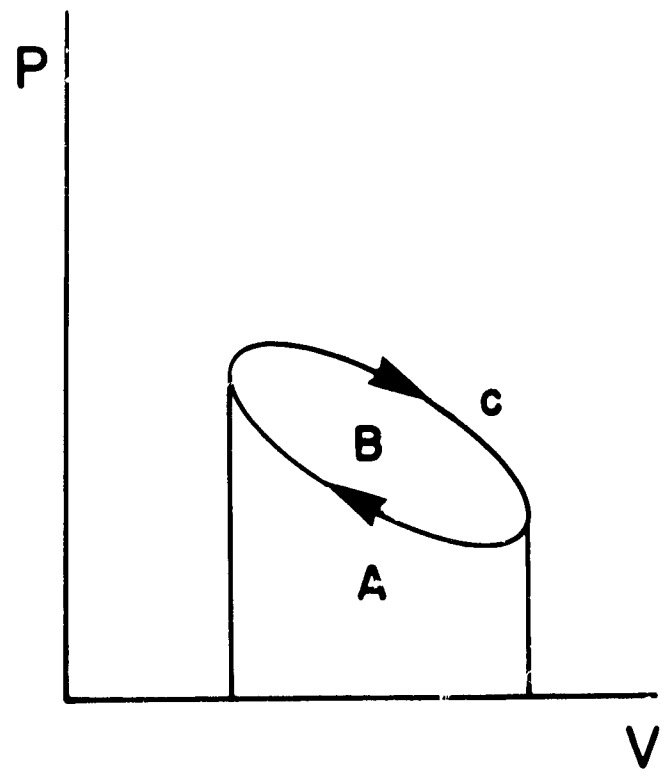

FIG. 32 PULSE TUBE CYCLE DIAGRAMS

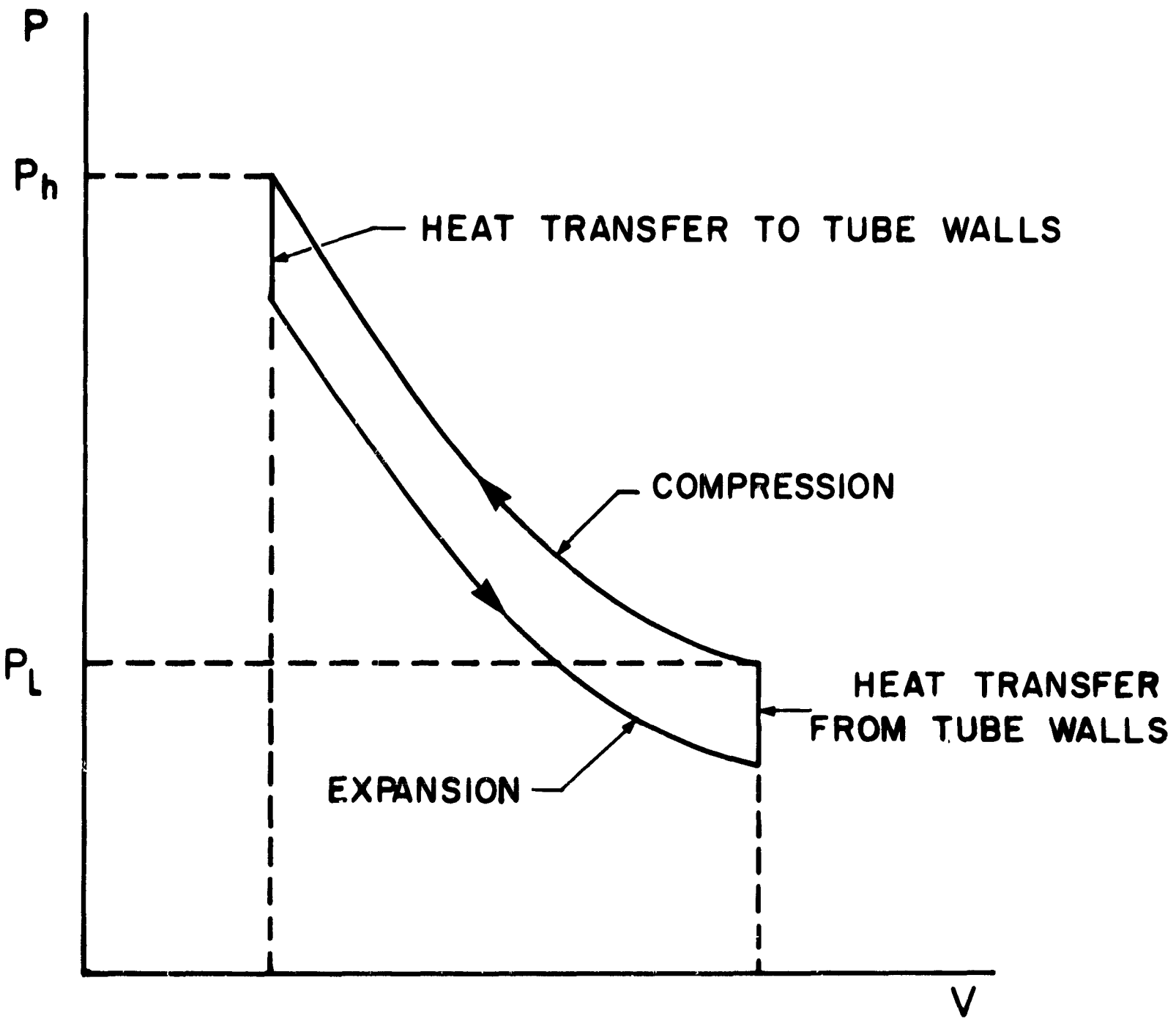

FIG. 33 INTEGRATED P-V DIAGRAM FOR GAS PACKETS IN PULSE TUBE

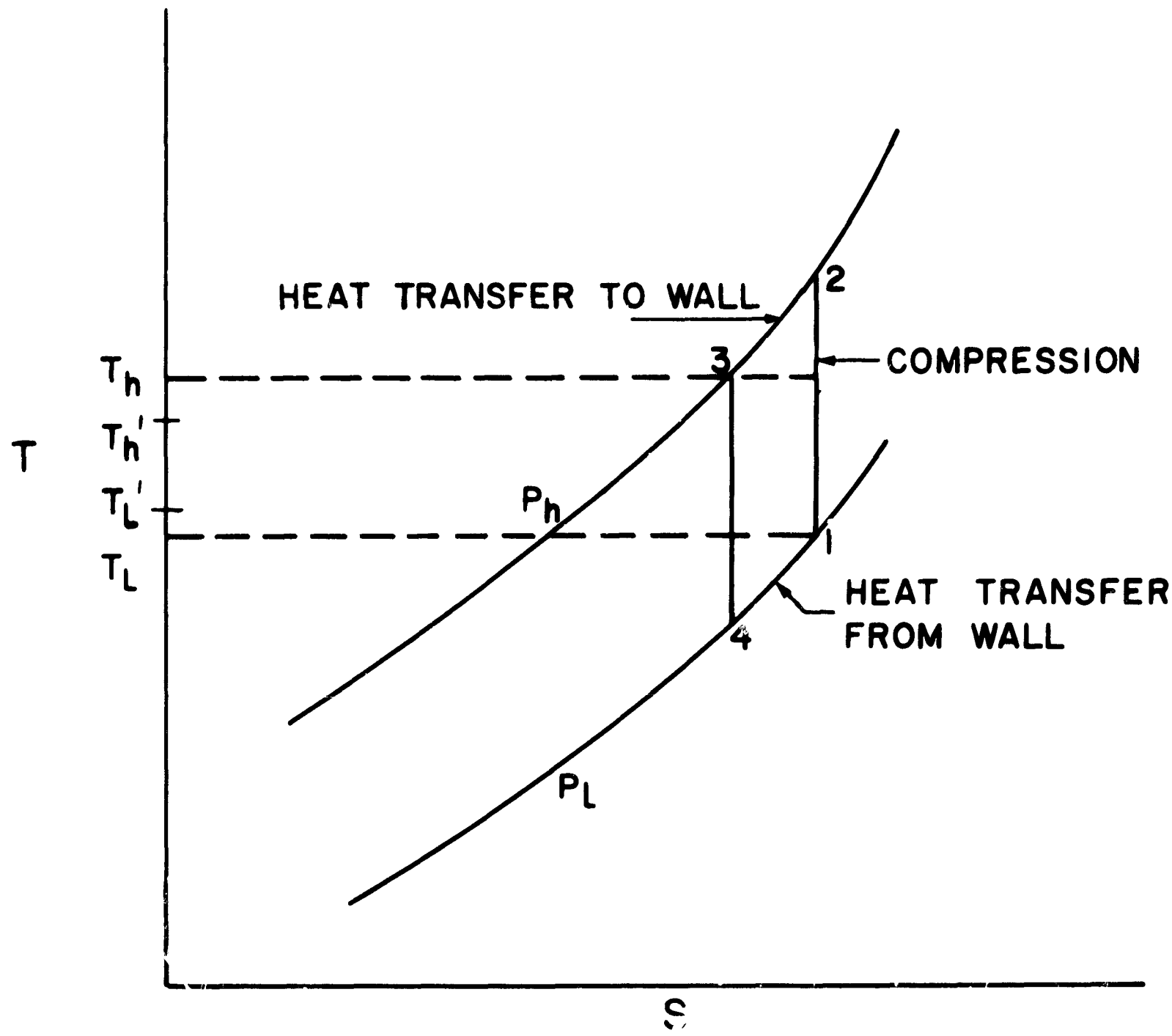

FIG. 34 T - S DIAGRAM FOR BRAYTON CYCLE

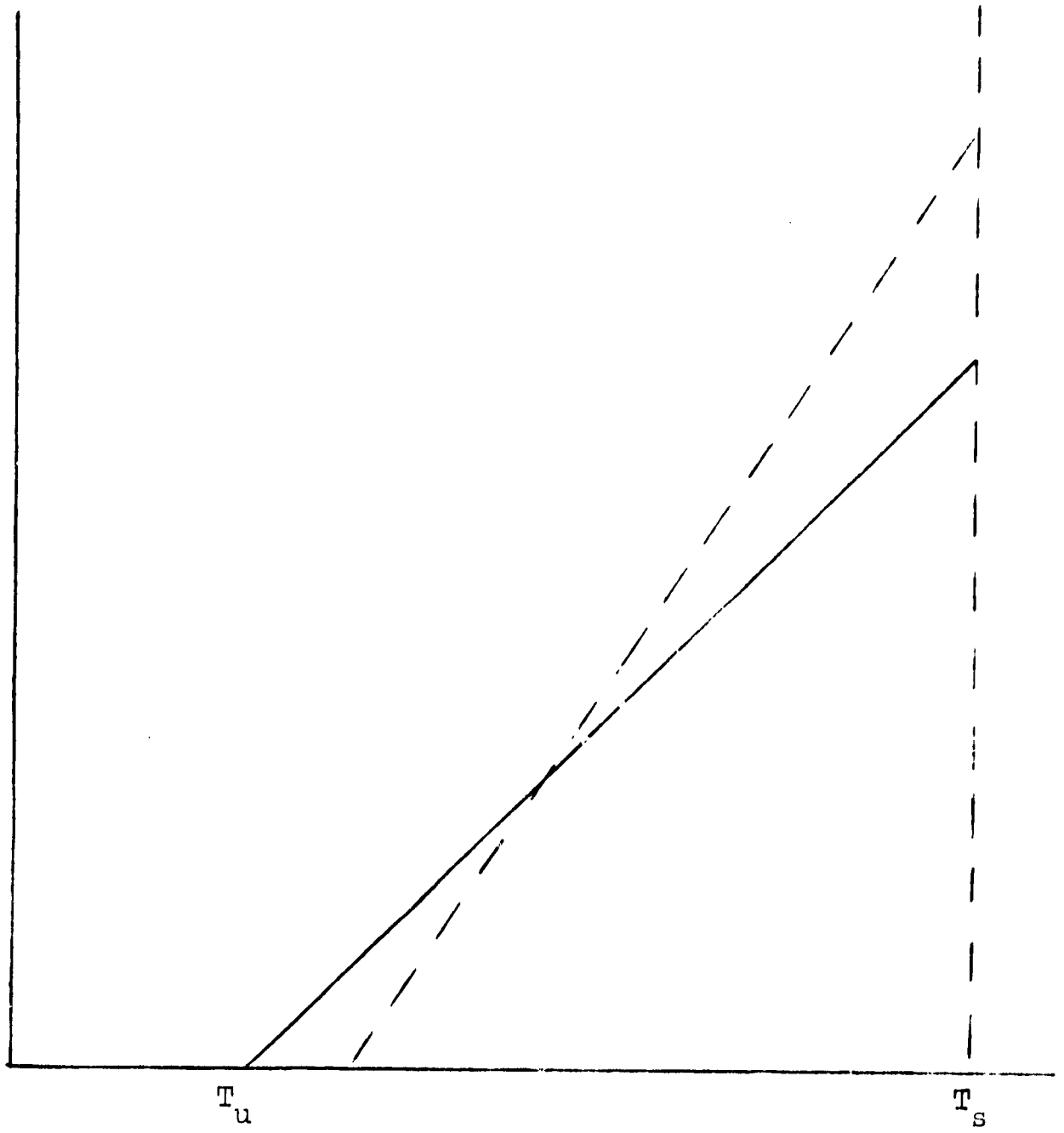

Figure 35

Pulse Tube Refrigeration as a Function of Cold End Temperature

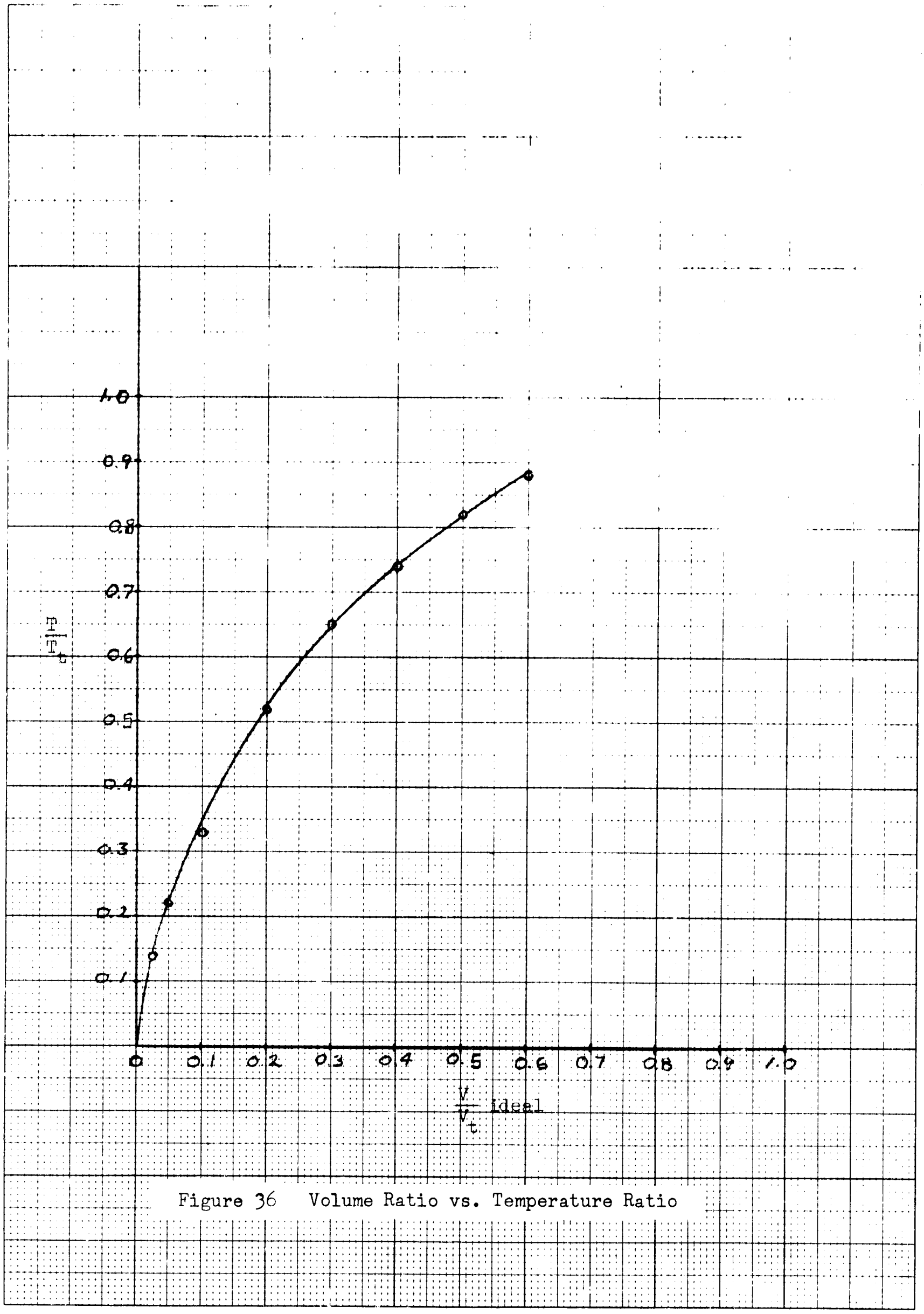

Figure 36 Volume Ratio vs. Temperature Ratio

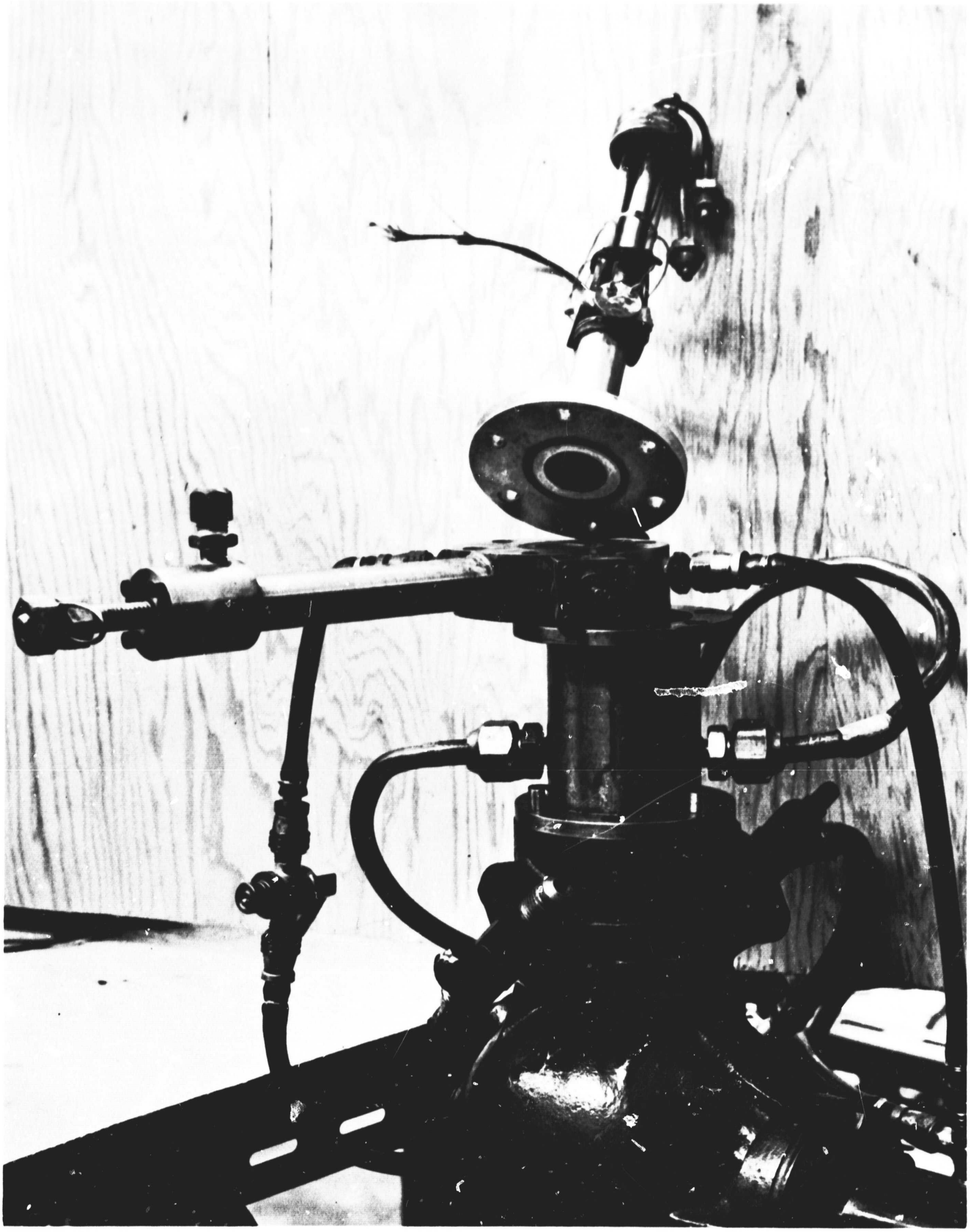

Figure 37 Reversible Pulse Tube Experimental Set Up, Showing Variable Volume Extension

Figure 38 Photograph of Multitube Pulse Tube Refrigerator without Regenerator and Flow Straighteners

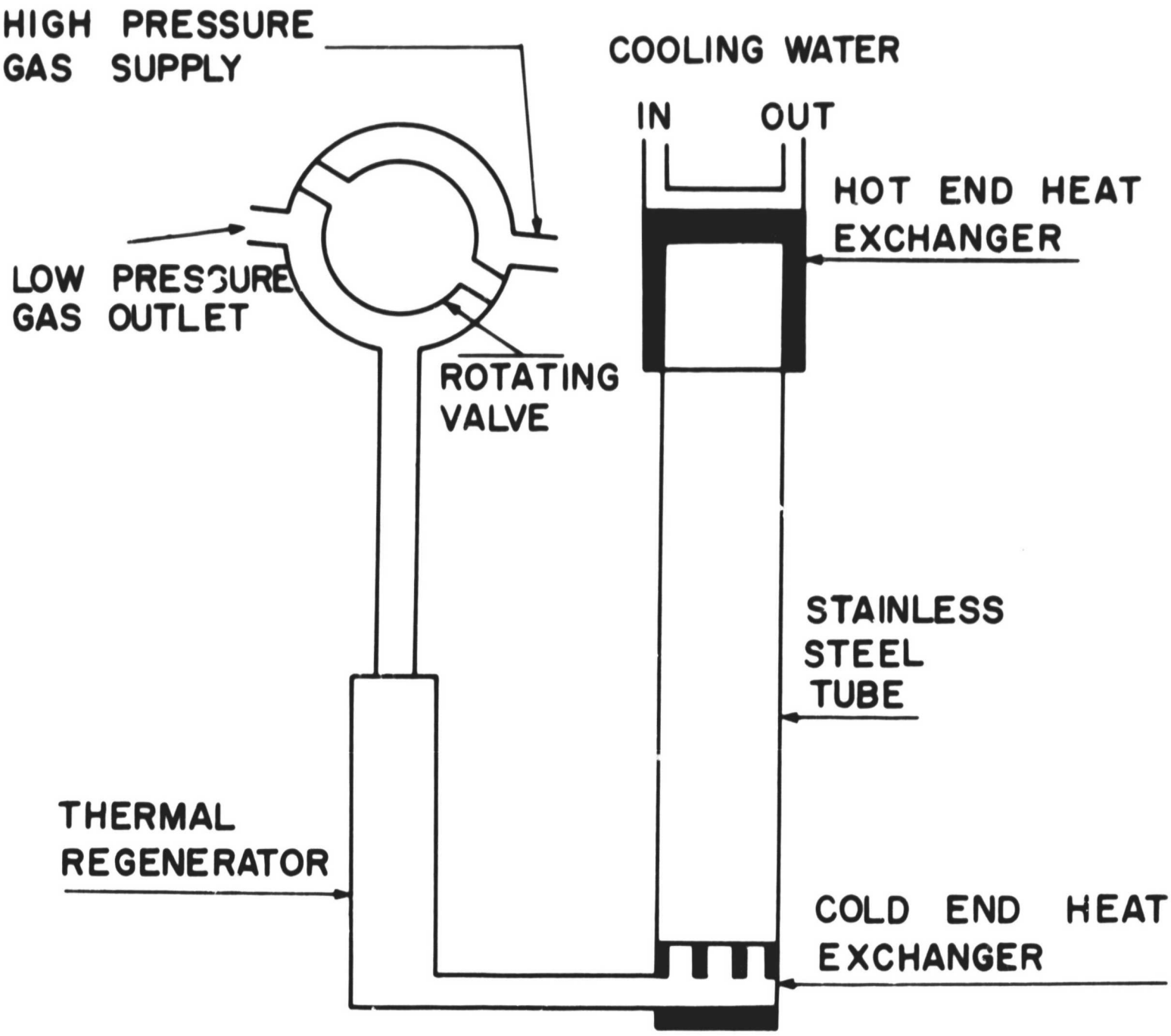

TYPICAL VALVED PULSE TUBE REFRIGERATOR

FIG. 39

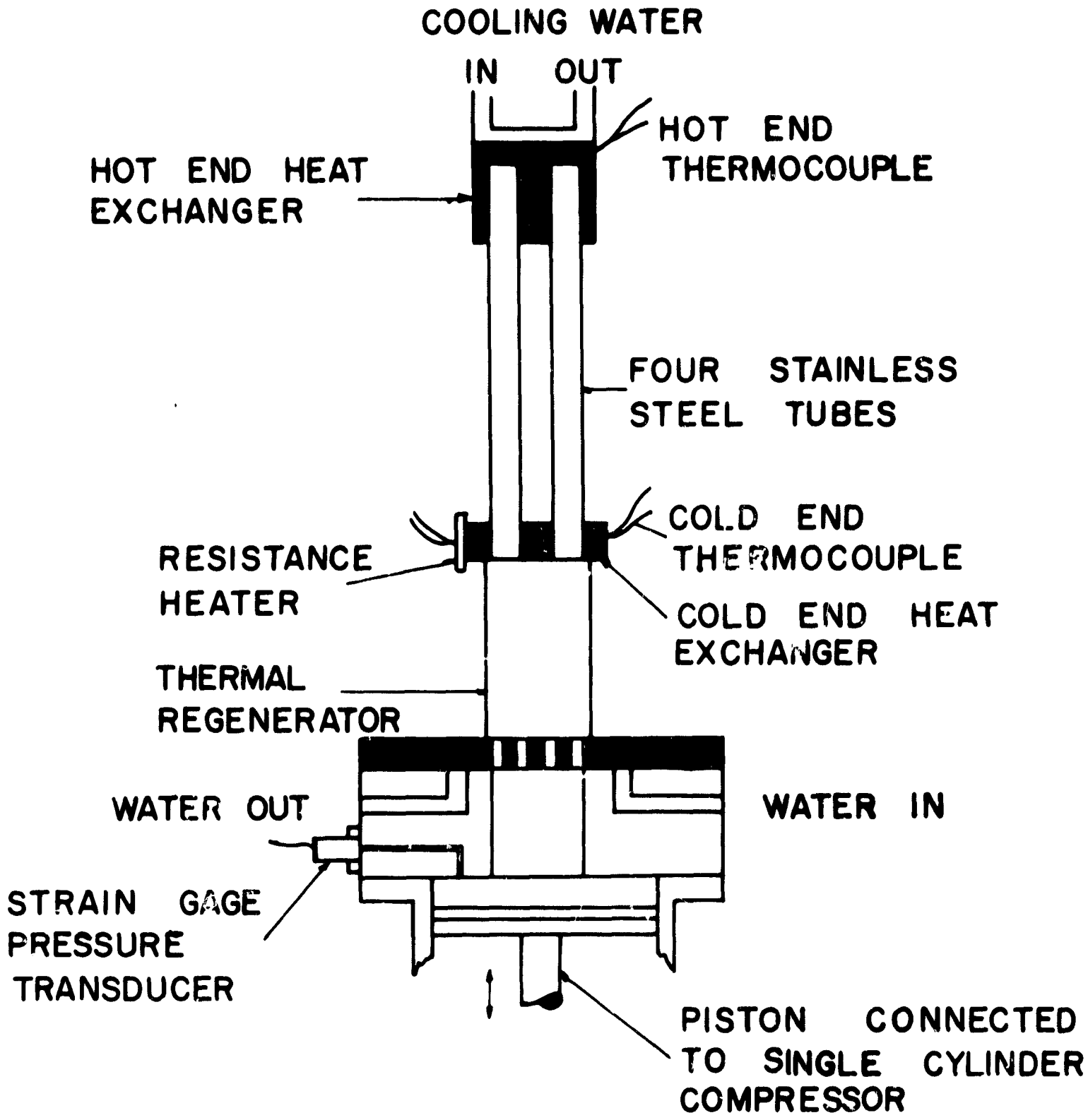

REVERSIBLE PULSE TUBE REFRIGERATOR
TO BE TESTED

FIG.40

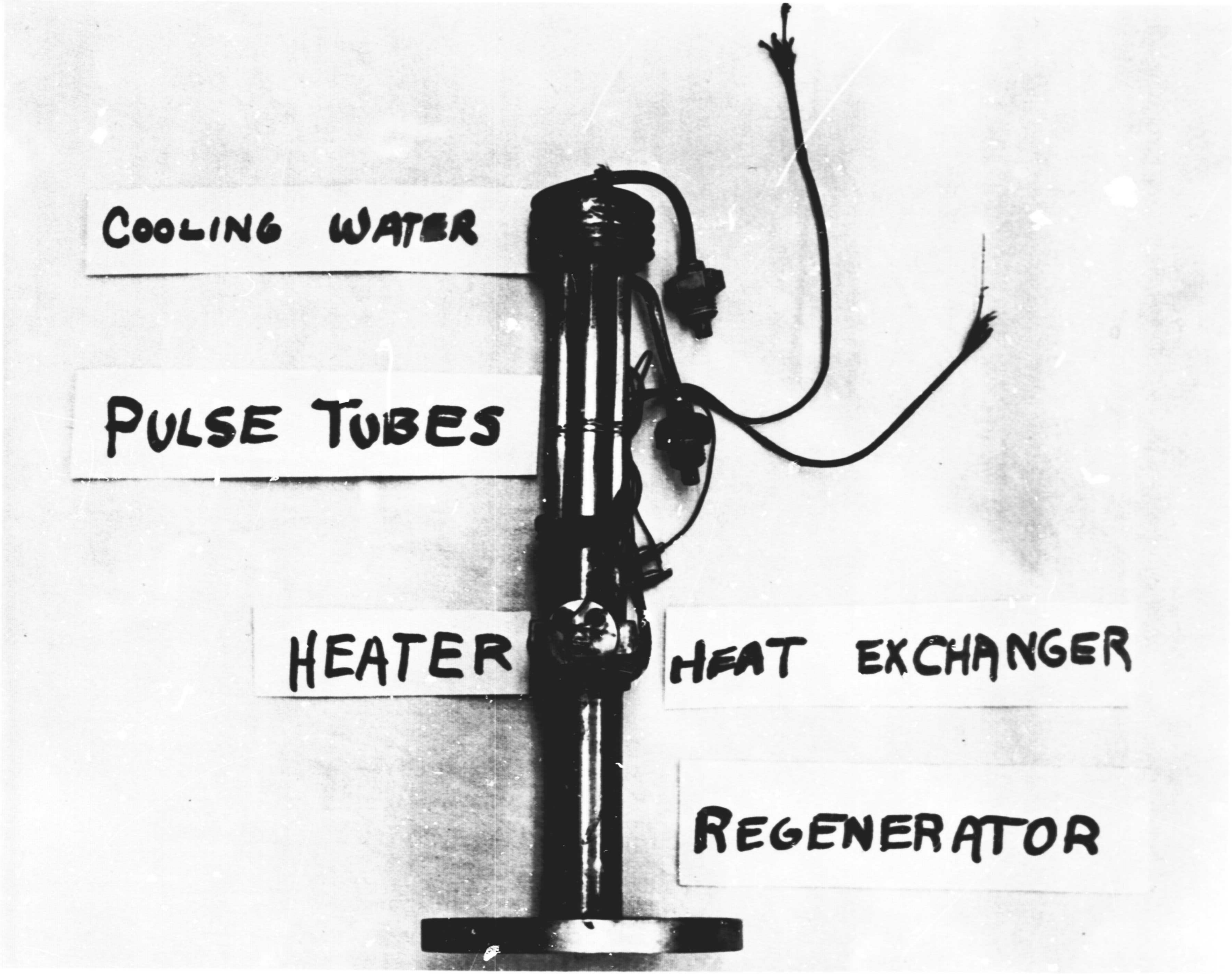

Figure 41 Photograph of Experimental Model of Reversible Puls, Tube Refrigerator

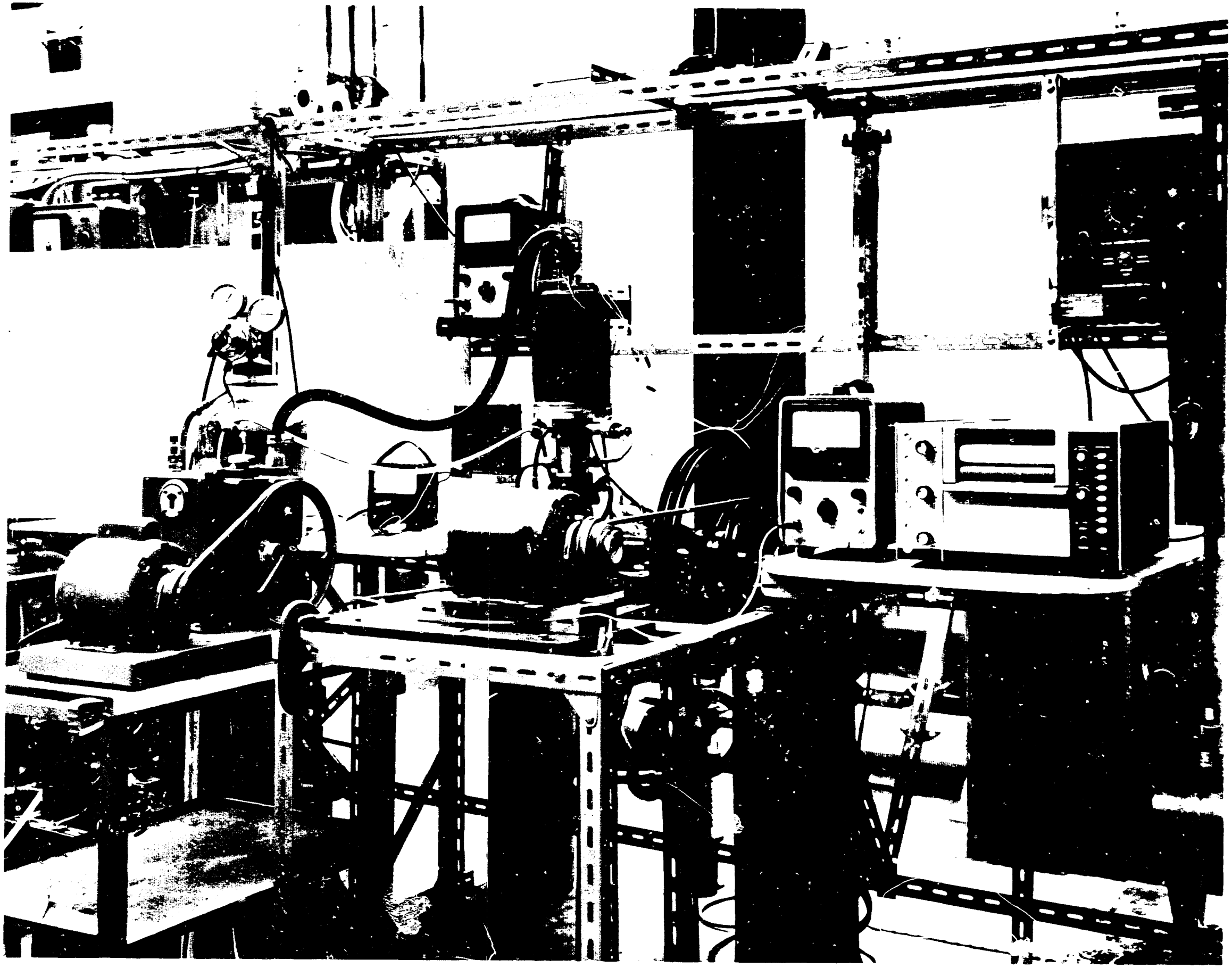

Figure 12 Experimental Set Up Used to Test Reversible Pulse Tube

FIG. 43

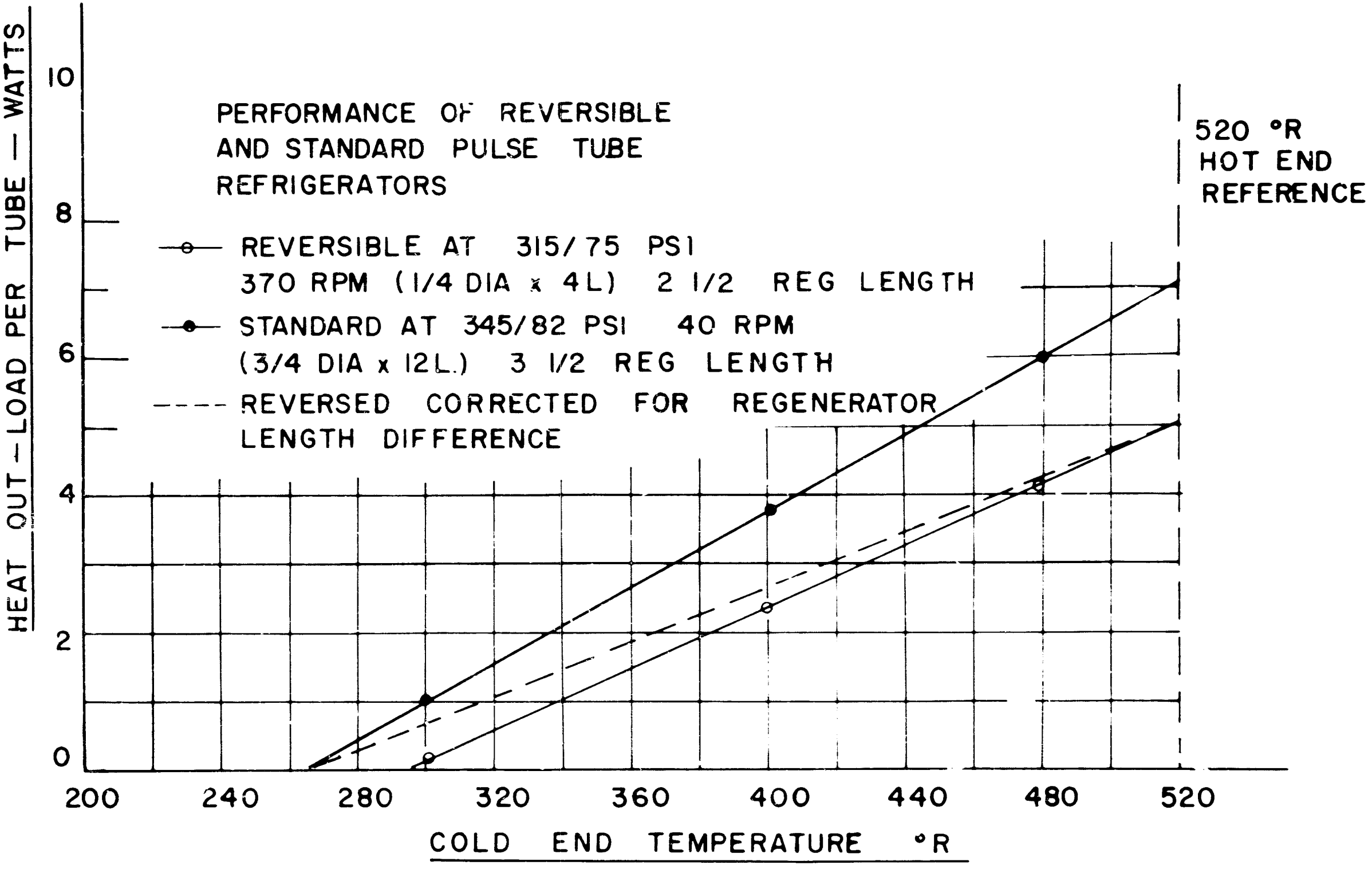
PERFORMANCE OF REVERSIBLE AND STANDARD PULSE TUBE REFRIGERATORS
REVERSIBLE AT 315/75 PSI 370 RPM (1/4 DIA x 4L) 2 1/2 REG LENGTH
STANDARD AT 345/82 PSI 40 RPM (3/4 DIA x 12L.) 3 1/2 REG LENGTH
REVERSED CORRECTED FOR REGENERATOR LENGTH DIFFERENCE
520 °R HOT END REFERENCE
HEAT OUT - LOAD PER TUBE - WATTS
0
2
4
6
8
10
200
240
280
320
360
400
440
480
520
COLD END TEMPERATURE °R

FIG. 44

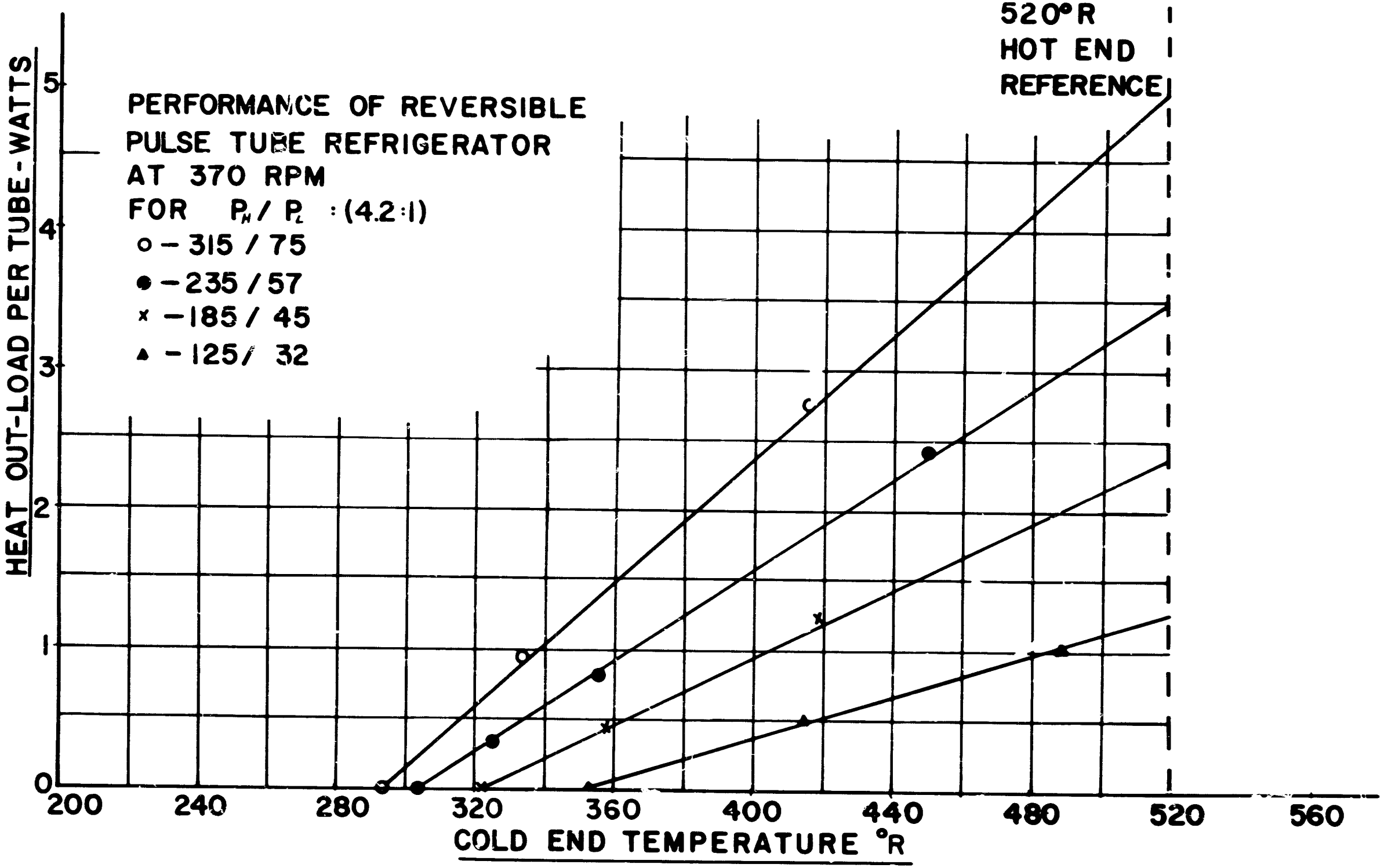
PERFORMANCE OF REVERSIBLE
PULSE TUBE REFRIGERATOR
AT 370 RPM
FOR P_H / P_L : (4.2:1)
o – 315 / 75
● – 235 / 57
× – 185 / 45
▲ – 125 / 32
520°R
HOT END
REFERENCE
HEAT OUT-LOAD PER TUBE-WATTS
0
1
2
3
4
5
200
240
280
320
360
400
440
480
520
560
COLD END TEMPERATURE °R

FIG. 45

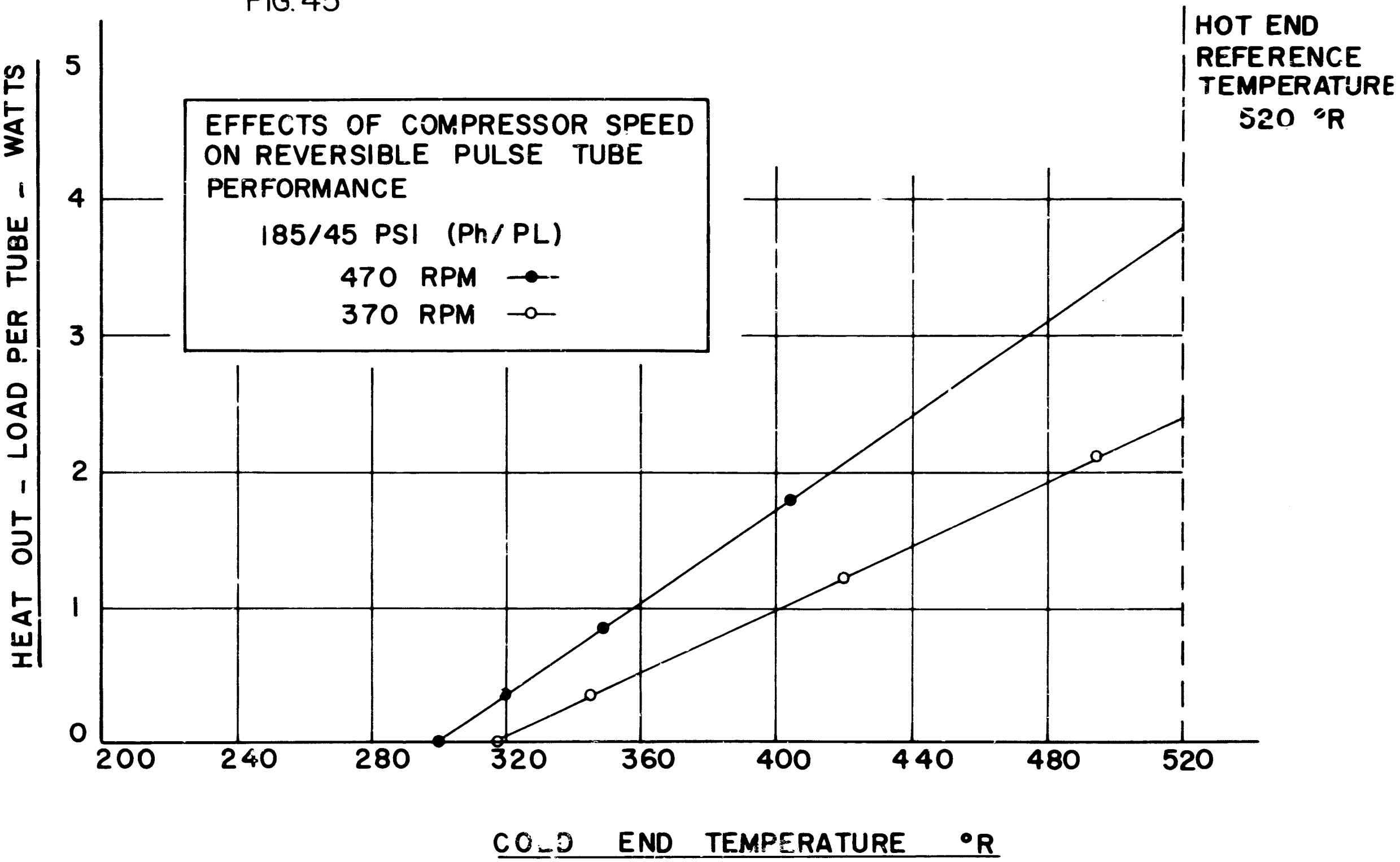
EFFECTS OF COMPRESSOR SPEED ON REVERSIBLE PULSE TUBE PERFORMANCE
185/45 PSI (Ph/PL)
470 RPM
370 RPM
HOT END REFERENCE TEMPERATURE 520 °R
HEAT OUT - LOAD PER TUBE - WATTS
0
1
2
3
4
5
200
240
280
320
360
400
440
480
520
COLD END TEMPERATURE °R

FIG. 46 TYPICAL PRESSURE TIME RELATIONS AT EQUAL Ph/PL FOR VALVED AND REVERSIBLE PULSE TUBES

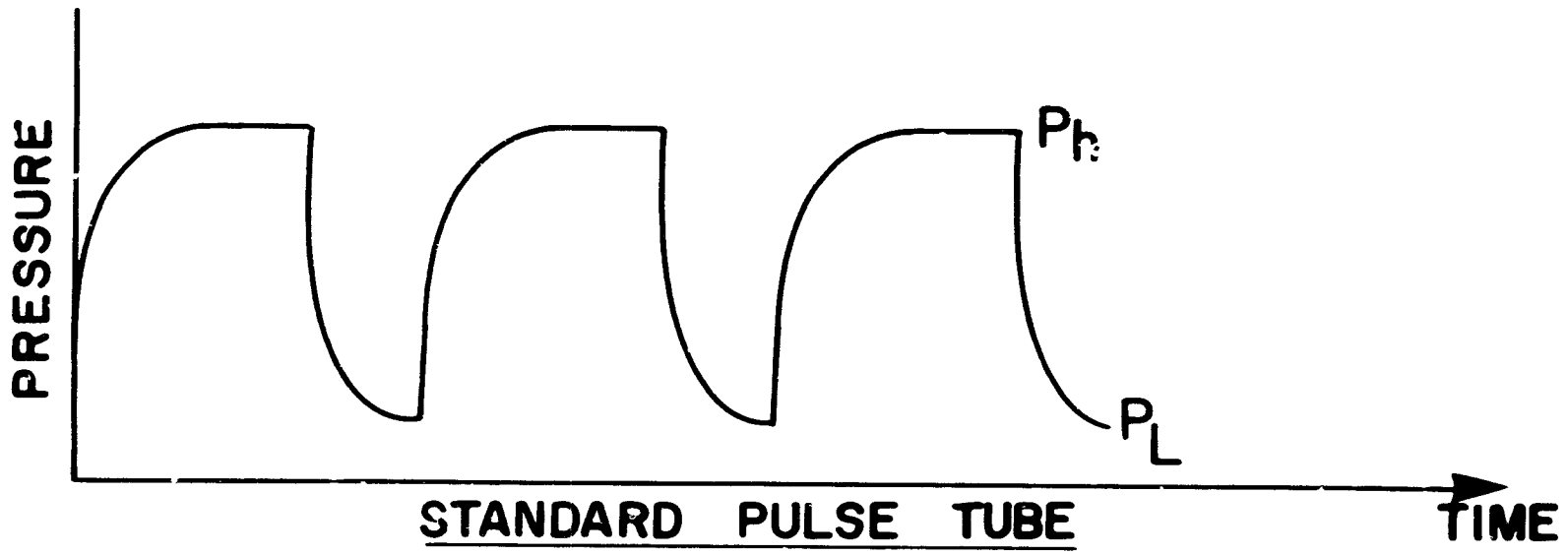

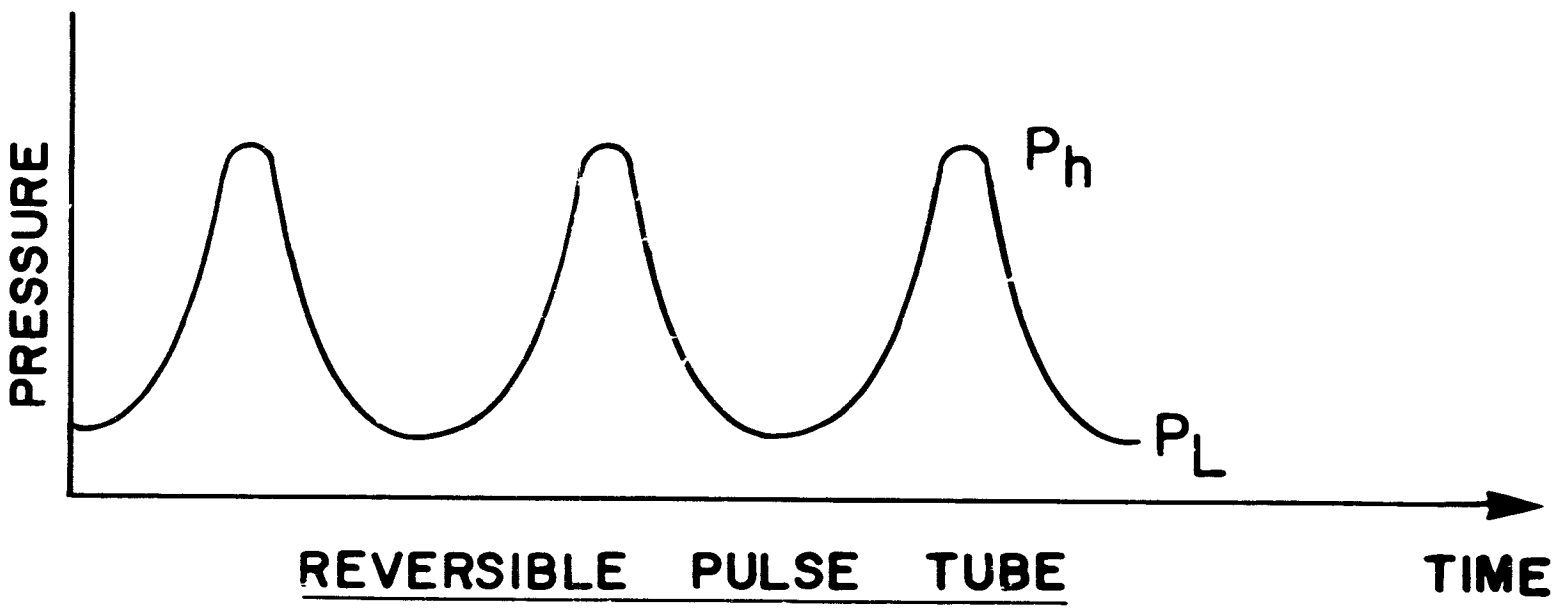

FIG. 47 SYSTEM POWER LOSSES IN REVERSIBLE PULSE TUBE TESTING APPARATUS

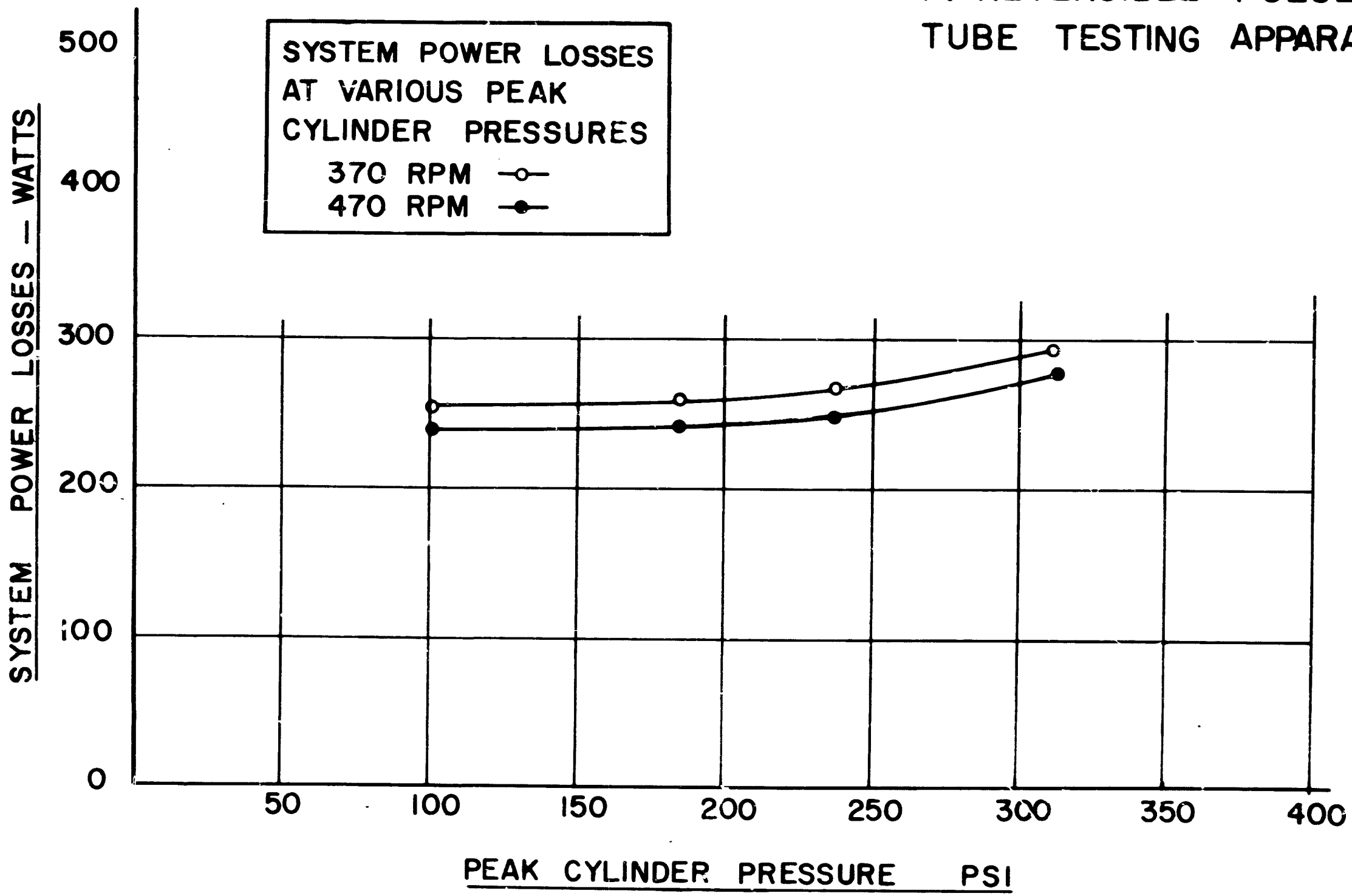

Figure 48

HEAT LOSS VS SCFM HELIUM

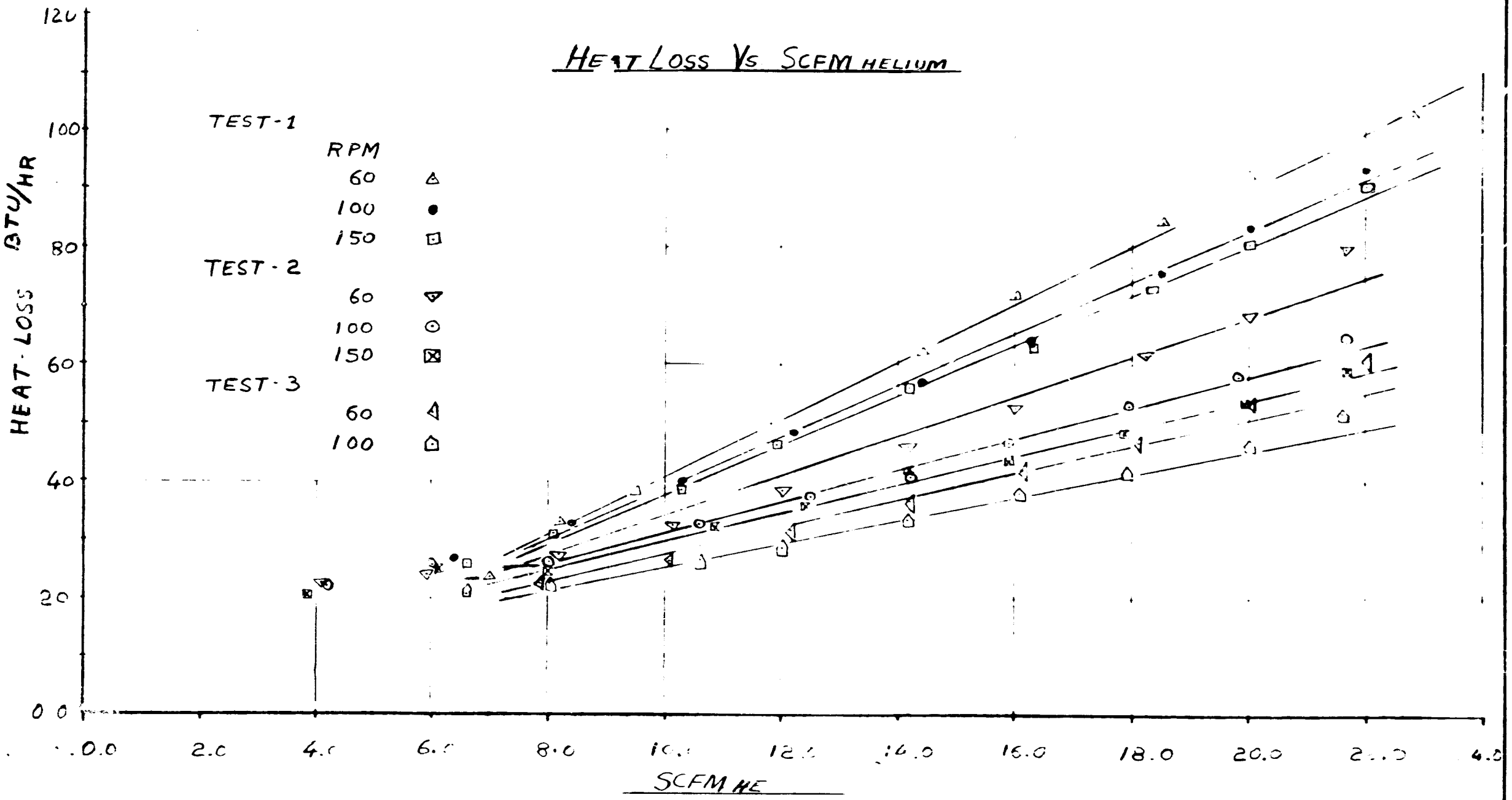

Figure 49

INEFFICIENCY VS. SCFM HELIUM

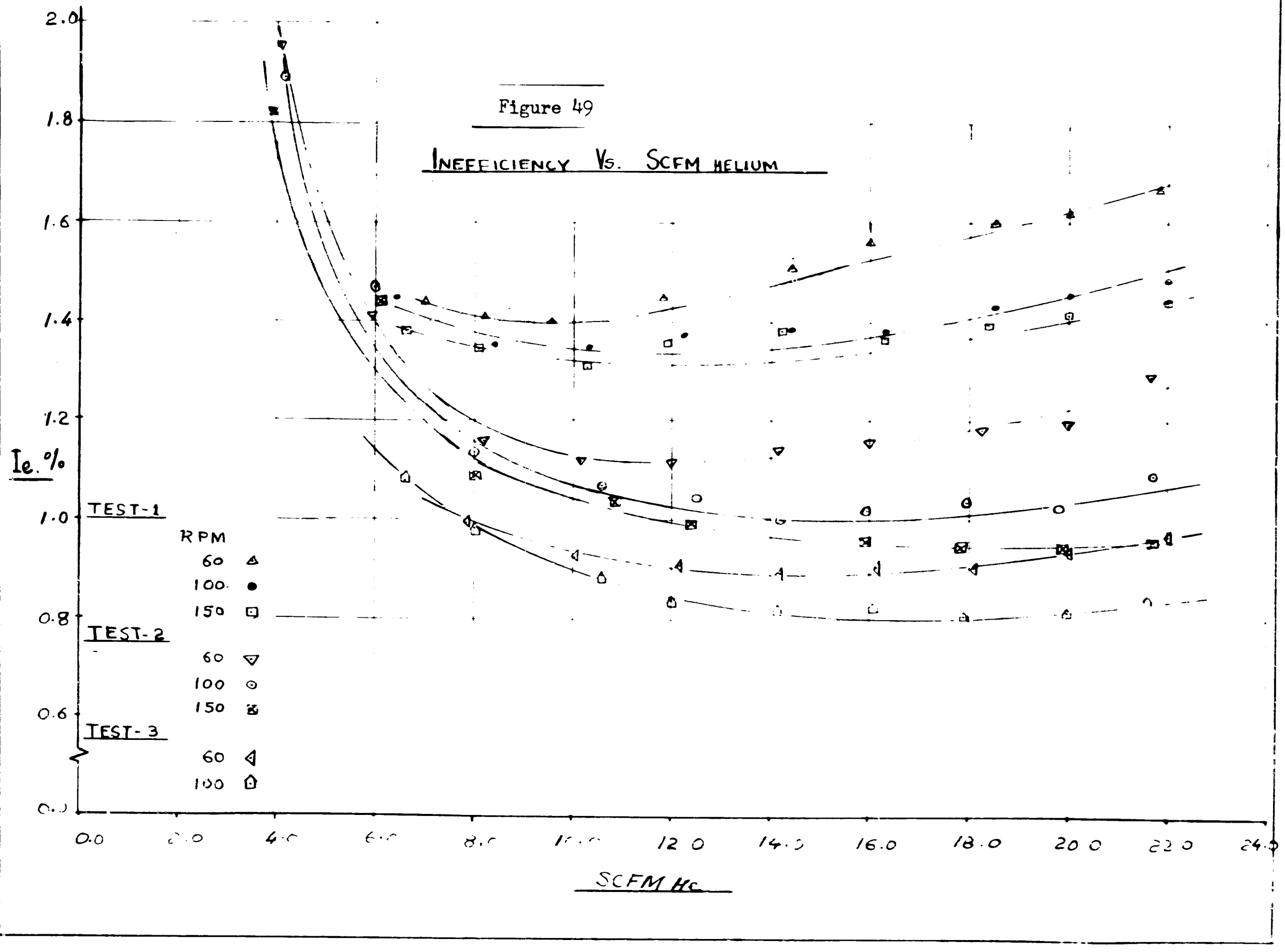

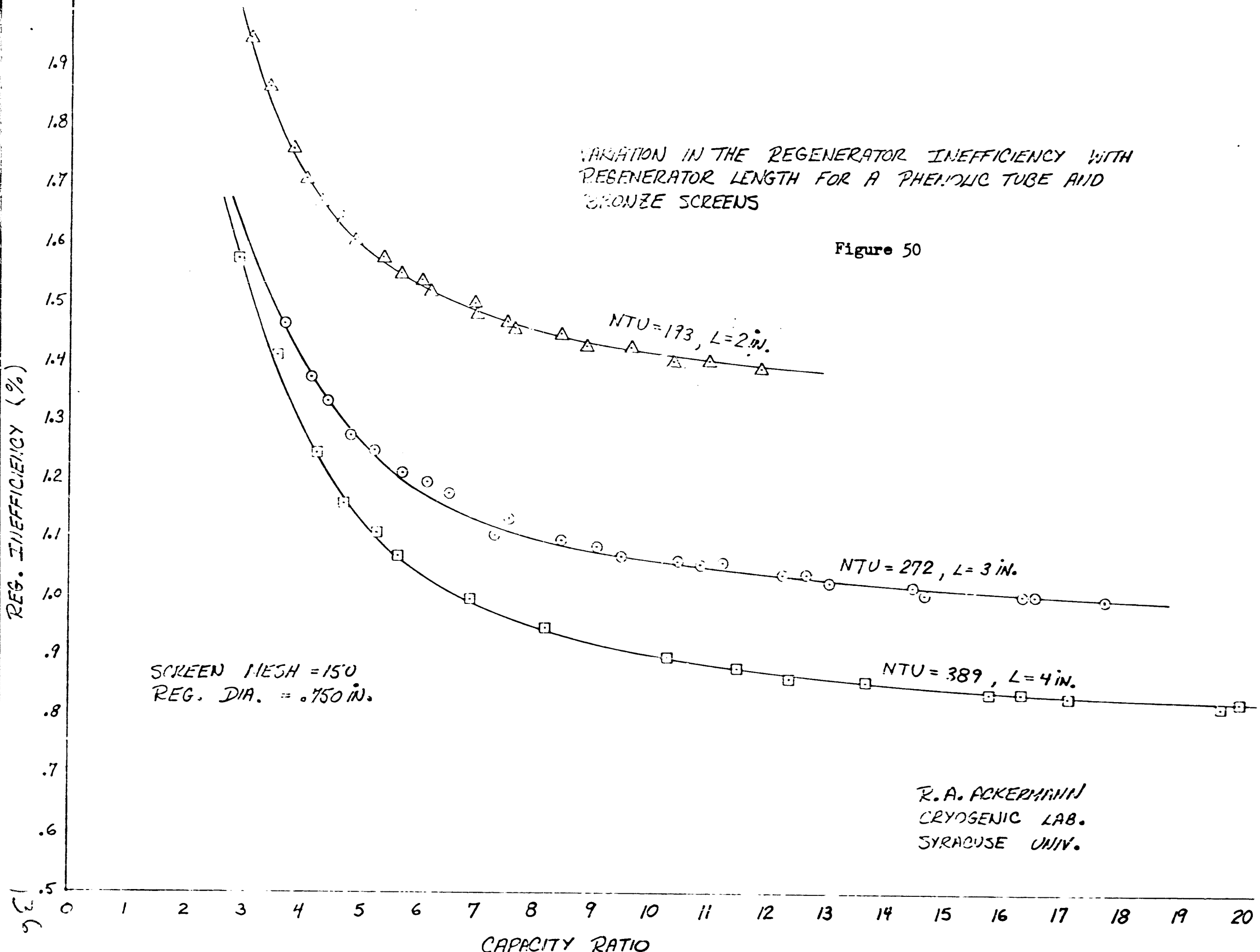

VARIATION IN THE REGENERATOR INEFFICIENCY WITH REGENERATOR LENGTH FOR A PHENOLIC TUBE AND BRONZE SCREENS

Figure 50

VARIATION IN THE REGENERATOR INEFFICIENCY WITH REGENERATOR LENGTH FOR A PHENOLIC TUBE AND BRONZE SCREENS

Figure 51

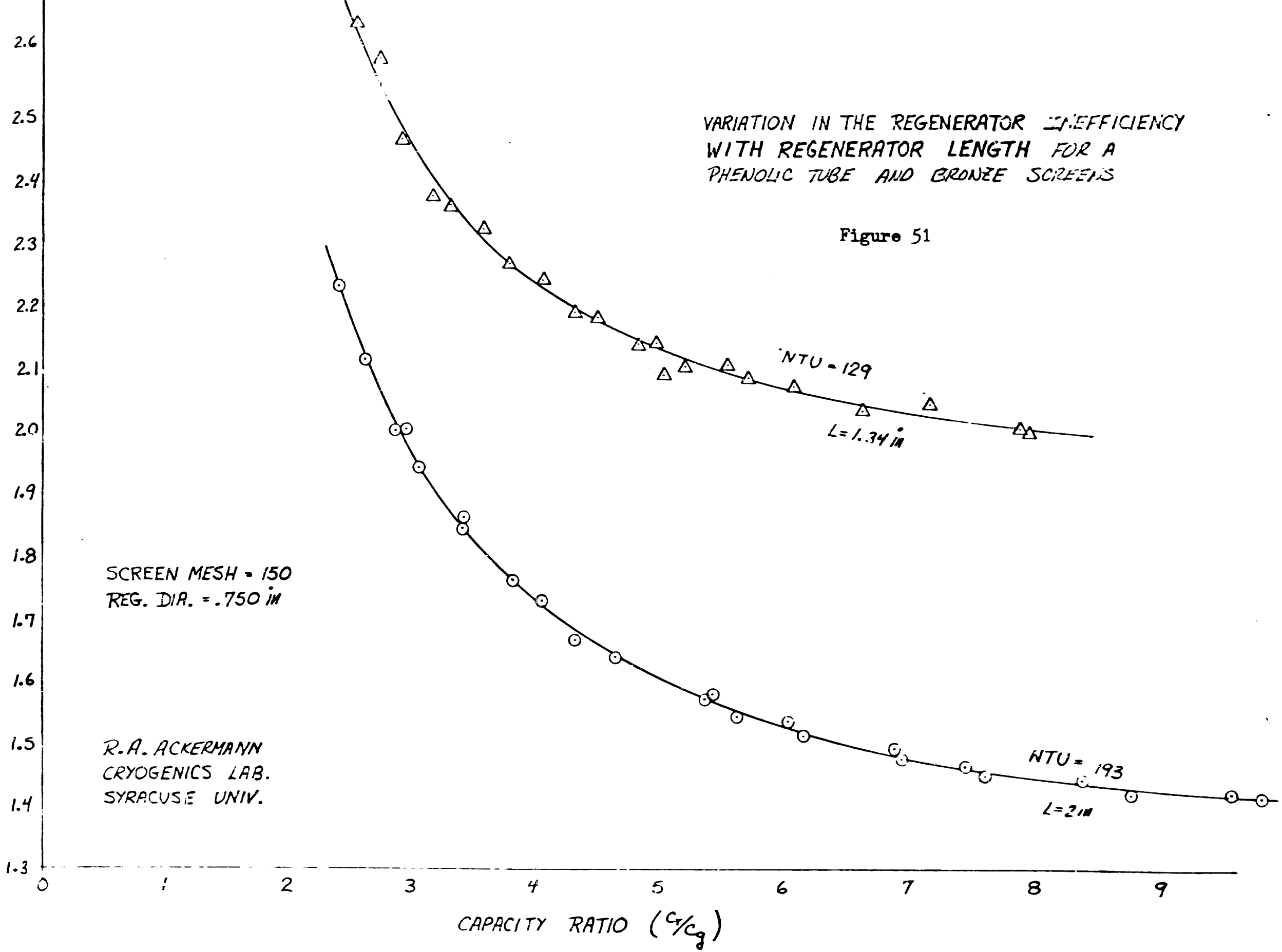

VARIATION IN THE REGENERATOR INEFFICIENCY WITH REGENERATOR LENGTH FOR A .020 IN THICK STAINLESS STEEL WALLED REGENERATOR AND BRONZE SCREENS

Figure 52

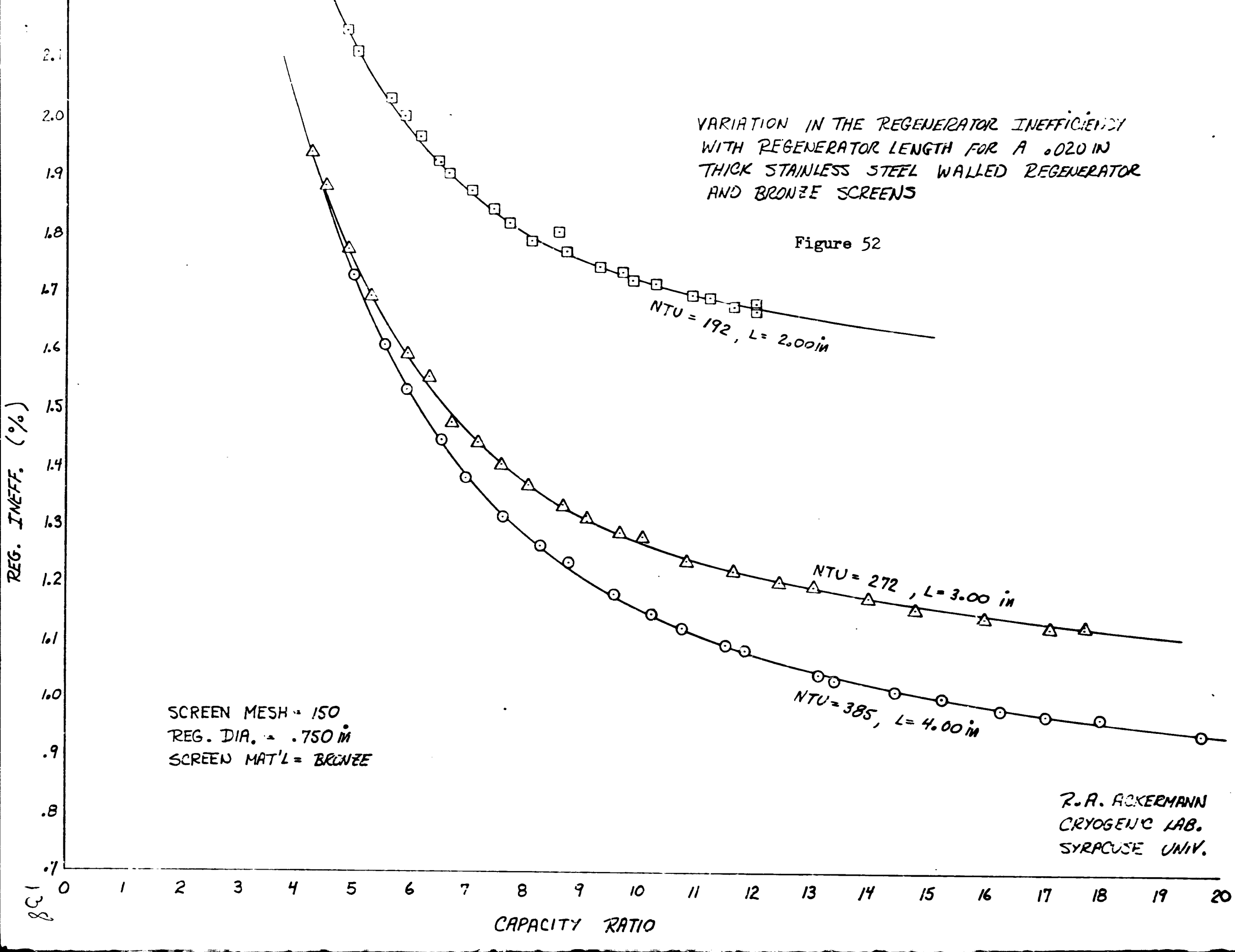

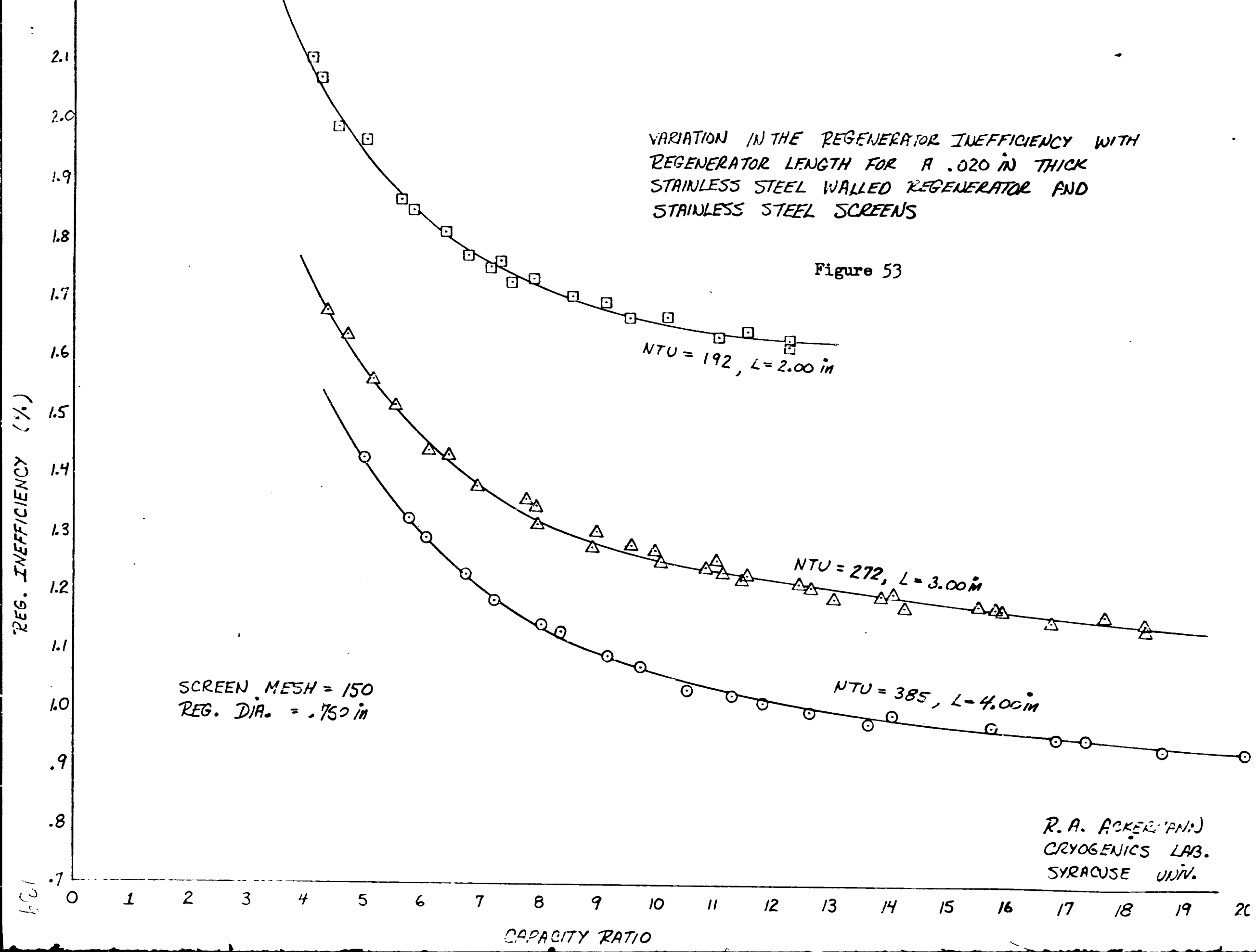

VARIATION IN THE REGENERATOR INEFFICIENCY WITH REGENERATOR LENGTH FOR A .020 in THICK STAINLESS STEEL WALLED REGENERATOR AND STAINLESS STEEL SCREENS

Figure 53

VARIATION IN THE REGENERATOR INEFFICIENCY
FOR LEAD SPHERES .015 TO .018 IN DIAMETERS

REG. DIA. = .750 IN

Figure 54

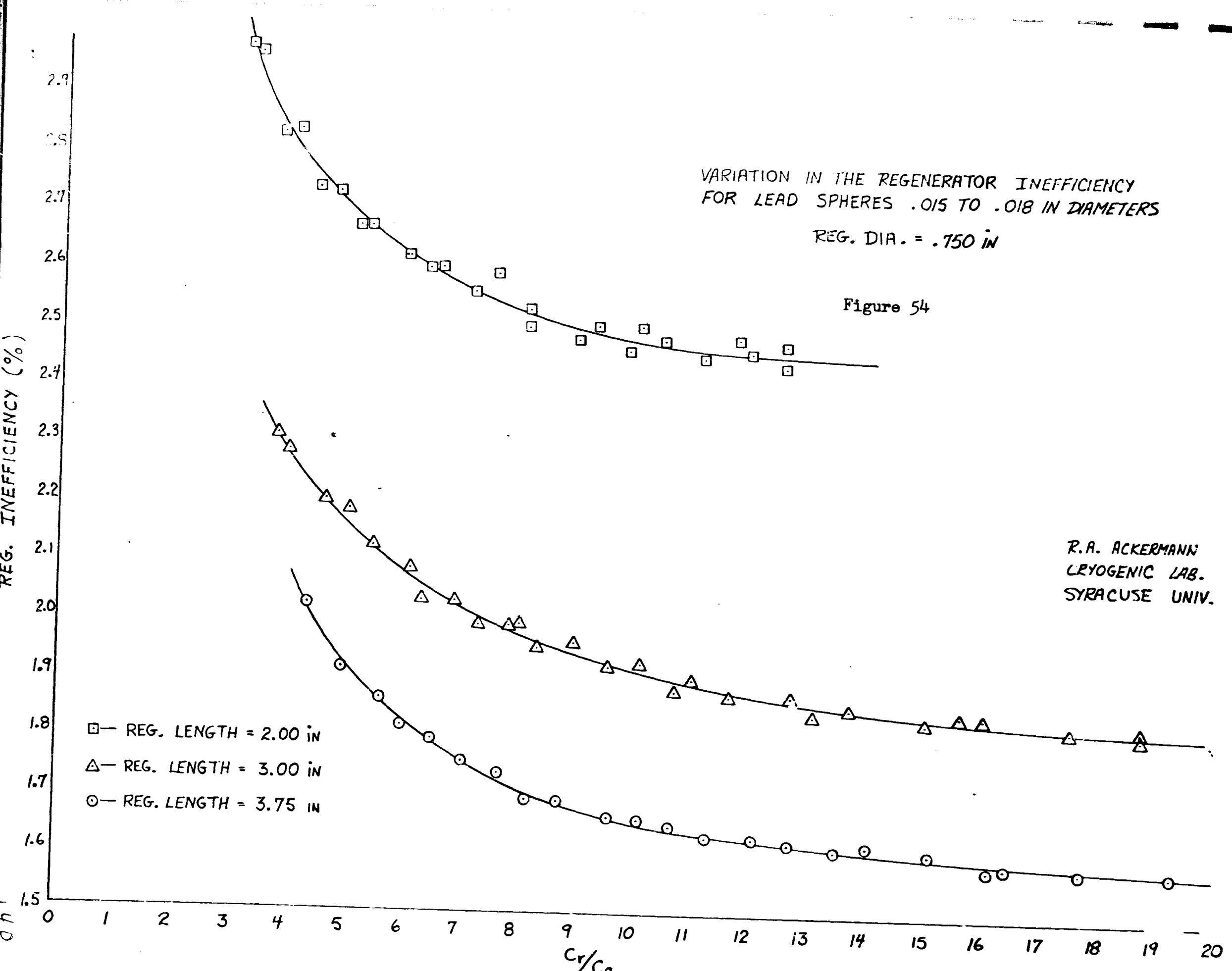

VARIATION IN THE REGENERATOR INEFFICIENCY
FOR TWO SPHERES .006 TO .007 IN. DIAMETERS
REG. DIA. = .750 IN.

Figure 55

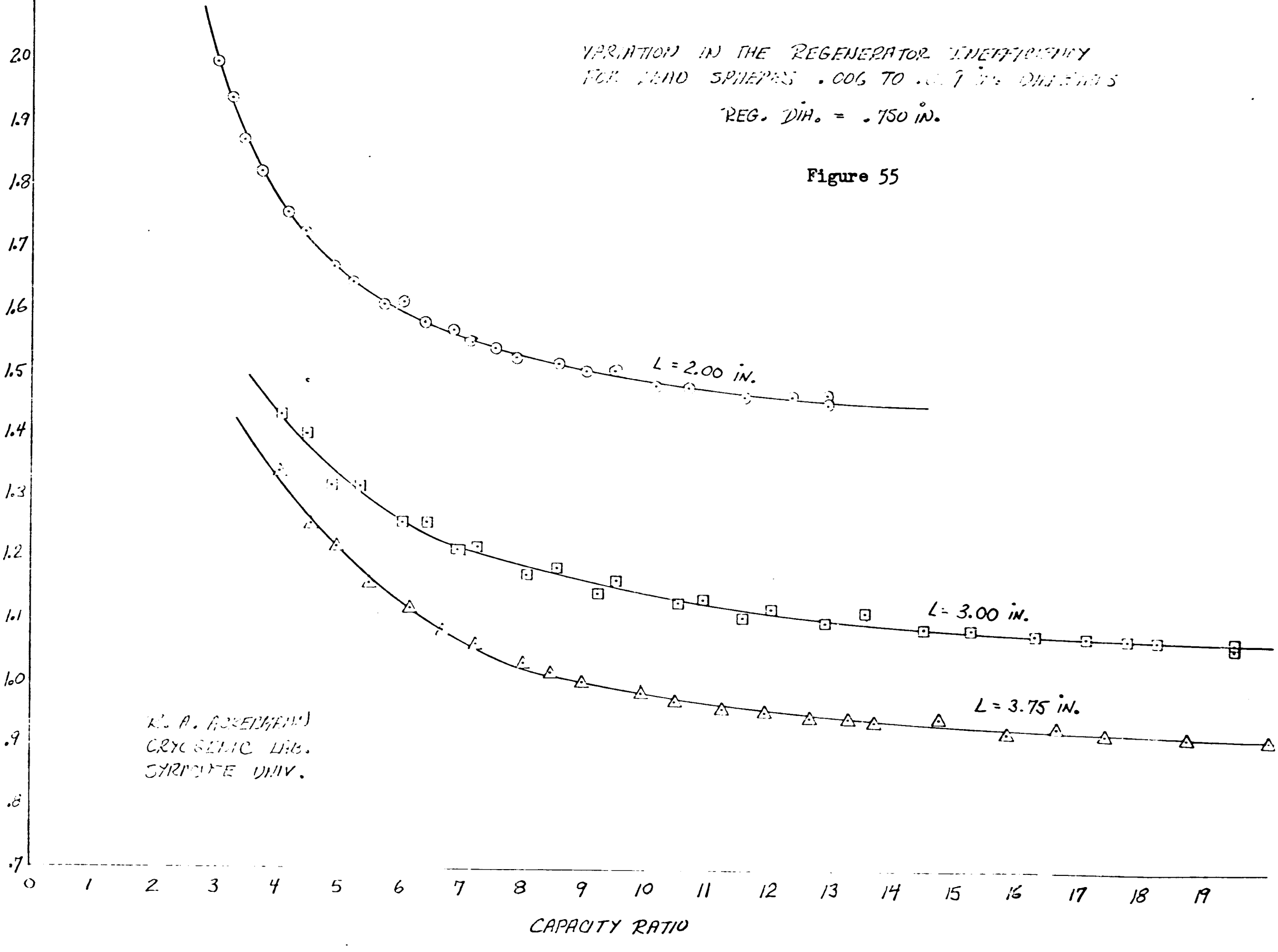

REGENERATOR INEFFICIENCY VARIATIONS
WITH HELIUM FLOW RATE

Figure 56

Screen mesh = 150
Reg. dia. = .750 in
Reg. length = 4.00 in
No. of screens = 670

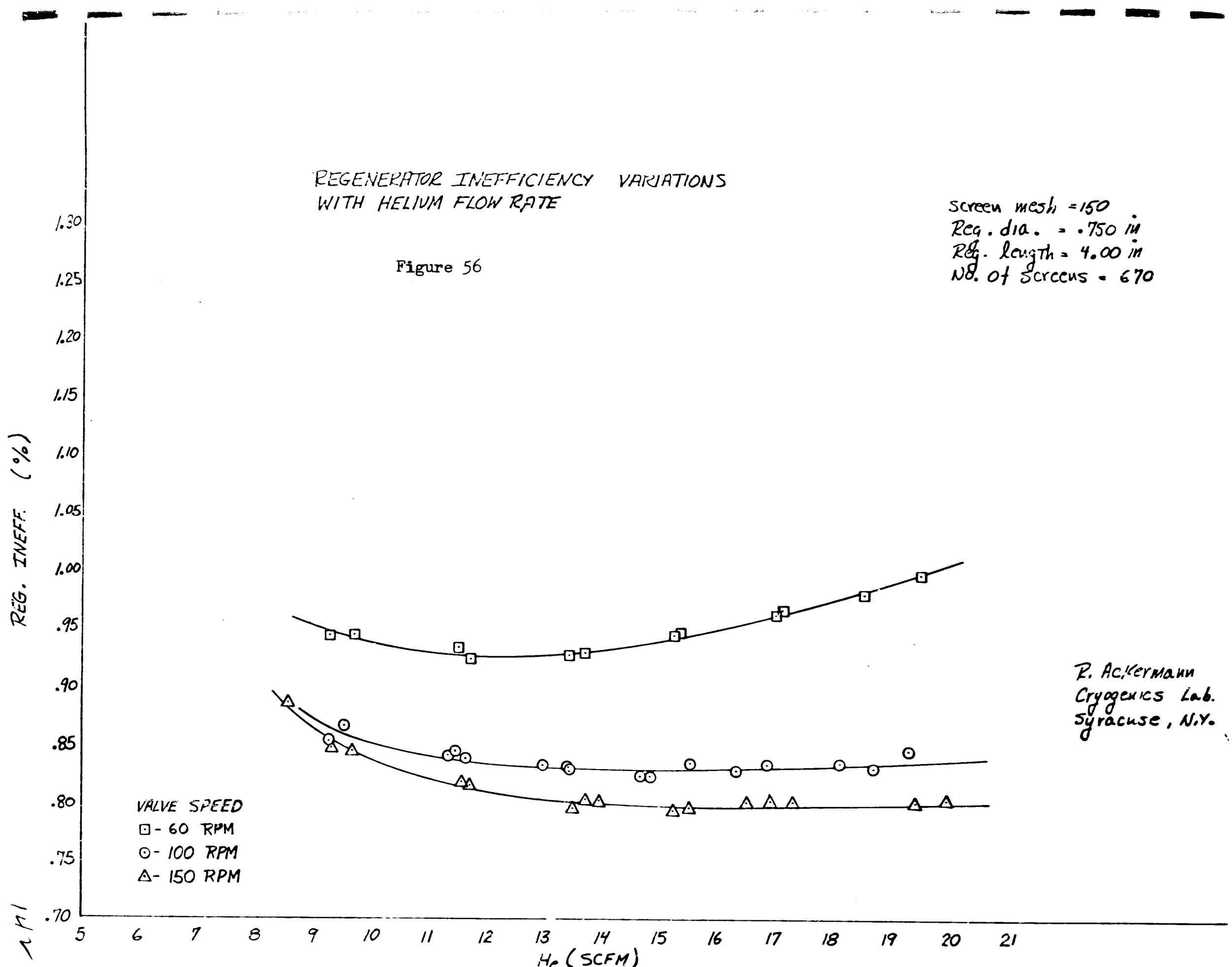

R. Ackermann
Cryogenics Lab.
Syracuse, N.Y.

REGENERATOR INEFFICIENCY VARIATION
WITH HELIUM FLOW RATE

Figure 57

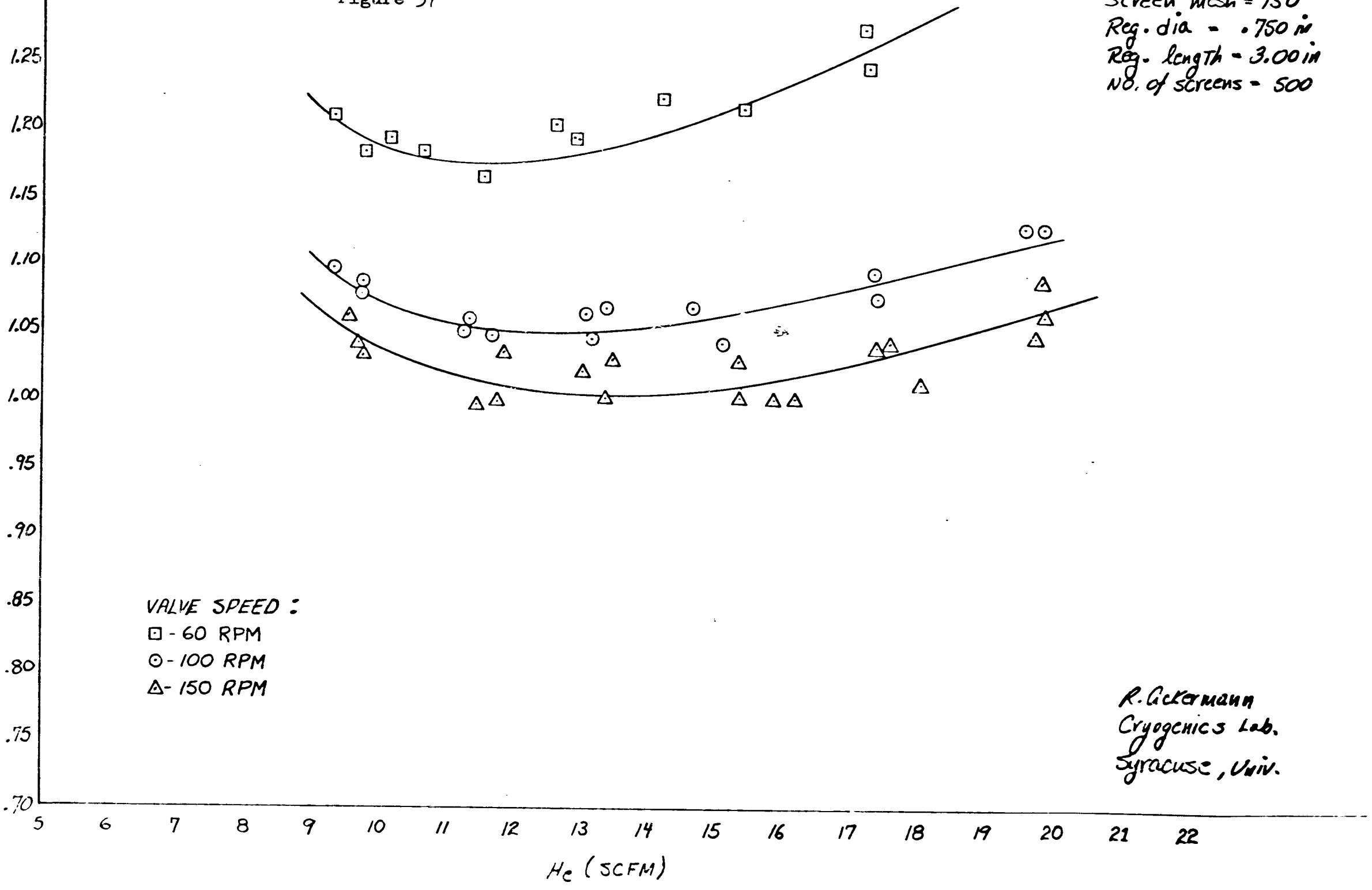

Screen mesh = 150
Reg. dia = .750 in
Reg. length = 3.00 in
No. of screens = 500

R. Ackermann
Cryogenics Lab.
Syracuse, Univ.

REGENERATOR INEFFICIENCY VARIATION WITH HELIUM FLOW RATE FOR A STAINLESS STEEL WALLED REGENERATOR

Figure 58

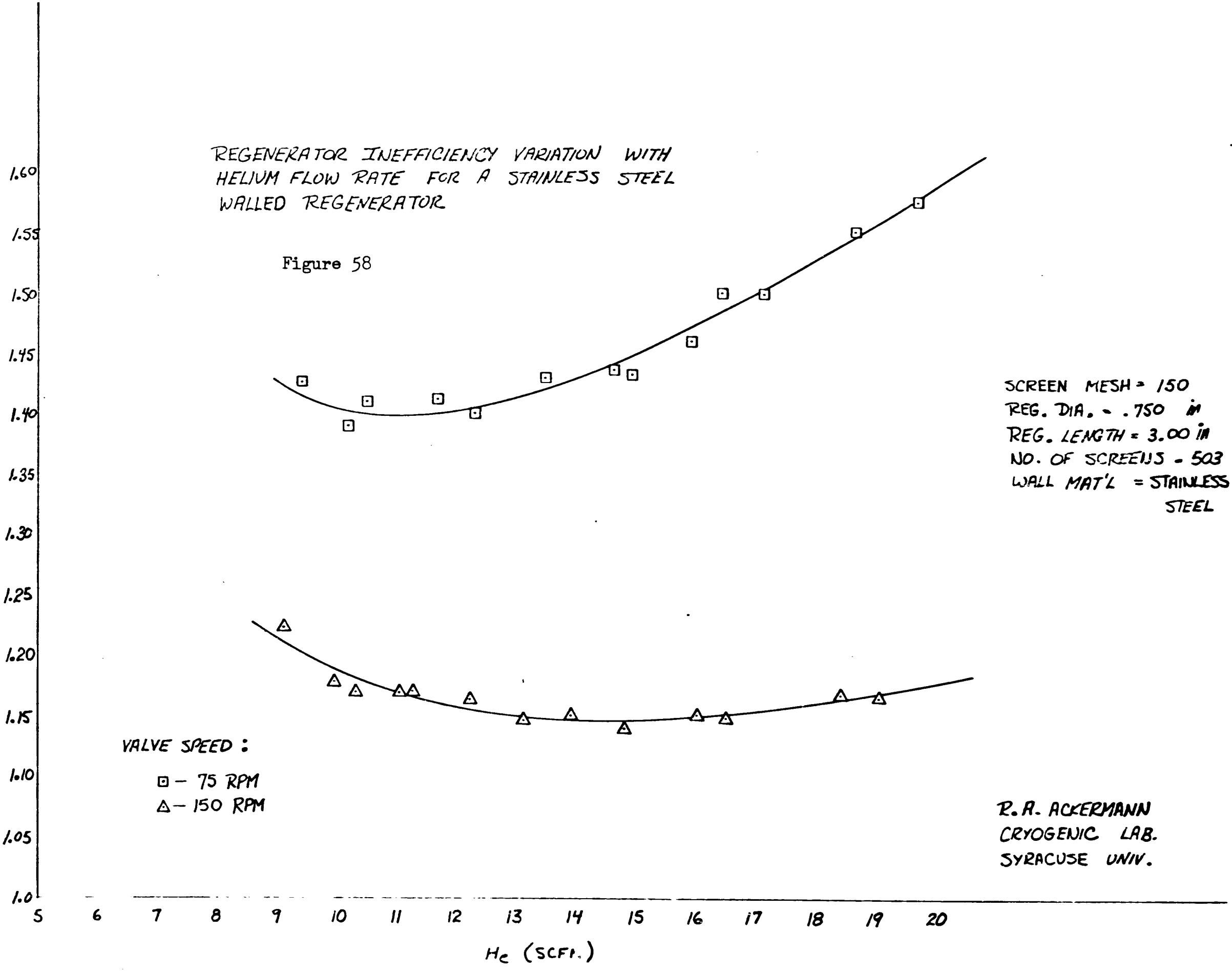

hh1

REGENERATOR INEFFICIENCY VARIATION
WITH HELIUM FLOW RATE

Figure 59

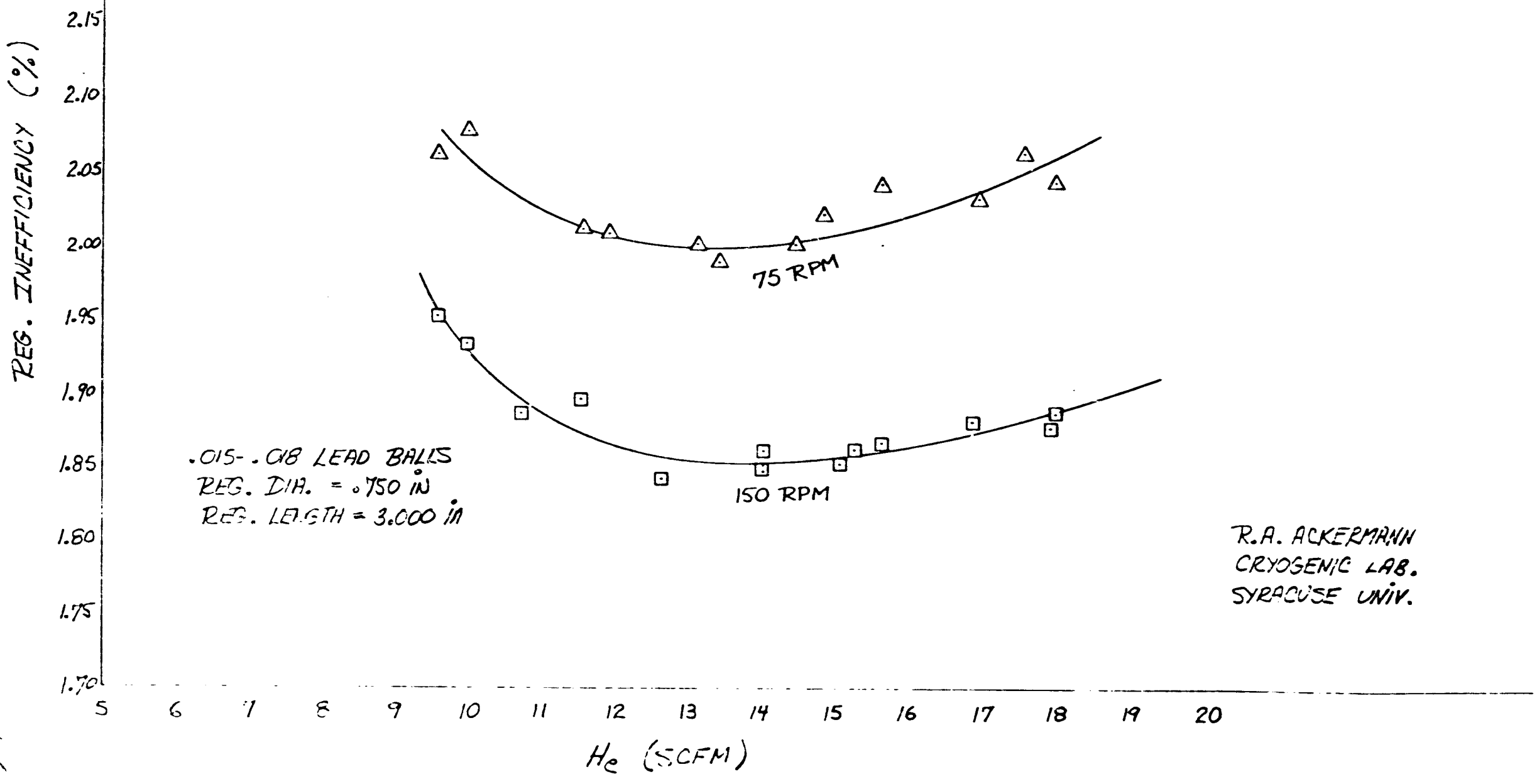

VARIATION IN REG. INEFFICIENCY WITH PACKING DENSITY FOR 150 MESH STAINLESS STEEL SCREENS

Figure 60

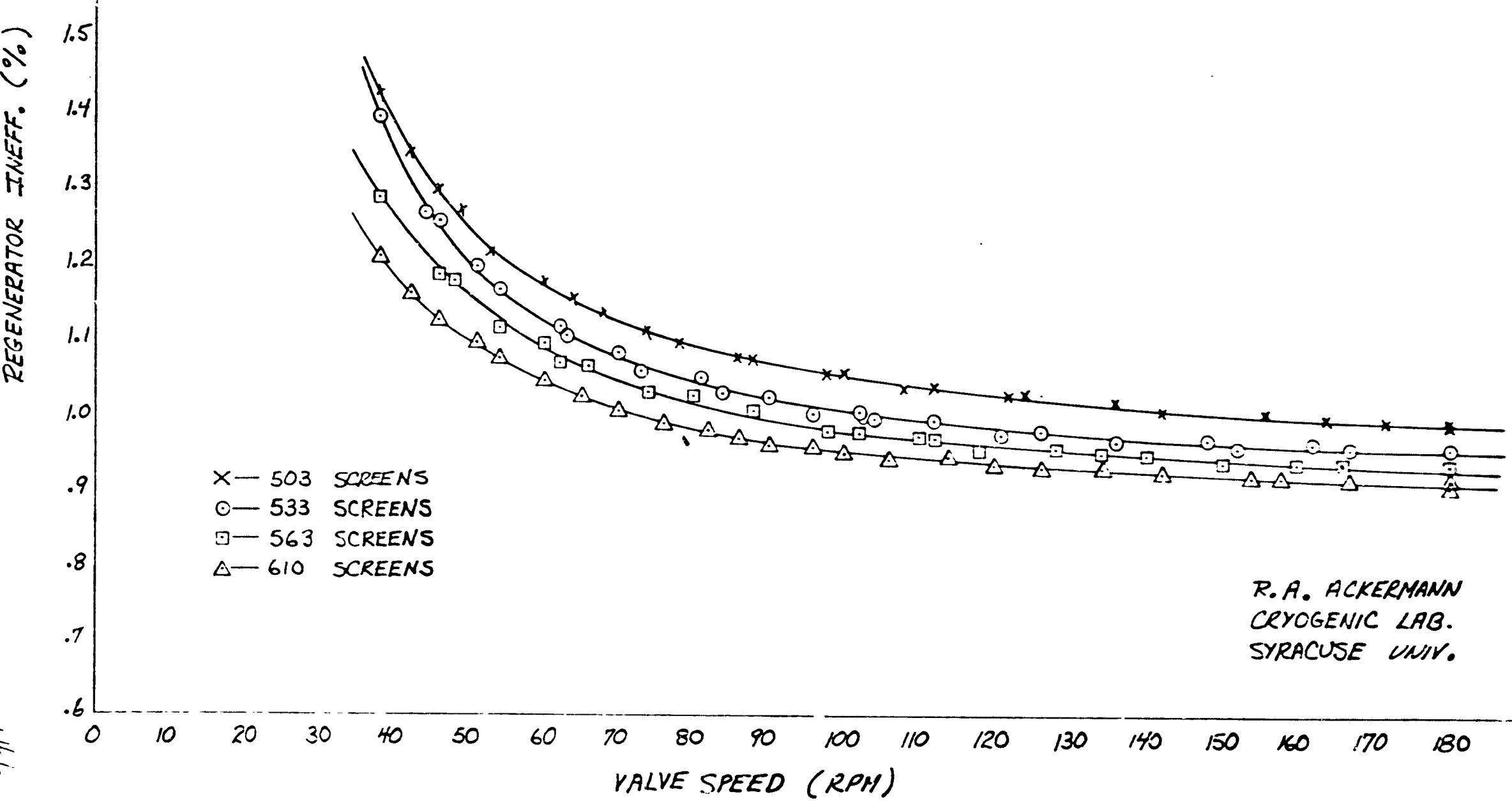

VARIATION IN REG. INEFFICIENCY WITH PACKING DENSITY FOR 150 MESH BRONZE SCREENS

Figure 61

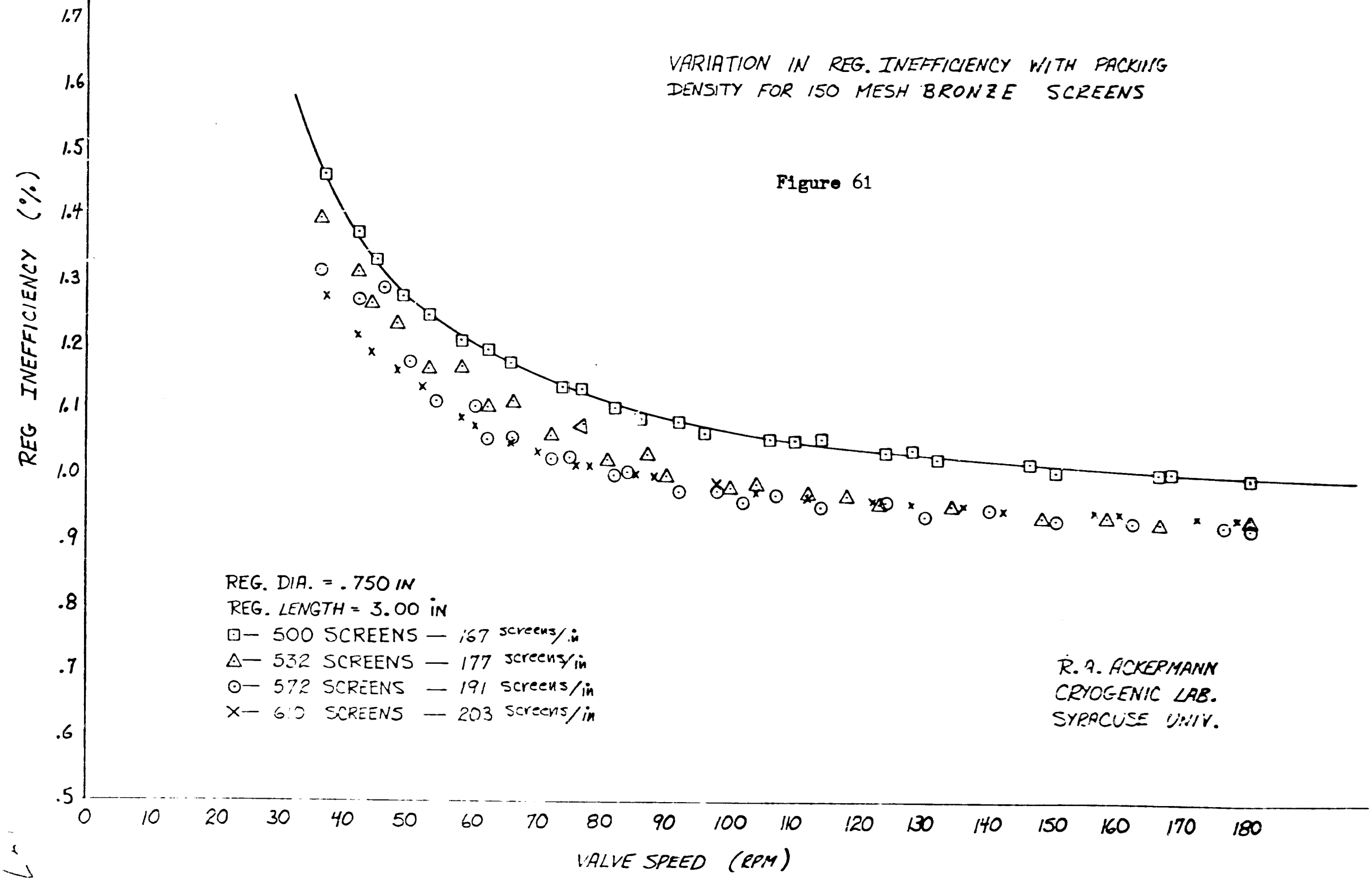

VARIATION IN REGENERATOR INEFFICIENCY
WITH SCREEN PACKING DENSITY

Figure 62

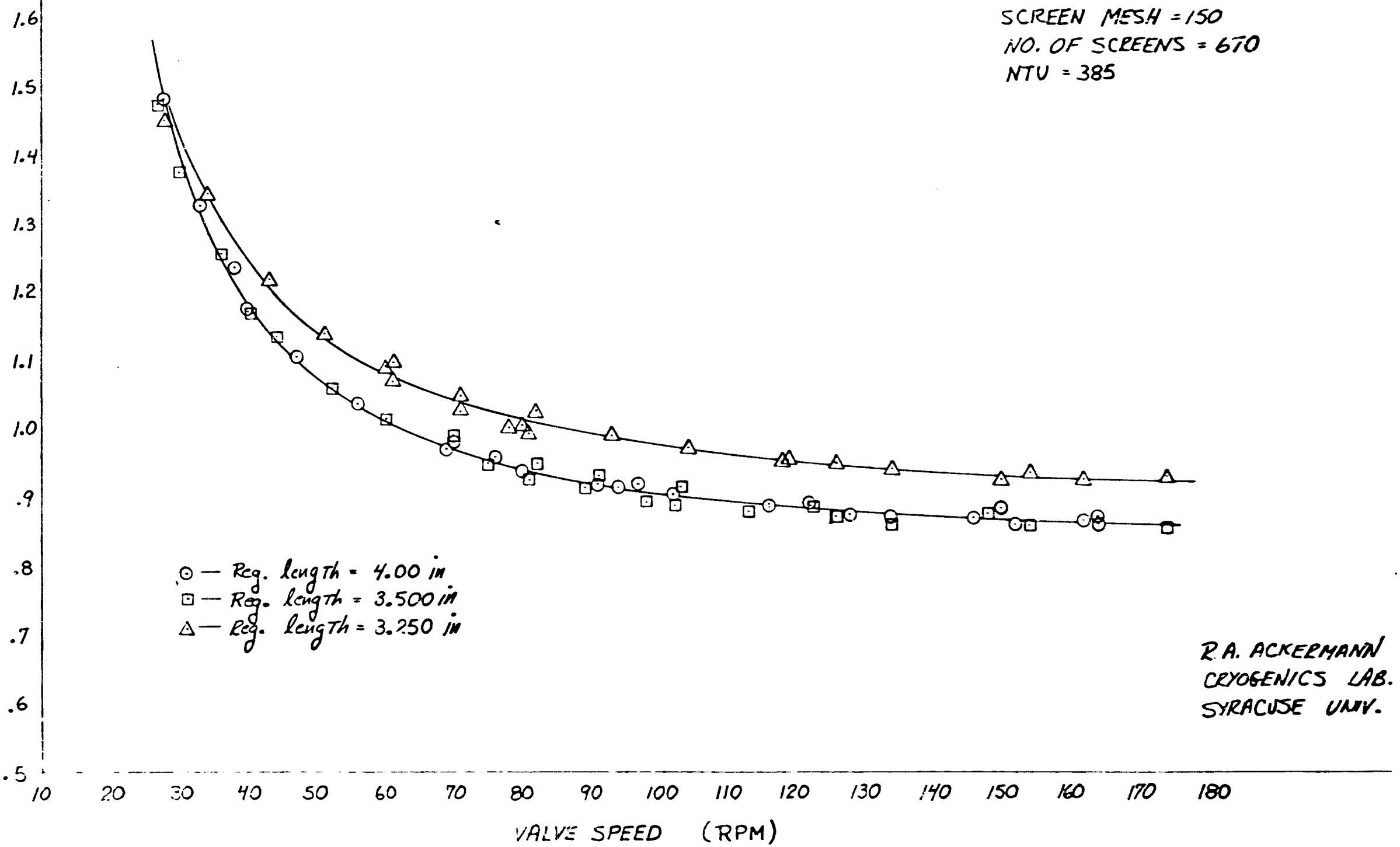

84

VARIATION IN REGENERATOR INEFFICIENCY
WITH SCREEN PACKING DENSITY

Figure 63

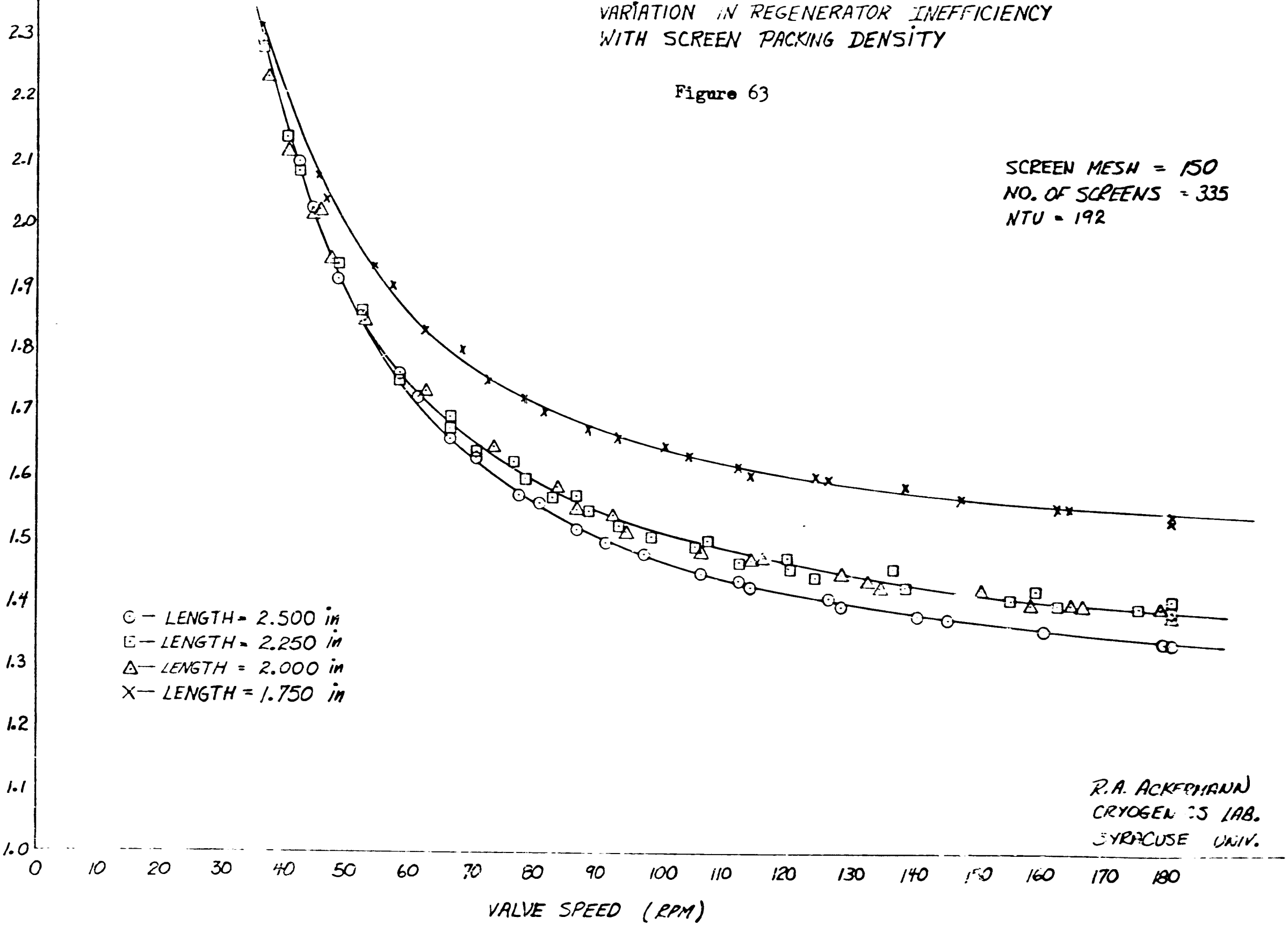

VARIATION IN THE REGENERATOR INEFFICENCY FOR A 2" LONG REGENERATOR WITH VARIABLE END CONDITIONS

Figure 64

SCREEN MESH = 150
REG. DIA. = .750 IN
NTU = 192

STAINLESS STEEL WALL

PHENOLIC WALL

⊙— .020 in THICK PERFORATED COPPER PLATE
△— ½" COPPER BLOCK
⊡— "S" CLIP

REG. INEFFICIENCY (%)

2.3 2.2 2.1 2.0 1.9 1.8 1.7 1.6 1.5 1.4 1.3 1.2 1.1 1.0

0 10 20 30 40 50 60 70 80 90 100 110 120 130 140 150 160 170 180

VALVE SPEED (RPM)

R. A. ACKERMANN
CRYOGENICS LAB.
SYRACUSE UNIV.

REGENERATOR TEST FLOW-DIAGRAM

FIGURE- 65

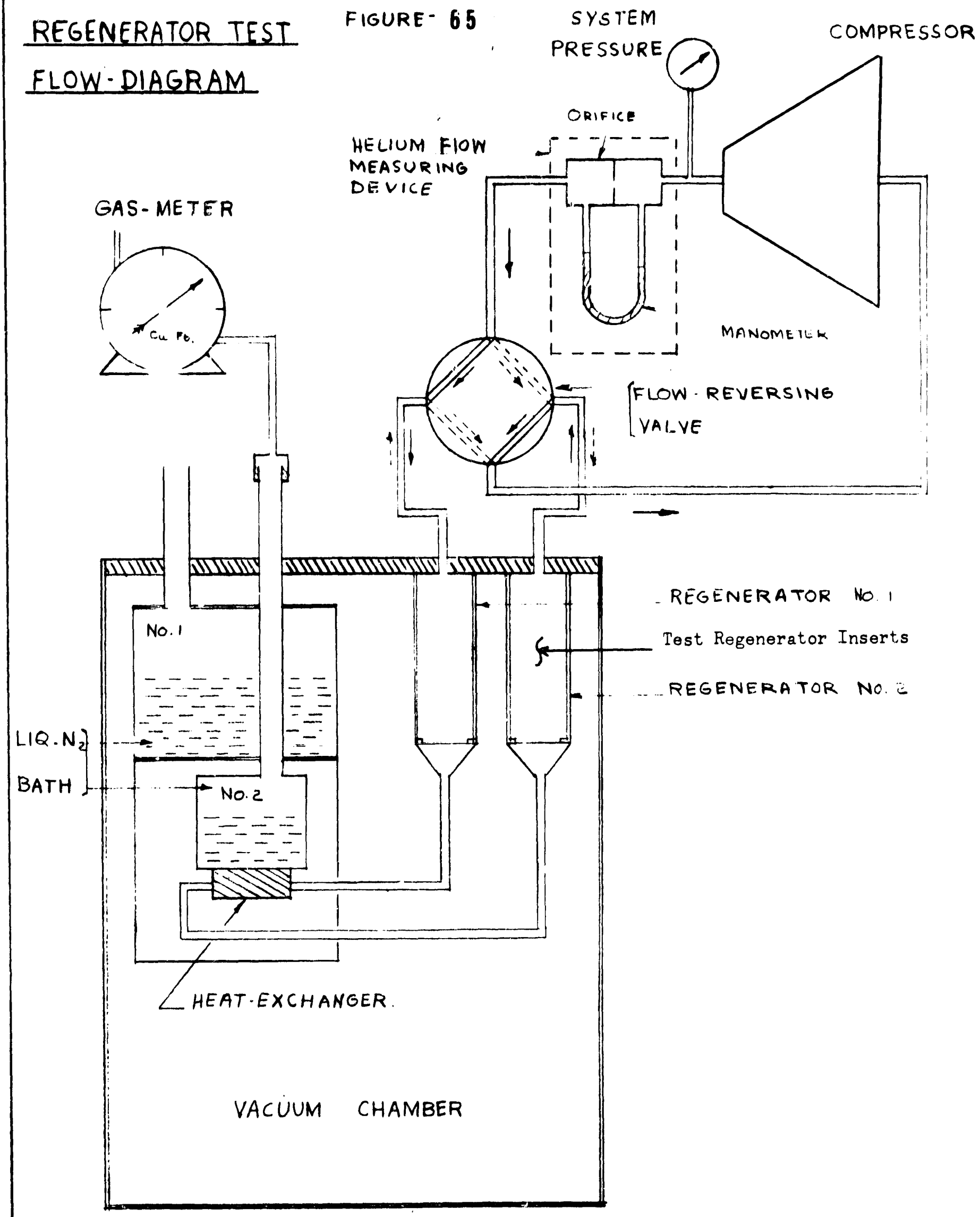

REFERENCES

1. Gordon J. Van Wylen, Thermodynamics, John Wiley & Sons, Inc., New York, 1959, page 18

2. W. E. Gifford, U. S. Patent #3,119,237, "Gas Balancing Refrigeration Method"

3. W. E. Gifford and H. O. McMahon, "A Low Temperature Heat Pump," Proc. of 10th Int. Congr. of Refrig., Vol. 1, Copenhagen, Denmark, August 1959

4. W. E. Gifford and T. E. Hoffman, Advances in Cryogenic Engineering, Vol. 6, K. D. Timmerhaus, ed., Plenum Press, Inc., New York, 1961

5. W. E. Gifford, Progress in Cryogenics, Vol. III, Heywood and Co., Ltd. London, 1961

BIBLIOGRAPHY

W. E. Gifford, U. S. Patent #2,966,035, "Refrigeration Method and Apparatus"

W. H. Hogan and R. W. Stuart, "Design Considerations for Cryogenic Refrigerators," ASME - Paper - 1963 - WA292, for meeting Nov. 17-22, 1963

R. W. Stuart and W. H. Hogan, Advances in Cryogenic Engineering, Vol. 10, K. D. Timmerhaus, ed., Plenum Press, Inc., New York, 1965